ISSN: 1945-3094 Volume 2, Number 7, July 2010

Scientific Research

Journal of Water Resource and Protection

ISSN: 1945-3094

www.scirp.org/journal/jwarp

Journal Editorial Board

ISSN: 1945-3094 (Print) ISSN: 1945-3108 (Online)

http://www.scirp.org/journal/jwarp

Editor-in-Chief

Editorial Board (According to Alphabet)

Editorial Assistant

Guest Reviewers (According to Alphabet)

J. Water Resource and Protection, 2010, 2, 609-689
Published Online July 2010 in SciRes (http://www.SciRP.org/journal/jwarp/)

TABLE OF CONTENTS

Volume 2 Number 7 July 2010

Journal of Water Resource and Protection (JWARP)

Journal Information

SUBSCRIPTIONS

The *Journal of Water Resource and Protection* (Online at Scientific Research Publishing, www.SciRP.org) is published monthly by Scientific Research Publishing, Inc., USA.

Subscription rates:

Print: $50 per issue.
To subscribe, please contact Journals Subscriptions Department, E-mail: sub@scirp.org

SERVICES

Advertisements
Advertisement Sales Department, E-mail: service@scirp.org

Reprints (minimum quantity 100 copies)
Reprints Co-ordinator, Scientific Research Publishing, Inc., USA.
E-mail: sub@scirp.org

COPYRIGHT

PRODUCTION INFORMATION

For manuscripts that have been accepted for publication, please contact:
E-mail: jwarp@scirp.org

J. Water Resource and Protection, **2010, 2, 609-618**
doi:10.4236/jwarp.2010.27070 Published Online July 2010 (http://www.SciRP.org/journal/jwarp)

Evaluation of Sawah Rice Management System in an Inland Valley in Southeastern Nigeria. II: Changes in Soil Physical Properties

John Chukwua Nwite[1], Charles Arizechukwua Igwe[1*], Toshiyukib Wakatsuki[2]
[1]*Department of Soil Science, University of Nigeria, Nsukka, Nigeria*
[2]*Faculty of Agriculture, Kinki University, Nara, Japan*
E-mail: *charigwe*1@*hotmail.com*
Received July 18, 2009; *revised August* 18, 2009; *accepted August* 28, 2009

Abstract

Establishment of effective *sawah* management system in parts of southeastern Nigeria may involve the manipulation of certain soil physical properties in form of ecological engineering works. This practice may affect the soil physical properties adversely. The objective of the study were basically to compare the influence of *sawah* and non *sawah* water management practices on the soil physical properties following rice cultivation with various inorganic and organic amendments. Parameters determined were soil bulk density, total porosity, moisture contents at field capacity (FC) and wilting point (WP), water-stable aggregates, dispersion ratio (DR), and hydraulic conductivity (Ks). *Sawah* managed soils reduced significantly the soil bulk density in the first and second year of planting thus increasing the soil total porosity during the same period Moisture content also improved in *sawah* management while WP increased significantly in the second year of planting. In spite of the destruction of soil structure as a result of cultural practices during rice cultivation the DR is improved on the long run by sawah water management. Moisture contents at FC and WP relates significantly with soil bulk density which also relates negatively with total porosity during the 2 years of cultivation. However, FC and WP may be very good tools in the estimation of bulk density. Again, the amendments were identified as promoting the development of soil aggregates and *Ks* on a long term.

Keywords: Water-Stable Aggregates, Bulk Density, Hydraulic Conductivity, Dispersion Ratio, Moisture Content

1. Introduction

The term *sawah* is defined as a leveled rice field surrounded by bunds with inlet and outlet connections to irrigation and drainage canals. It originated from Malayo-Indonesian term '*paddi*' which means rice plants. However, the term 'paddy' refers to rice grain with husks in the whole of West Africa. Wakatsuki *et al*. [1] therefore used the term *sawah* to distinguish between rice grain with husk, rice field and rice plant. Establishment of effective *sawah* management system for in- creased rice production in southeastern Nigeria involves the manipulation of certain soil physical properties in form of ecological engineering works. This manipulation of soil physical properties may involve deep earth movement and tillage to achieve a better topographic setting and optimal soil physical condition. Wakatsuki and Masunaga [2] remarked that ecological engineering of the inland watershed by the local people are required to increase agricultural productivity. These techniques according to them include leveling, bonding, and construction of canals and head dykes. Most soils in the West African sub-region are highly weathered and very fragile [3-7]. Mbagwu [4] reported that physical degradation of soils in the tropics resulted from soil erosion by water and mechanical land clearing using bulldozers. Lal [8] and Mbagwu *et al*. [9] showed that this degradation was manifested in high bulk density, low total and macro porosity, reduced water infiltration and transmission rate and low water retention and available water capacity within the root zone.

Rengasamy *et al.* [10] had earlier indicated that many soils used for irrigated or dry land agriculture are difficult to manage owing to their tendency to develop unsatisfactory structure particularly in their surface layers. Breakdown of aggregates leads to surface crusting, re-

duced water infiltration, restricted plant establishment and growth. The reason for the breakdown is normally as a result of slaking and dispersion of aggregates. These negative physical conditions of the soils added to poor nutrient status of such soils according to Mbagwu [4] resulted in poor crop-productivity and often abandonment of such lands leading to reduction in resource base of rural farmers.

Nnabude and Mbagwu [11] had used abandoned biological waste to improve the physical condition of some soils used in rice production in southeastern Nigeria. They insisted that application of rice mill waste on a Typic Haplustult in southeastern Nigeria resulted in significant improvement in bulk density, permanent water wilting point and total porosity. The use organic waste to restore the physical condition of soils solves two problems; one is the removal from the environment which they pollute and secondly supply of soil plant nutrient and eventual amelioration of soil physical properties. The use of biological wastes in the management of degraded soils or soils used for *sawah* rice management production is sustainable [12,13]. Most of the previous research where biological wastes were used for sustainable management of soils was mainly on upland and rainfed cultivation. None of these uses have been reported in *sawah* managed cropping system especially in southeastern Nigeria where these wastes are heaped with problems on the disposal. The objective of the study was therefore to 1) compare the influence of *sawah* and non *sawah* water managements on the physical characteristics of the soil, 2) to determine the contributions of the amendments on the soil physical properties and 3) the relationships among the soil physical properties.

2. Materials and Methods

2.1. Location and Field Study

The location of the study and the field design of this study are already given in the part I of this study [14]. The mineralogy of the soil is mainly kaolinite and the so-called interlayer minerals [15]. The major physical characteristics of the soil are shown (**Table 1**).

The field, which was under fallow for more than 5 years, was disk-ploughed and disk-harrowed to a depth of about 20 cm before puddling and treatments. The plot was divided into 2 portions, one part for *sawah* and the second part for non-*sawah* water management. In the non-*sawah* managed field, there was no defined water management and no bunding of plots in the field. Water was allowed to flow in and out as it comes but in the *sawah* field water was controlled and maintained to an approximate level of between 5 and 10 cm from two weeks after transplanting to the stage of ripening of the grains. In each of the plots the following treatments, arranged as a Split-Plot on a Randomized Complete Block Design (RCBD) were as shown (**Table 1**); each treatment was replicated 3 times and each plot was 6 m × 2.5 m. The NPK fertilizer consisted of 400 kg/ha as compound fertilizer, poultry dropping was applied at the rate of 5 tons/ha and Rice husk dust applied at 10 tons/ha. The RD on decomposition is widely applied by local farmers as source of plant nutrient. The nutrient contents of these organic amendments were determined. The mature PD and RD were spread on the plots that received them and incorporated manually into the top 20 cm soil depth 2 weeks before planting. All amendments were applied only in 2004 and their residual effect maintained for the 2 years.

The test crop was a high yielding rice variety *Oryza sativa* var. Tox 3108. This cultivar is widely used by farmers in the area. This was first planted in a nursery field and later transplanted to the main fields after 4 weeks in nursery. At maturity rice grains were harvested dried and yield computed at 90% dry matter content. This was done for the two years (2004 and 2005). At the end of each harvest soil samples were collected from each replicate of every plot for physical analyses.

2.2. Laboratory Methods

Particle size distribution of the less than 2-mm fine earth

Table 1. Some physical properties of the top soil (0-20 cm) before ploughing and amendment.

Soil Property	Value
Clay%	10
Silt%	21
Total sand %	69
Textural class	SL
Organic Carbon% (C)	1.61
Gravimetric moisture content (%) at	
–0.1 MPa (Field capacity) FC	27
–1.5 MPa (Permanent wilting point) PWP	9.2
Saturated hydraulic conductivity K_s (cm h^{-1})	7.0
Bulk density Mg/m^3	1.29
Total porosity%	51.2
Mean-weight diameter (MWD) mm	0.50

Table 2. Treatment combinations and their symbols.

I	F	NPK Fertilizer (20:10:10). Locally recommended rate for rice
II	PD	Poultry droppings
III	RD	Rice husk dust
IV	RD + PD	Rice husk dust + Poultry droppings
V	PD + F	Poultry droppings + NPK Fertilizer
VI	RD + F	Rice husk dust + NPK Fertilizer
VII	F + PD + RD	NPK Fertilizer + Poultry droppings + Rice husk dust
VIII	CT	Control (No soil amendment)

fractions was measured by the hydrometer method as described by Gee and Bauder [16]. The clay obtained from particle size analysis with chemical dispersant is regarded as total clay (TC) and silt as total silt (TSilt), while clay and silt obtained after particle size analysis using deionised water only were the water-dispersible clay (WDC) and water-dispersible silt (WDSi). The soil organic carbon was determined by the Walkley and Black method described by [17]. Dispersion ratio which is an index of soil dispersion was calculated as;

$$\text{Dispersion ratio (DR)} = [(\text{WDSi} + \text{WDC})/(\text{TSilt} + \text{TC})] \quad (1)$$

The higher the DR, the more the ability of the soil to disperse in water. The soil saturated hydraulic conductivity was measured using Klute and Dirksen method [18]. Soil bulk density was measured by the core method [19]. Total porosity (Tp) was obtained from bulk density (ρ_b) values with assumed particle density (ρ_s) of 2.65 Mg/m^3 as follows,

$$\text{Porosity} = \text{Tp} = 100(1 - \rho_b/\rho_s) \quad (2)$$

The soil moisture contents at 0.1 and 1.5 MPa suction were determined by Klute [18] method while the available water capacity was calculated as the difference between moisture retention at 0.1 and 1.5 MPa [*i.e.* field capacity (FC) and permanent wilting point (PWP)].

The method of Kemper and Rosenau [20] was used to separate the water-stable aggregates (WSA). In this method 40 g of < 4.75 mm air-dried soils were put in the topmost of a nest of four sieves of 2.00, 1.00, 0.50, and 0.25 mm mesh size and pre-soaked for 30 min in deionized water. Thereafter the nest of sieves and its contents were oscillated vertically in water 20 times using 4 cm amplitude at the rate of one oscillation per s. After wet-sieving, the resistant soil materials on each sieve and the unstable (< 0.25 mm) aggregates were quantitatively transferred into beakers, dried in the oven until steady weight is achieved. The percentage ratio of the aggregates in each sieve represents the water-stable aggregates (WSA) of size classes; > 2.00, 2.00-1.00, 1.00-0.50, 0.50-0.25 and < 0.25 mm. Aggregate stability was measured as the mean-weight diameter (MWD) of stable aggregates as equation

$$\text{MWD} = \Sigma X_i W_i \quad (3)$$

where X_i is the mean diameter of the i^{th} sieve size and W_i is the proportion of the total aggregates in the i^{th} fraction. The higher the MWD values, the higher proportion of macroaggregates in the sample and therefore better stability.

2.3. Data Analyses

An analysis of variance of each soil properties between water management systems and amendments was performed on the soil data generated from the laboratory. The differences among the mean values were tested with the LSD. Also correlation coefficients of the relationships between some of the soil properties were determined using the SPSS.10 computer package.

3. Results and Discussion

3.1. The Influence of Water Managements and Amendments on Soil Bulk Density and Total Porosity

During the first year of planting the bulk density was between 1.2 Mg/m^3 to 1.46 Mg/m^3 in the non *sawah* water management system and 1.19 to 1.46 Mg/m^3 in the *sawah* system (**Table 3**). The results indicated that there was a significant difference within the bulk density with amendments. Also the mean bulk density of soils in the *sawah* system was significantly lower than the corresponding mean bulk density of the non *sawah* system. Higher bulk density according to Mbagwu *et al*. [9] signified compaction and undesirable soil structure that affects roots and plant growth negatively. Again, the same trend as was shown for bulk density in the first year was also indicated in the second year of planting. Bulk density varied significantly with amendments while a significant lower bulk density was obtained from the *sawah* system than the non *sawah* system. In all cases whether in *sawah* or non *sawah* management, rice husk dust reduced the mean bulk density of the soil. Nnabude and Mbagwu [11] showed that rice waste, either burnt or fresh condition could be effective in the improvement of soil properties. The importance of lower bulk density in the soil as portrayed by the *sawah* managed plots is the improvement of soil aeration, tilt and better water infiltration in addition to unreserved root penetration.

The total porosity also followed the trend in the soil bulk density (**Table 3**). While total porosity differed significantly with soil amendments in both first and second year of planting, it also differed significantly with water managements. In both years total porosity were always significantly higher in *sawah* managed system than in non *sawah* managed system (**Table 3**). The results here also showed the beneficial contribution of the organic amendments in improving the soil total porosity. Furthermore, *sawah* managed system could provide management strategies as to the improvement of soils liable to compaction and other negative physical properties when puddle for rice production.

3.2. The Influence of Water Managements and Amendments on Moisture Content at Field Capacity (FC) and Wilting Point (WP)

While amendments showed no significant differences with moisture content at field capacity (FC) in the first

year, there was non significant difference in the FC values in the same year (**Table 4**). However, the value of FC in *sawah* system is higher when compared to non *sawah*. Also in the second year the FC did not differ sig nificantly with amendments and with water managements. Again the trend showed that although non significant, relatively higher value of FC was obtained in *sawah* than in non *sawah* managed plot. The inference that could be drawn from this is that *sawah* managed plots may hold water more at the level of field capacity than the non *sawah* managed. This hypothesis may be exploited in the restoration of these soils occurring within the inland valleys of the agro ecological zone in the area of water management for sustainable production.

In the first year just like the FC, the moisture content at wilting point (WP) was significant with amendments but not with water management. However, the trend was that higher average value was obtained in the *sawah* managed plots more than the non *sawah* managed plot (**Table 4**). In the second year of planting, it was significant both for the amendment and water management. In most cases the amendments improved the moisture content at WP while *sawah* water management improved significantly the WP (**Table 4**). This result further confirms the superiority of *sawah* in soil moisture reserve over non *sawah*. In these soils which discharge its moisture contents very quickly, it will be an advantage that with *sawah* practice, more moisture may be reserved at WP, than other practices.

3.3. The Influence of Water Managements and Amendments on Soil Water-Stable Aggregates and Mean-Weight Diameter

Table 5 presents Water-stable aggregate (WSA) sizes > 2.00 mm and < 0.25 mm. These two aggregate sizes were chosen because of their extreme vales and sizes. While the WSA > 2.00 mm were the large aggregates, the < 0.25 mm are the smallest aggregate sizes. The WSA > 2.00 mm are not significant with neither amendment nor

Table 3. Effect of sawah system and amendments on bulk density and total porosity of 0-20 cm top soil.

	1st Year			
Amendments	Non Sawah		Sawah	
	Bulk Density Mg/m^3	Total Porosity%	Bulk Density Mg/m^3	Total Porosity%
F	1.29	51.4	1.46	44.9
PD	1.45	45.8	1.15	56.7
RD	1.12	57.9	1.20	54.4
RD + PD	1.34	49.4	1.20	54.9
PD + F	1.31	50.2	1.29	51.4
RD + F	1.46	44.8	1.19	55.4
F + PD + RD	1.25	52.7	1.32	50.4
CT	1.29	51.2	1.33	49.7
Mean	1.31	50.4	1.27	52.2
LSD (0.05)	0.14	5.9	0.14	5.9
Non Sawah × Sawah Bulk density		0.03		
Non Sawah × Sawah Total porosity		1.12		
	2nd Year			
F	1.25	52.8	1.35	48.9
PD	1.31	50.8	1.13	57.5
RD	1.13	57.1	1.23	53.5
RD + PD	1.27	51.9	1.18	55.7
PD + F	1.30	50.6	1.23	53.5
RD + F	1.45	45.3	1.13	57.0
F + PD + RD	1.26	52.7	1.28	51.6
CT	1.27	52.1	1.28	51.7
Mean	1.28	51.7	1.23	53.7
LSD (0.05)	0.10	3.9	0.10	3.9
Non Sawah × Sawah Bulk density		0.026		
Non Sawah × Sawah Total porosity		1.12		

NS = non-significant

Table 4. Effect of sawah system and amendments on moisture content at field capacity (FC) and wilting point (WP) of 0-20 cm top soil.

	1st Year			
Amendments	Non Sawah		Sawah	
	FC%	WP%	FC%	WP%
F	37.9	14.0	30.4	9.2
PD	24.8	7.2	40.4	15.5
RD	44.9	18.0	38.5	16.2
RD + PD	36.6	12.8	39.7	14.4
PD + F	40.5	15.3	36.9	14.2
RD + F	26.9	7.5	41.7	16.6
F + PD + RD	41.1	15.8	30.4	11.6
CT	27.0	9.2	34.6	12.1
Mean	35.0	12.5	36.6	13.7
LSD (0.05)	NS	3.9	NS	3.9
Non Sawah × Sawah FC		NS		
Non Sawah × Sawah WP		NS		
		2nd Year		
F	41.9	16.3	35.6	14.1
PD	24.6	6.8	43.2	17.9
RD	45.4	18.7	38.5	14.7
RD + PD	35.7	13.4	38.7	14.5
PD + F	38.9	13.9	40.2	17.6
RD + F	29.9	10.1	39.5	16.8
F + PD + RD	37.2	12.9	31.2	11.1
CT	27.0	7.7	35.3	13.9
Mean	35.1	12.5	37.8	15.1
LSD (0.05)	NS	4.38	NS	4.38
Non Sawah × Sawah FC		NS		
Non Sawah × Sawah WP		2.04		

NS = non-significant

water managements. In the < 0.25 mm aggregate sizes in the first year, amendments contributed significantly in increasing the values which were not desirable as aggregates within these range are said to be very unstable especially when submerged [6,21]. The WSA < 0.25 mm were also not significant with water management. In the second year WSA reduced significantly in *sawah* management and differed significantly with amendment (**Table 5**). Average value shows that in non *sawah* WSA was 13.69% in the second year and went down to 9.97% in the *sawah* system. This was an advantage as Abu-Hamdeh *et al*. [22] observed that as clod size increased, detachment rate increased and interaggregate tensile strength decreased and often leading to greater rate of splash erosion. The WSA < 0.25 mm correspondingly increased in *sawah* managed over non *sawah* managed in the second year significantly (**Table 5**).

Mean-weight diameter (MWD) did not change significantly with water management and amendments in the first year (**Table 5**). In the second year of planting MWD changed significantly with amendments and water managements. In the non *sawah* management an average value of 0.75 mm was obtained as against an average of 0.56 mm in *sawah* managed plots. These lower values of MWD in *sawah* managed plots may be advantageous when considered in the entire dynamics of low land or flooded rice production. This condition may be more favourable to rice requirements in terms of the physical soil condition to enable puddling.

3.4. The Influence of Water Managements and Amendments on Soil Dispersion Ratio and Saturated Hydraulic Conductivity

Dispersion ratio (DR) is an index which measures the ease of soil particles to disperse and erode, indicates that

higher values of DR signify higher propensity to erode especially when submerged. **Table 6** among other properties showed the DR with amendments and with water managements. In the first year of operation amendments contributed significantly to changes in DR but not in water managements. However lower average value of DR was obtained in *sawah* managed. In the second year both the amendments and the water managements contributed significantly to DR. An average DR value of 0.78 was obtained in non *sawah* managed plot while a mean value of 0.58 was for *sawah* system. The implication of these results are that although low values of MWD and high WSA < 0.25 mm were obtained in *sawah* managed soils, yet their rate of potential erodibility was low. Igwe [6] and Igwe [7] used this index to show the potential soil loss values for similar soils within the agro ecological zone.

Although the saturated hydraulic conductivity (*Ks*) was not significant with water management in first and second years, yet the amendments were able to change the saturated hydraulic conductivity significantly (**Table 6**). In both year *Ks* was always nominally higher in *sawah* managed plots than the non *sawah* plots. This was a reflection of the earlier results on bulk density, total porosity and aggregate stability of the soils.

3.5. Relationships among the Soil Physical Properties

In the first year of planting irrespective of the type of water managements, bulk density which is a very strong index of the soil structure negatively correlated with total porosity, moisture contents at field capacity (FC) and

Table 5. Effect of sawah system and amendments on large Water-stable aggregates (WSA > 2.00 mm), fine aggregates (WSA < 0.25 mm) and mean-weight diameter (MWD) of 0-20 cm top soil.

	1st Year					
	Non-Sawah			Sawah		
	WSA > 2.0	WSA < 0.25	MWD	WSA > 2.0	WSA < 0.25	MWD
F	5.2	77.9	0.39	7.89	71.8	0.48
PD	6.25	72.3	0.43	5.95	73.4	0.43
RD	9.21	71.9	0.53	7.04	70.6	0.50
RD + PD	7.97	71.3	0.51	6.16	75.0	0.42
PD + F	9.00	69.6	0.52	8.71	68.2	0.53
RD + F	7.73	69.8	0.49	5.04	74.1	0.40
F + PD + RD	9.53	64.9	0.55	5.69	72.3	0.42
CT	9.51	69.5	0.55	6.57	74.0	0.44
Mean	8.05	70.9	0.50	6.63	72.4	0.45
LSD (0.05)	NS	6.2	NS	NS	6.2	NS
Non-Sawah × Sawah WSA > 2.00 mm				NS		
Non-Sawah × Sawah WSA < 0.25 mm				NS		
Non-Sawah × Sawah MWD				NS		
	2nd Year					
F	15.9	60.5	0.80	9.13	67.7	0.58
PD	14.4	59.2	0.82	13.5	64.6	0.71
RD	11.9	60.5	0.70	10.7	68.9	0.58
RD + PD	14.8	60.3	0.76	9.0	68.2	0.55
PD + F	15.6	56.6	0.83	8.4	67.1	0.54
RD + F	11.4	60.9	0.66	8.8	66.3	0.55
F + PD + RD	11.8	59.4	0.67	8.8	67.7	0.54
CT	13.7	61.9	0.72	9.8	66.9	0.59
Mean	13.69	59.9	0.75	9.97	67.2	0.58
LSD (0.05)	4.86	5.78	0.18	4.86	5.78	0.18
Non-Sawah × Sawah WSA > 2.00 mm				3.64		
Non-Sawah × Sawah WSA < 0.25 mm				4.2		
Non-Sawah × Sawah MWD				0.10		

NS = non-significant

Table 6. Effect of sawah system and amendments on Dispersion ratio (DR) and saturated hydraulic conductivity (*Ks*) of 0-20 cm top soil.

Amendments	1st Year			
	Non Sawah		Sawah	
	DR	*Ks* (cm/h)	DR	*Ks* (cm/h)
F	0.47	5.07	0.66	7.61
PD	0.61	5.34	0.42	12.9
RD	0.72	15.1	0.67	21.5
RD + PD	0.67	3.43	0.78	12.7
PD + F	0.80	21.3	0.70	4.80
RD + F	0.73	14.9	0.65	11.6
F + PD + RD	0.66	20.8	0.79	11.7
CT	0.74	6.6	0.62	10.9
Mean	0.68	11.6	0.66	11.7
LSD (0.05)	0.16	9.4	0.16	9.4
Non Sawah × Sawah DR		NS		
Non Sawah × Sawah *Ks*		NS		
	2nd Year			
F	0.63	6.16	0.41	10.8
PD	0.78	8.18	0.58	14.6
RD	0.86	19.0	0.65	25.7
RD + PD	0.87	6.36	0.67	14.4
PD + F	0.82	22.8	0.69	9.89
RD + F	0.81	15.6	0.35	13.5
F + PD + RD	0.74	24.14	0.49	19.3
CT	0.76	7.29	0.76	12.6
Mean	0.78	13.7	0.58	15.1
LSD (0.05)	0.18	9.6	0.18	9.6
Non Sawah × Sawah DR		0.18		
Non Sawah × Sawah *Ks*		NS		

NS = non-significant

wilting point (WP) (**Table 7**). Also in the first year total porosity positively correlated with FC and WP, while FC positively correlated with saturated hydraulic conductivity (*Ks*) (r = 0.44*). Again the WP positively correlated significantly with *Ks* (r = 0.47*). The levels of significant correlation within the WSA are shown. However, the dispersion ratio (DR) positively correlated significantly with MWD (r = 0.43*).

In the second year the significant negative correlation between bulk density, FC and WP were also obtained (**Table 7**). Positive significant correlations were also obtained between the total porosity, FC and WP thus indicating the importance of soil moisture contents in the formation of soil structure generally and these soils in particular. Also trend of correlations found between the positively with MWD (r = 0.52*) When all the results obtained for the two years were WSA in the first year also repeated in the second year. Again the dispersion ratio (DR) significantly correlated combined the relationships among the soil properties took a different shape. In these combined results soil organic carbon assumed a different role than the ones obtained for individual years. **Table 7** also shows the correlation matrix for the years combined. Soil organic carbon (OC) negatively correlated with bulk density (r = –0.40*) and WSA < 0.25 mm (r = –0.49*). OC also positively correlated significantly with total porosity, WSA > 2.00 mm, MWD and saturated hydraulic conductivity (*Ks*). The implication of these is that the overall effect of OC can be viewed from its cumulative contribution rather than the immediate action. In a degraded Ultisol in southeastern Nigeria. Mbagwu (1992) highlighted the roles of organic amendments in improving the soil structure and perhaps the fertility supply. As in the individual years the bulk density significantly correlated negatively with FC and WP while Ks positively correlated significantly with FC (r = 0.34*) and WP (r = 0.31*). This result showed that the moisture contents of the soil to a large extent control the *Ks* which in addition are a function of the soil bulk density.

As a result of the importance of bulk density as a soil structural index, it was subjected further to regression analyses aimed at determining the properties determined that influenced it most. The correlation coefficients that were high were selected for this analysis. The results for the first year, second year and the two years combined are presented (**Table 8**). In the first year the moisture contents at FC and WP explained about 81% of the variation in bulk density while individually WP explained 78% and FC 67% of the variation in bulk density. It follows that both FC and WP could be used to predict or estimate the bulk density of this soil. During the second year the R^2 for FC and WP were not as high as in the first year with both FC and WP explaining 45% or less of the variability in bulk density. An analyses of DR in the second year as a determinant of degradation showed that the properties that had correlated significantly with gave low R^2 values (**Table 8**). In the combined years (**Table 8**), both FC and WP jointly explained about 61% of the variation in bulk density. Individually FC and WP explained 56% and 61% respectively of the variation in bulk density of the soils. The contribution of WP in this cumulative determination may be linked to other factors such as clay contents and other intrinsic chemical prop-

Table 7. Correlation coefficients matrix of soil physical properties.

				1st Year	N = 16					
	OC	BD	TP	FC	WP	WSA1	WSA2	MWD	DR	*Ks*
OC	—									
BD	–0.28	–								
TP	0.27	–0.98*	–							
FC	0.16	–0.82*	0.81*	–						
WP	0.16	0-05	0.87*	0.97*	–					
WSA1	0.38	–0.88*	–0.08	0.04	0.02	–				
WSA2	–0.20	–0.13	0.15	0.07	0.04	–0.80*	–			
MWD	0.38	–0.01	–0.03	0.05	0.06	0.97*	–0.85*	–		
DR	0.20	0.13	–0.15	–0.13	–0.10	0.45*	–0.42*	0.43*	–	
Ks	0.25	–0.37	0.34	0.44*	0.47*	0.23	–0.37	0.26	0.27	-
				2nd Year	N = 16					
OC	–									
BD	–0.31	–								
TP	0.35	–0.99*	–							
FC	0.13	–0.78*	0.75*	–						
WP	0.26	–0.78*	0.76*	0.93*	–					
WSA1	–0.23	0.18	-0.15	0.02	–0.22	–				
WSA2	0.24	–0.24	0.24	0.02	0.31	–0.77*	–			
MWD	–0.21	0.20	–0.17	0.01	–0.21	0.99*	–0.81*	–		
DR	0.09	0.23	–0.26	–0.18	–0.32	0.53*	–0.64*	0.52*	–	
Ks	0.12	–0.11	0.08	0.14	0.09	–0.25	0.14	–0.30	–0.04	–
					All Years Combined		N = 32			
OC	–									
BD	–0.40*	–								
TP	0.36*	–0.99*	–							
FC	0.14	–0.77*	0.75*	–						
WP	0.22	–0.81*	0.79*	0-95*	–					
WSA1	0.54*	–0.13	0.12	0.08	0.03	–				
WSA2	–0.49	0.09	–0.08	–0.02	–0.01	–0.91*	–			
MWD	0.54*	–0.14	0.14	0.05	0.04	0.98*	–0.95*	–		
DR	0.16	0.14	–0.14	–0.13	–0.21	0.39*	–0.37*	0.33*	–	
Ks	0.31*	–0.33*	0.30	0.34*	0.31*	0.21	–0.23	0.18	0.16	–

OC = organic carbon; BD = bulk density; TP = total porosity; FC = field capacity; WP = wilting point; WSA1& 2 = WSA > 2.00, < 0.25 mm respectively: DR = dispersion ratio; Ks hydraulic conductivity; *Significant at p > 0.05

Table 8. Linear regression relationships between bulk density, dispersion ratio and other physical properties.

Regression Equation	R^2	SE
1st Year		
BD = 1.796 – 0.014FC	0.67	0.062
BD = 1.65 – 0.028WP	0.78	0.051
BD = 1.50 + 0.013FC – 0.05WP	0.81	0.049
2nd Year		
BD = 1.48 – 0.02WP	0.44	0.07
BD = 1.61 – 0.01FC	0.45	0.065
BD = 1.56 – 0.006FC – 0.006WP	0.45	0.07
DR = 0.24 + 0.66MWD	0.24	0.14
DR = 2.26 – 0.03WSA < 0.25 mm	0.41	0.12
DR = 0.31 + 0.32WSA > 2.00 mm	0.28	0.14
DR = 2.98 + 0.06WSA > 2.00 mm – WSA < 0.25 mm – 1.49MWD	0.47	0.13
Two Years Combined		
BD = 1.57 – 0.022WP	0.61	0.061
BD = 1.71 – 0.012FC	0.56	0.065
BD = 1.54 + 0.002FC – 0.03WP	0.61	0.06

erties not determined.

4. Conclusions

The study revealed the following

1) *Sawah* managed soils reduced significantly the soil bulk density and thereby increasing the soil total porosity.

2) Well managed water regime can also on the long run improve the WP, water-stable aggregates and the MWD of the soils

3) In spite of the destruction of soil structure as a result of cultural practices during rice cultivation the DR is improved on the long run by *sawah* water management.

4) Moisture contents at FC and WP relates significantly with soil bulk density which also relates nega tively with total porosity. However, FC and WP may be very good tools in the estimation of bulk density. Again, the amendments were identified as promoting the development of soil aggregates and *Ks* on a long term. Arising from the study, a number of possible further researches have been suggested for the development of yield in water stress area in the sub-Saharan Africa and the comparison of pump water supply from lakes, rain fed and gravity irrigation from adjacent lakes or streams in rice cultivation.

5. References

[1] T. Wakatsuki, M. M. Buri and O. O. Fashola, "Ecological Engineering for Sustainable Rice Production and the Restoration of Degraded Watersheds in West Africa," *Proceedings of Rice Research Conference*, Bali, 12-14 September 2005, pp. 336-366.

[2] T. Wakatsuki and T. Masunaga, "Ecological Engineering for Sustainable Food Production of Degraded Watersheds in Tropics of Low pH Soils: Focus on West Africa," *Soil Science and Plant Nutrition*, Vol. 51, No. 5, 2005, pp. 629-636.

[3] J. S. C. Mbagwu, "The Agricultural Soils of Nigeria: Properties and Agronomic Significance for Increased Productivity," *Beitrage für Tropical Landwirtschaften und Veterinari Medizin*, Vol. 27, 1989, pp. 395-409.

[4] J. S .C. Mbagwu, "Improving the Productivity of a Degraded Ultisol in Nigeria Using Organic and Inorganic Amendments. Part 2: Changes in Physical Properties," *Bioresource Technology*, Vol. 42, No. 3, 1992, pp. 167-175.

[5] S. Hirose and T. Wakatsuki, "Restoration of Inland Valley Ecosystems in West Africa," Norin Tokei Kyokai, Tokoyo, 2002, p. 572.

[6] C. A. Igwe, "Erodibility of Soils of the Upper Rainforest Zone, Southeastern Nigeria," *Land degradation & Development*, Vol. 14, No. 3, 2003, pp. 323-334.

[7] C. A. Igwe, "Erodibility in Relation to Water-Dispersible clay for Some Soils of Eastern Nigeria," *Land degradation & Development*, Vol. 16, No. 1, 2005, pp. 87-96.

[8] R. Lal, "Soil Erosion Problems on Alfisols in Western Nigeria. VI. Effects of Erosion on Experimental Plots," *Geoderma*, Vol. 25, No. 3-4, 1981, pp. 215-230.

[9] J. S. C. Mbagwu, R. Lal and T. W. Scott, "Effects of Desurfacing Alfisols and Ultisols in Southern Nigeria. II. Changes in Soil Physical Properties," *Soil Science Society of America Journal*, Vol. 48, 1984, pp. 834-838.

[10] P. Rengasamy, R. S. B. Greene, G. W. Ford and A. H. Mehanni, "Identification of Dispersive Behaviour and Management of Red-Brown Earths," *Australian Journal of Soil Research*, Vol. 22, No. 4, 1984, pp. 413-431.

[11] P. C. Nnabude and J. S. C. Mbagwu, "Soil Water Rela-

tions of a Nigerian Typic Haplustult Amended with Fresh and Burnt Rice-Mill Wastes," *Soil & Tillage Research*, Vol. 50, No. 3-4, 1999, pp. 207-214.

[12] A. K. Makarim, D. K. Cassel and M. K. Wade, "Effect of Land Reclamation Practices on Chemical Properties of an Acid, Infertile Oxisol in Western Sumatra," *Soil Technology*, Vol. 2, 1989, pp. 27-39.

[13] D. K. Cassel, M. K. Wade and A. K. Makarim, "Crop Response to Management of a Degraded Oxisol Site in West Sumatra," *Soil Technology*, Vol. 3, No. 2, 1990, pp. 99- 112.

[14] J. C. Nwite, C. A. Igwe and T. Wakatsuki, "Evaluation of Sawah Rice Management System in an Inland Valley in Southeastern Nigeria. I: Soil Chemical Properties and Rice Yield," *Paddy and Water Environment*, Vol. 6, No. 3, 2008, pp. 299-307.

[15] S. S. Abe, T. Masunaga, S. Yamamoto, T. Honna and T. Wakatsuki, "Comprehensive Assessment of the Clay Mineralogical Composition of Lowland Soils in West Africa," *Soil Science and Plant Nutrition*, Vol. 52, No. 4, 2006, pp. 479-488.

[16] G. W. Gee and J. W. Bauder, "Particle-size Analysis," In: A. Klute Ed., *Methods of Soil Analysis*, Part 1, American Society of Agronomy, Madison, 1986, pp. 91-100.

[17] D. W. Nelson and L. E. Sommers, "Total Carbon, Organic Carbon and Organic Matter," In: A. L. Page, R. H. Miller, D. R. Keeney, Eds., *Methods of Soil Analysis*, Part 2, America Society of Agronomy, Madison, 1982, pp. 539-579.

[18] A. Klute and C. Dirksen, "Hydraulic Conductivity and Diffusivity," In: A. Klute, Ed., *Methods of Soil Analysis*, Part 1, American Society of Agronomy, Madison, 1986, pp. 694-783.

[19] G. R. Blake and K. H. Hartge, "Bulk Density," In: A. Klute, Ed., *Methods of Soil Analysis*, Part 1, American Society of Agronomy, Madison, 1986, pp 363-382.

[20] D. W. Kemper and R. C. Rosenau, "Aggregate Stability and Size Distribution," In: A. Klute, Ed., *Methods of Soil Analysis*, Part 1, American Society of Agronomy, Madison, 1986, pp. 425-442.

[21] C. A. Igwe, F. O. R. Akamigbo and J. S. C. Mbagwu, "Physical Properties of Soils of Southeastern Nigeria and the Role of Some Aggregating Agents in their Stability," *Soil Science*, Vol. 160, No. 6, 1995, pp. 431-441.

[22] N. H. Abu-Hamdeh, S. A. Abo-Qudais and A. M. Othman. "Effect of Soil Aggregate Size on Infiltration and Erosion Characteristics," *European Journal of Soil Science*, Vol. 57, No. 5, 2006, pp. 609-616.

J. Water Resource and Protection, **2010, 2, 619-628**
doi:10.4236/jwarp.2010.27071 Published Online July 2010 (http://www.SciRP.org/journal/jwarp)

Chesapeake Bay Tidal Characteristics

Yi Xiong[1], Charlie R. Berger[2]
[1]*Department of Civil and Environmental Engineering, Mississippi State University, Starkville, USA*
[2]*US Army Corps of Engineers, Coastal and Hydraulics Laboratory–ERDC, Vicksburg, USA*
E-mail: *xiongyiwv@yahoo.com*
Received January 23, 2010; *revised March* 19, 2010; *accepted May* 7, 2010

Abstract

The basic knowledge of tidal characteristics in Chesapeake Bay is a prerequisite to understand the tidal processes in Chesapeake Bay. The tidal characteristics in Chesapeake Bay were assessed in this paper using basic tidal hydraulic analysis. Tidal elevation, currents and salinity data of Chesapeake Bay from National Oceanic and Atmospheric Administration (NOAA) were retrieved, and analyzed to understand Chesapeake Bay tide. General knowledge of location, geometry, tides, freshwater inputs, wind, salinity, etc in Chesapeake Bay was described. Sediment distribution of Chesapeake Bay was briefly described and discussed. Amplitude and phase of the selected major constituent, form factor, phase difference between tide elevations and currents at a few tidal elevation stations within Chesapeake Bay were calculated. Tidal prism was figured out using cubature method. The analysis approach could also be used as a source of reference for basic tidal study in other tide-affected field.

Keywords: Chesapeake Bay, Tidal Characteristics

1. Introduction

Chesapeake Bay encountered a severe environmental suffering during past a few decades, due to nitrogen, phosphorus and sediment pollution. It has been recognized that environmental quality factors are directly dependent on the tides in the Bay [1].

Chesapeake Bay is the largest bay in US. The Chesapeake Bay and its tributaries are the best studied estuaries in the world [2]. The Chesapeake Bay "main stem", defined by tidal zones, is approximately 195 mi (315 km) long and 3.5 to 35 mi (5.6 to 56 km) wide, and has a surface area of nearly 4,400 mi^2 (11,601 km^2). The main stem is entirely within Maryland and Virginia. Nearly 50 rivers, with thousands of tributary streams and creeks, drain the approximately 64,000 mi^2 (166,000 km^2) forming the Chesapeake Bay Basin. The basin contains more than 150,000 stream miles (241,500 km) in the District of Columbia and parts of six states: New York, Pennsylvania, Maryland, Virginia, West Virginia, and Delaware [3]. **Figure 1** shows the location of Chesapeake Bay in accordance with "NOAA Tides and Currents". In addition, the fourteen tidal elevation stations and seven tidal current stations are indicated (see **Table 1** for details).

The Chesapeake estuary is a drowned river and it is partially mixed. The depths are relatively shallow, so that mixing of at least moderate magnitude extends to the depths. In the total estuary approximately 50% of the system is less than 20 ft (6 m) deep, 35% has depths greater than 30 ft (9 m), 18% greater than 40 ft (12 m), and only 8% greater than 60 ft (18.3 m) [2].

Tides and freshwater inputs from the various tributaries of the Chesapeake Bay control the hydraulics of the bay [1]. National Research Council (2004) mentioned that three main factors influencing Chesapeake Bay's circulation: freshwater inflow, the geometry of the basin, and tidal strength. Due to its small depth-length ratio, Chesapeake Bay accommodates slightly more than one semidiurnal tidal wave at all times, which results in a special tidal characteristics within Chesapeake Bay. Although the Bay has more than 50 tributary rivers, only 3 —the Susquehanna, Potomac, and James—account for more than 80% of the total freshwater input, with Susquehanna accounting for nearly half of the total (49%). All Eastern Shore Rivers combined contribute less than 4% of the total. In the average year, the total amount of freshwater discharged into the Bay (71 km^3 or 17 mi^3) is roughly equivalent to the tidal mean volume of the Chesapeake Bay estuarine system (76 km^3 or 18 mi^3) – the combined volume of the Bay proper and its tributary estuaries. The flows of the Bay's major rivers are typical of mid-latitude rivers: high discharges in spring, pro-

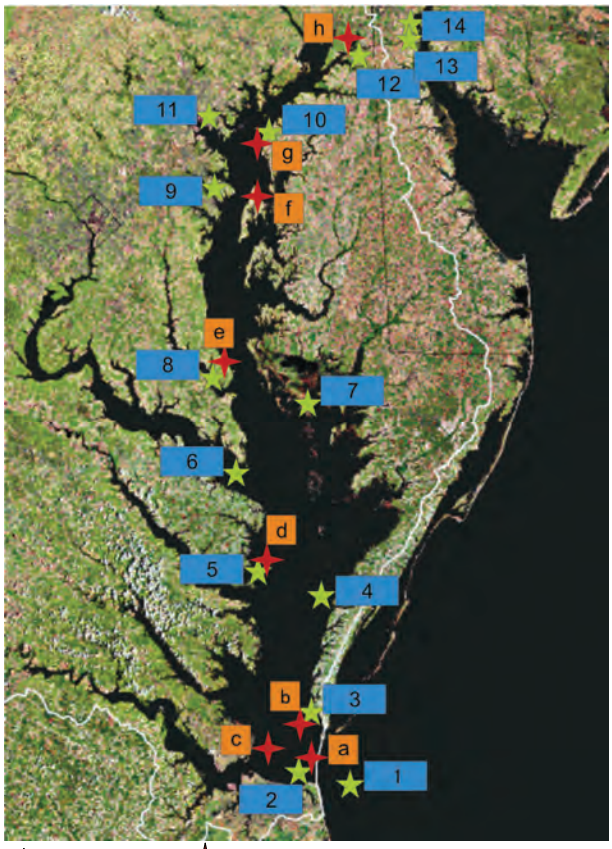

Figure 1. Chesapeake bay map.

duced by snow melt and spring rains; low flows in late summer and early fall, followed by moderate flows through-out the remainder of the year [4]. Fresh water in Chesapeake Bay has a mean residence time of 7 months [5].

Wind is also reported as an important energy input in Chesapeake Bay. Zhong and Li [6] proposed that tidal and wind forcing appears to have nearly equal importance in Chesapeake Bay. Chesapeake Bay is classified as a partially–stratified estuary [7].

The main channel is of 5 to 7 km (4.4 mi) width and 23 m (75 ft) depth at the mouth of the Chesapeake Bay [8]. Bathymetries in the Upper Chesapeake Bay are characterized by a steep east-west slope and a relatively gentle north-south slope. A narrow and deep navigation channel exceeding 9 m (30 ft) follows the contour of the eastern coast, bounded to the west by broad banks [9]. The Chesapeake & Delaware Canal runs 14 miles long, 450 feet wide and 35 feet deep across Maryland and Delaware, connecting the Delaware River with the Chesapeake Bay and the Port of Baltimore. The C&D Canal is owned and operated by the U.S. Army Corps of Engineers, Philadelphia District.

The mean tidal range decreases from 0.9 m (3 ft) at the Bay's entrance (Chesapeake BBT) to a minimum of 0.3 m (1.0 ft) at Annapolis, then rises to 0.7 m (2.3 ft) at the head. Average tidal current amplitudes decrease from a maximum of 1.03 m/s (3.38 ft/s) at the mouth to a minimum of 0.13 m/s (0.43 ft/s) in the middle Bay, but increase to 0.59 m/s (1.94 ft/s) at Baltimore in the upper Bay [6].

The tidal and current range on the eastern shore is generally higher than that on the corresponding western shore, which is mostly explained as the result of earth rotation. However, Wang and Chao [9] proposed that the deep channel is the root cause of the current intensification, while the earth's rotation does not play a crucial role.

The salinity increases from zero at the head of the estuary to nearly that of seawater at the mouth. In the upper Chesapeake Bay and in each tributary estuary there are considerable seasonal variations in salinity which diminish in magnitude in magnitude toward the mouths of these estuaries [2].

Figures 2 and **3** are one-month and three-day tides at Chesapeake Light (8638979), respectively. These two plots reveal that the tide is predominantly driven by semidiurnal constituent. The magnitudes of Spring and Neap tide ranges are approximately 1.7 m (5.6 ft) and 0.7 m (2.3 ft), respectively, as shown in **Figure 2**. Also, the mean tide range is around 1.2 m (3.9 ft).

The understanding of tidal characteristics is the premise to learn tidal and sediment transport processes in estuarine areas. Investigation on hydrodynamic environment of the bay is in favor of comprehending pollutant transport and mechanism of deep water zone maintaining [10]. Therefore, it is desirable to perform a general basic tidal study in Chesapeake Bay in order to further understand the tidal characteristic in Chesapeake Bay. In addition, the basic tidal analysis approaches can be optionally used in other estuaries.

2. Tidal Characteristics within Chesapeake Bay

2.1. Stations and General Issues

Table 1 lists the tidal stations (See **Figure 1** for the locations) and **Table 2** describes their tidal characteristics. M_2 constituent is obviously the dominant constituent with the next largest constituent being an order of magnitude less in amplitude. Annapolis has the lowest M_2 tidal elevation, while the higher tide occurs at both the entrance of the Bay and the C&D Canal. Also, the tide on eastern shore has the higher amplitude than that on western shore. In addition, Salas-Monreal and Valle-Levinson [11] provided the mean depths of transects through a few stations.

Table 1. Tidal characteristics at water elevation stations.

Station	Station ID	Latitude (N)	Latitude (W)	location
Chesapeake Light Tower	8638979	36°54.3′	75°41.8′	Ocean
Chesapeake BBT	8638863	36°58.0′	76°6.8′	
Kiptopeke	8632200	37°9.9′	75°59.3′	Lower bay
Rappahammock Light	8632837	37°32.3′	76°0.9′	
Windmill Point	8636580	37°36.9′	76°17.4′	
Lewisetta	8635750	37°59.8′	76°27.9′	
Bishops Head	8571421	38°13.2′	76°2.3′	Mid bay
Solomons Isand	8577330	38°19.0′	76°27.1′	
Annapolis	8575512	38°59.0′	76°28.9′	
1tolchester Beach	8573364	39°12.8′	76°14.7′	Upper bay
Baltimore**	8574680	39°16.0′	76°34.7′	
Chesapeake City	8573927	39°31.6′	75°48.6′	
Reedy Point	8551910	39°33.5′	75°34.4′	C&d canal
Delaware City	8551762	39°34.9′	75°35.3′	

Note: * For C&D canal tide analysis only; ** For salinity discussion only

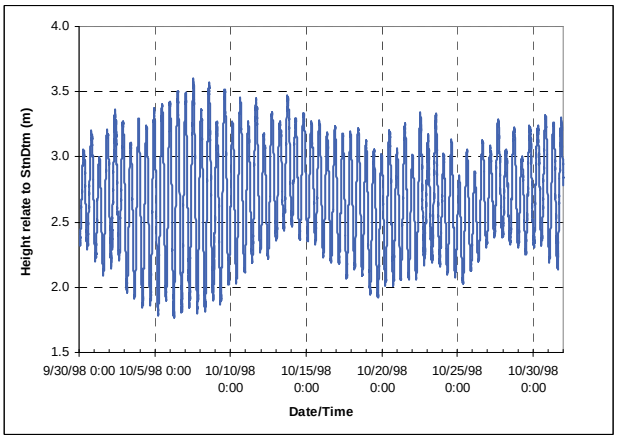

Figure 2. One-month ocean tide at chesapeake light.

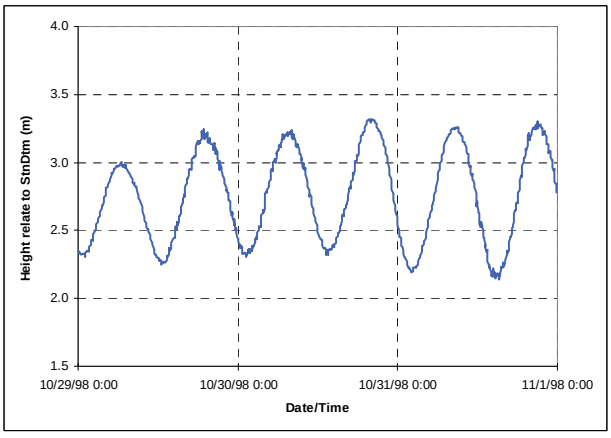

Figure 3. Three-day ocean tide at chesapeake light.

Table 3 gives the Chesapeake Bay current stations from Chesapeake Bay Port (See **Figure 1** for the locations).

The relative importance of the diurnal and semidiurnal tidal constituents and tide classification can be expressed in terms of form factor as shown in **Table 2** [12], which is defined as,

$$F = \frac{K_1 + O_1}{M_2 + S_2}$$

where K_1, O_1, M_2, and S_2 are the amplitudes of the corresponding tidal constituents. In terms of the form factor, F, the tides may be roughly classified as shown in **Table 4**.

The calculated form factors reveal that semidiurnal tide is almost throughout Chesapeake Bay except for the standing wave in three upper Bay stations (Annapolis, Tolchester Beach, and Baltimore) with higher latitudes.

The natural fundamental period T_n can be calculated as below,

$$T_n = \frac{2s}{\sqrt{g\bar{h}}}$$

where s is the length of Chesapeake Bay, 320 km; g is the gravity acceleration, 9.81m/s^2, $\bar{h}$ is the mean depth of Chesapeake Bay, 5 m [13]. The calculated natural fundamental period T_n, 25.38 hours, is closer to the diurnal tidal period, thus, amplification of diurnal tide could be observed. In accordance with Schwartz [14], the diurnal tide could be amplified at near the semidiurnal nodal area where semidiurnal tide range is small (see **Figure 4**). In accordance with **Figure 4**, Windmill Point is located near the semidiurnal nodal area, around –230 km (–149 mi) from the upstream end. The form factor at Windmill Point, representing mixed mainly semidiurnal tide, is slightly higher than those at adjacent stations with semidiurnal tide as shown in **Table 2**. Consequently, approximate nodal area locations of Windmill Point might be a reason for the observed a little bit amplification of diurnal signal at Windmill Point. Referring to Huang *et al*. [9], as Rappahammock Light and Bishop Head have higher M_4/M_2 than other stations within Chesapeake Bay, shallower tidal wave would be assumed at these two locations. Therefore, more attentions might have to be paid to there due to probable significant sediment transport processes around these two stations.

Figure 4 is the calculated M_2 tidal amplitudes in Chesapeake Bay with friction by superposition of the incident and reflective waves. The friction is represented by an exponential function [15]—$\exp(-\mu x)$ (μ is the amplitude damping coefficient; x is the travel distance starting from the mouth of the Bay, m). Then, the super

Table 2. Tidal characteristics at water elevation stations.

Station	Depth(m)	Amplitude of Constituents (m)							Form Factor
		M2	S2	K1	O1	M4	M6	M8	
Chesapeake Light Tower	18.30								
Chesapeake BBT	9.14	0.380	0.069	0.058	0.045	0.005	0.006	0.000	0.229
Kiptopeke	7.70	0.388	0.068	0.059	0.046	0.005	0.005	0.000	0.230
Rappahammock Light		0.239	0.034	0.041	0.030	0.014	0.005	0.000	0.260
Windmill Point		0.175	0.030	0.030	0.023	0.009	0.003	0.000	0.259
Lewisetta	8.50	0.184	0.028	0.023	0.019	0.004	0.003	0.000	0.198
Bishops Head		0.267	0.033	0.042	0.029	0.018	0.002	0.001	0.237
Solomons Island	15.00	0.171	0.026	0.027	0.023	0.005	0.003	0.000	0.254
Annapolis		0.139	0.022	0.059	0.048	0.004	0.003	0.000	0.665
Tolchester Beach	5.30	0.174	0.024	0.069	0.058	0.004	0.000	0.000	0.641
Baltimore**		0.159	0.023	0.069	0.056	0.008	0.000	0.000	0.687
Chesapeake City		0.434	0.059	0.032	0.014	0.026	0.009	0.003	0.093
Reedy Point		0.773	0.100	0.089	0.068	0.055	0.033	0.007	0.180
Delaware City		0.744	0.100	0.095	0.068	0.060	0.033	0.006	0.193

Note: * For C&D canal tide analysis only; ** For salinity discussion only The depths data at the stations are excerpted from Salas-Monreal and Valle-Levinson (2008).

Table 3. Chesapeake bay current stations.

Station	Station ID	Location
a. Cape Henry LB '2CH'	cb0102	Lower Bay
b. York Spit LBB 22	cb0201	
c. Thimble Shoal LB '18'	cb0301	
d. Rappahannock Shoal Channel LBB '60'	cb0801	Mid Bay
e. Cove Point LNG Pier	cb1001	
f. Chesapeake Channel LBB '92'	cb1101	Upper Bay
g. Tolchester Front Range	cb1201	
h. Chesapeake City	cb1301	C&D Canal

Table 4. Tide classification.

Form Factor, F	Types of Tide
0~0.25	Semidiurnal
0.25~1.50	Mixed Mainly Semidiurnal
1.50~3.00	Mixed Mainly Diurnal
>3.00	Diurnal

position of the incident and reflective waves can be expressed as,

$$\eta(t,x) = a_{M_2}\cos(\sigma t - kx)$$
$$= A\{\exp(-\mu(s+x))\cos(\sigma t - kx) + \exp(-\mu(s-x))\cos(\sigma t + kx)\}$$

where $\eta(t,x)$ is water surface profile for the integrated wave, m; a_{M2} is the M_2 constituent amplitude, m, A is the M_2 constituent amplitude of the progressive wave at the entrance, m; K is wave number, m^{-1}; σ is wave angular frequency, s^{-1}. Therefore, the M_2 constituent amplitude within Chesapeake Bay is,

$$a_{M2} = A\{\exp(-\mu(s+x)) + \exp(-\mu(s-x))\cos 2kx\}$$

Both the M_2 constituent amplitudes at CBBT (0.380 m at –320 km) and Tolchester Beach (0.174 m at –40 km) are used to figure out the damping coefficient, $\mu = 1.65 \times 10^{-6}$, which adjusts the amplitudes of both incident and reflective waves along the travel distance. Similar to Boon [13], **Figure 4** represent that two minimum tidal amplitudes occur at around –80 km (–50 mi) and –230 km (–143 mi) from the upstream end, which approximately corresponding to somewhere close to Annapolis and Windmill Point, respectively. The amplitudes at both Windmill Point and Annapolis are relative low comparing with other stations, which matches the result as shown in **Figure 4**. Because of friction and energy dissipation, the amplitude at the upper Bay is generally lower even with the effect of reflection in accordance with **Table 2** and **Figure 4**, although the M_2 constituent amplitude at upper Bay might be overestimated in **Figure 4** due to the assumed constant damping coefficient, μ. In brief, there are two areas with lower M_2 constituent amplitude, and a generally decrease of the amplitude of the dominant M_2 constituents, as tide moves upstream. Standing wave characteristics and narrowness at Chesapeake City result in higher M_2 tide there.

Figure 5 depicts the 3-day salinity at three stations,

and the salinity decreases gradually from the mouth (~22 ppt at CBBT) up to the upper Chesapeake Bay (~6 ppt at Baltimore). The salinity at CBBT is more sensitive to the tidal elevation, while the salinities at Lewisetta and Baltimore are almost constant in this short time period. The peak salinity at CBBT is in response to the water surface elevation to some extent in accordance with **Figure 5**.

For this partially mixing Bay, seasonal-varied freshwater flow might be most influencing factor affecting salinity distribution in Chesapeake Bay.

The deep channel, along with earth rotation and freshwater effects (due to predominant freshwater from Western Shore), might make a lower salinity on western shore. Stronger stratification could be observed at upper end with lower tidal velocity. Vertical stratification is not discussed in detail for data deficiency.

In recent decades, Chesapeake Bay has had widespread water quality problems due to fine sediment. Sediment distribution is usually dominated by hydraulic condition and material origin [10]. Tidal current, freshwater, wind, etc could be the factors affecting the process of sediment transport and the distribution of sediment. Without considering freshwater input, **Table 5** shows the calculated near bed velocity amplitude of tidal stations based on dominant M_2 constituent. The near bed velocity amplitude can be expressed as

$$V_b = \frac{a_{M_2} gk}{\sigma} \frac{1}{\cosh(kh)}$$

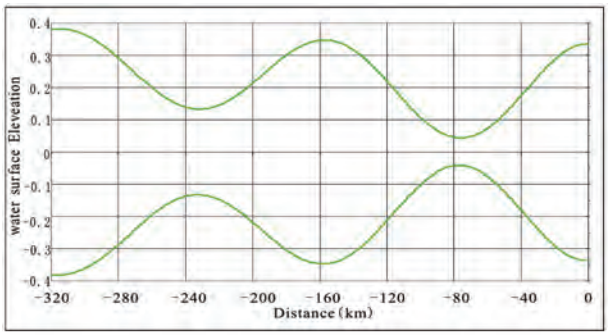

Figure 4. Calculated M_2 constituent tidal amplitudes in chesapeake bay with friction.

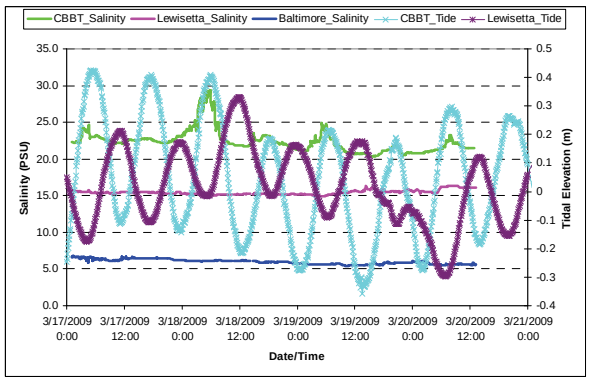

Figure 5. Salinity in chesapeake bay

where V is near bed velocity amplitude at the location of the station, m/s; h is water depth, m. The higher the velocity amplitude, the more important the sediment process at the station. In accordance with the criteria, the sediment process at both lower Bay and C&D Canal is significant. **Table 5** also depicts that velocity amplitude at the bed on the eastern shore is generally higher than that on the corresponding western shore due to the higher amplitude of M_2 constituent. Therefore, the gradient of bottom shear stress from eastern shore to western shore could be assumed for a general sediment transport estimate.

Freshwater brings great amount of fine sediment, while the force resulting from freshwater flow is in both local scale and lower magnitude. Therefore, tidal force could be more important in the general sediment transport and re-distribution at Chesapeake Bay. Tidal current dominate the process of sediment transport, controlling the distribution of sediment and development of seabed [10]. The long-term annual average of suspended material contributed by the Chesapeake Bay basins is approximately 4.3 million tons per year. About 90 percent of this material came from the three largest rivers (Susquehanna, Potomac, and James). It was assumed that the great majority of the sediment supplied from the freshwater flow is fine-grained silts and clays [3]. More fine sediment is supposed to be accumulated at western shore, as freshwater inflows are located mostly close to western shore.

Consequently, differentiating sediment transport & distribution in western shore from that in eastern shore is necessary in both water quality modeling and the following restoration practice.

Sediment distribution along the length of Chesapeake Bay is even more elusive due to complex interactions among tide, freshwater input, wind, bathymetry, etc. Data indicated that the greatest sediment volume is associated with the bay mouth, which further suggests that the continental shelf has been more significant source of sediment to the Bay with high tidal velocity (see **Table 5**) than the Susquehanna River and other watershed tributaries [3]. Although sand is the predominant sediment type in the lower Bay, part is composed of clay and silt-sized material and there also is good evident for its significant net up estuary transport [3]. Therefore, a quantification of northward Bay fine sediment transport determines the water quality in both lower Bay and other tidal-affected area. In another word, controlling the fine sediment movement in lower Bay could be an important step to improve water quality in the Bay.

2.2. Tide at Entrance (Chesapeake BBT)

Corresponding to the Spring and Neap tidal variations Tide range varies between 0.5 m (1.6 ft) and 1.0 m (3.3 ft)

at the entrance of Chesapeake Bay (See **Figure 6**).

2.3. Tidal Currents

Figure 7 shows the general currents within Chesapeake Bay at current stations as shown in **Figure 1**. Not solely related to the tidal elevation, the magnitude of current at each station is affected but multi-factors such as cross area, freshwater flow, etc. Phase difference is noticed in accordance with **Figure 7**. Although there is no observed data at current station cb1001, which is close to narrowing Solomons Island, higher velocity could be the fact at this station for the smaller cross section.

Figure 8 shows both the tidal elevation at Chesapeake BBT and current at cb0102. Since cb0102 is rather close to Chesapeake BBT, so the current at cb0102 could be approximately used for Chesapeake BBT. Generally, not much phase difference is observed between the tide and current, which matches the result of in-phase generated by Whitford [8]. However, wind might be the primary reason for the discrepancy during 03/18/2009 12:00—03/19/2009 06:00.

Excluding the effect of wind, **Figure 9** depicts tidal elevation at Chesapeake BBT, currents at both cb0102 and cb0301 during the period of 09/21/2008 16:00—09/22/2008 13:00 (wind speed is nearly zero). An approximate in-phase result is observed in **Figure 9**, which matches the accepted mainly progressive wave at the entrance.

The characteristics of mainly standing waves are obviously observed at both Annapolis and Tolchester Beach as shown in **Figures 10** and **11**, respectively. Lower tidal velocity occurs at Tolchester Beach with the standing wave.

In accordance with **Figures 10** and **11**, more saw-toothed pattern tides in upper Bay indicate more upland tides.

2.4. Phase Aspect of the Tide Elevation in Chesapeake Bay

NOAA Predicted tidal elevations at 9 stations within Chesapeake Bay are shown in **Figure 12**. The changes of the tidal amplitudes are observed along the main channel seem to be a consequence of the interaction between the tide and the Bay morphology as well as the wave reflection, and are described by the law of energy conservation [16]. It is observed that the whole bay experienced a low tide on January, 9, 2009. Comparing the tidal phase lag for M_2 constituent from the entrance against the plots in **Figure 12**, it is not dif ficult to find that they are in good agreement.

Table 6 lists the tidal phase lag from the entrance (Chesapeake BBT) in terms of the dominated M_2 constituent. **Table 7** lists the tidal phase lag from the entrance (Chesapeake BBT) in terms of the K_1 constituent. The region from Chesapeake BBT to Lewisetta is more like a progressive wave region. However, there is a narrowing of the channel around Solomons Island, and there is only around half hour lag for M_2 and two and half hours for K_1. Therefore, a standing wave is indicated and the tide is likely to be amplified around Solomon Island.

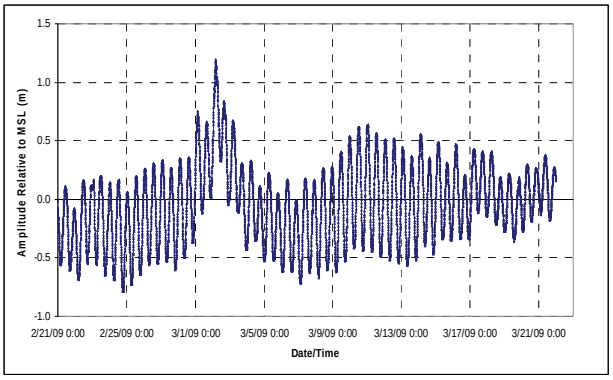

Figure 6. Observed spring and neap tide cycle at entrance (chesapeake BBT).

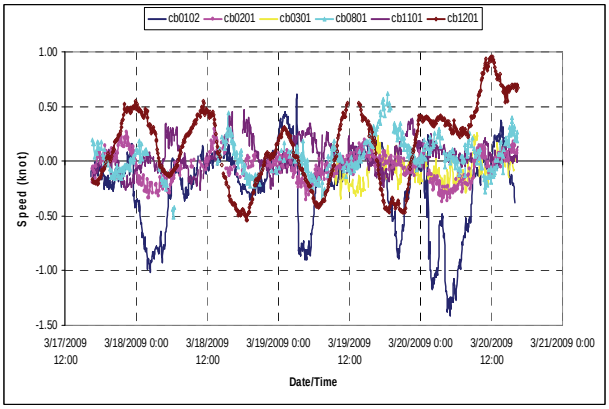

Figure 7. Observed tidal currents within chesapeake bay.

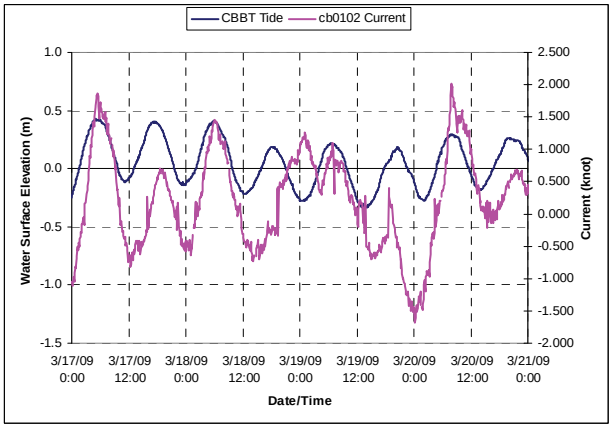

Figure 8. Tide and current at the entrance with wind effect (chesapeake BBT).

2.5. Tide Prism

Cubature method is employed to calculate the tidal prism (03/18/2009) of Chesapeake Bay in accordance with the tide on 03/18/2009 in **Figure 12**. The identification of subareas is shown in **Figure 13**, and the tidal prism is calculated as shown in **Table 8**.

The tidal prism is about for M_2 constituent is around 1.25×10^9 m^3 (4.41×10^{10} ft^3) as shown in **Table 8**. Freshwater flow is around 4,250 m^3/s (150,000 ft^3/s) in March in accordance with USGS.

Table 5. Near bed velocity amplitude of tidal stations based on M_2.

Station	Depth (m)	Amplitude of Constituent M_2 (m)	Near Bed Velocity Amplitude Vb (m/s)
Chesapeake Light Tower	18.30		
Chesapeake BBT	9.14	0.380	0.394
Kiptopeke	7.70	0.388	0.438
Rappahammock Light [@]	**8.00**	0.239	0.265
Windmill Point [@]	**8.00**	0.175	0.194
Lewisetta	8.50	0.184	0.198
Bishops Head [@]	**8.00**	0.267	0.296
Solomons Island	15.00	0.171	0.138
Annapolis [@]	**6.00**	0.139	0.178
Tolchester Beach	5.30	0.174	0.237
Baltimore ** [@]	**5.00**	0.159	0.223
Chesapeake City *	10.00	0.434	0.430
Reedy Point *	10.00	0.773	0.766
Delaware City *	10.00	0.744	0.737

Note: [@] Depth Data are assumed with uncertainty

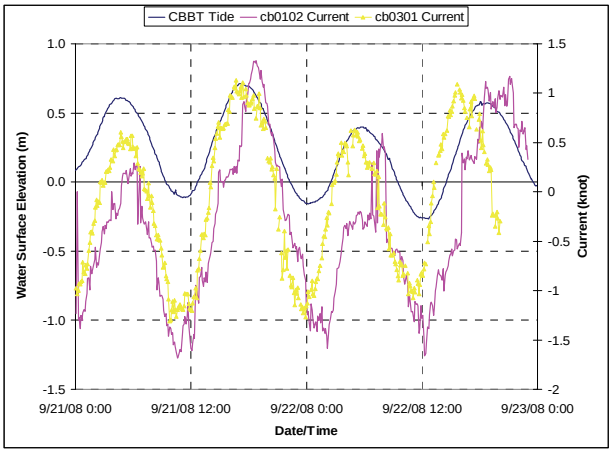

Figure 9. Tide and current at the entrance (chesapeake BBT).

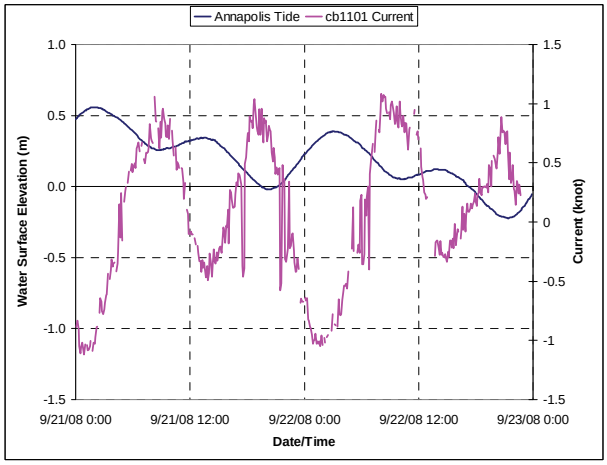

Figure 10. Tide and current at annapolis.

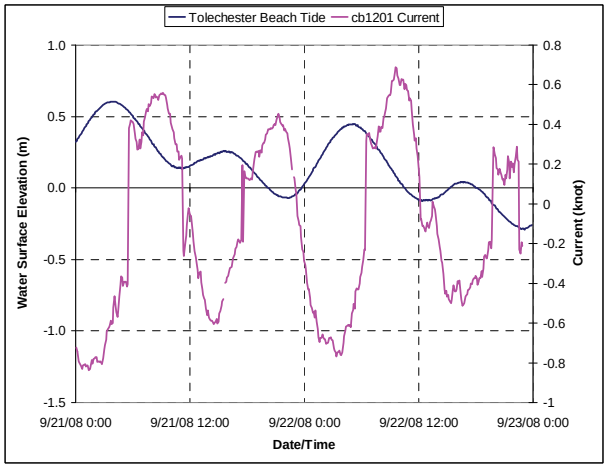

Figure 11. Tide and current at tolchester beach.

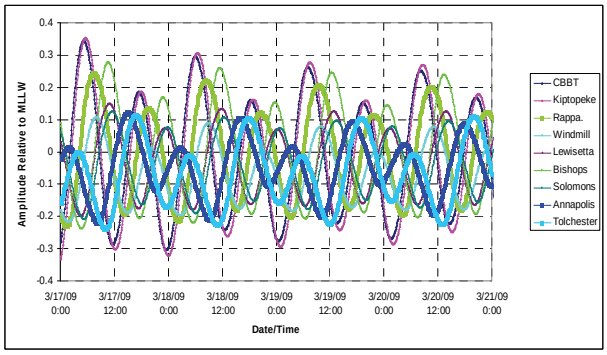

Figure 12. Predicted tides elevations within chesapeake bay.

Therefore, freshwater volume in 12.42 hours is 1.90×10^8 m^3 (6.71×10^9 ft^3) approximately. Consequently, the Canter Cremer Estuary Number can be figured out as N = 0.15, which shows that the Chesapeake Bay is partially mixed as N > 0.10 in this specific time period. Consequently, the tidal prism formula [17] in terms of M_2 constituent gives a lower limit of flushing time of 3.2 days.

Table 6. Tidal phase lag for M_2 from the entrance (chesapeake BBT).

Station	Station ID	Types of Tide	Epoch (˚)	Phase Lag From Entrance in (degree ˚)	Phase Lag From Entrance in hour
Chesapeake BBT	8638863	Semi-diurnal	21.0	0.0	0.00
Kiptopeke	8632200		32.5	11.5	0.40
Rappahammock Light	8632837	Mixed Mainly	86.8	65.8	2.27
Windmill Point	8636580	Semi-diurnal	103.2	82.2	2.84
Lewisetta	8635750	Semi-diurnal	176.4	155.4	5.36
Bishops Head	8571421		181.9	160.9	5.55
Solomons Island	8577330	Mixed Mainly	198.8	177.8	6.13
Annapolis	8575512	Semi-diurnal	291.6	270.6	9.34
Tolchester Beach	8573364		346.6	325.6	11.23

Table 7. Tidal phase lag for K_1 from the entrance (chesapeake BBT).

Station	Station ID	Types of Tide	Epoch (˚)	Phase Lag From Entrance in (degree ˚)	Phase Lag From Entrance in hour
Chesapeake BBT	8638863	Semidiurnal	184.9	0	0.00
Kiptopeke	8632200		193.4	8.5	0.57
Rappahammock Light	8632837	Mixed Mainly	222.4	37.5	2.49
Windmill Point	8636580	Semidiurnal	226.7	41.8	2.78
Lewisetta	8635750	Semidiurnal	276.2	91.3	6.07
Bishops Head	8571421		283.3	98.4	6.54
Solomons Island	8577330	Mixed Mainly	315.6	130.7	8.69
Annapolis	8575512	Semidiurnal	356.7	171.8	11.42
Tolchester Beach	8573364		3.3	178.4	11.86

2.6. C&D Canal Analysis

The Canal could be regarded as open to Chesapeake Bay (Left end open). **Figure 14** shows the observed tidal elevations at Chesapeake City and Reedy Point located on C&D Canal. M_2 constituent is the dominant constituent at both these two stations in accordance with **Table 2**. Consequently, information on the progressive wave in C&D Canal is summarized in **Table 9**. Ideally, the tidal elevation at Chesapeake City would be nearly zero for its location on node, and the standing waves at both stations are in phase. However, some distortions on both amplitude and phase occur due to the imperfect reflection resulting from Upper Chesapeake Bay's morphology.

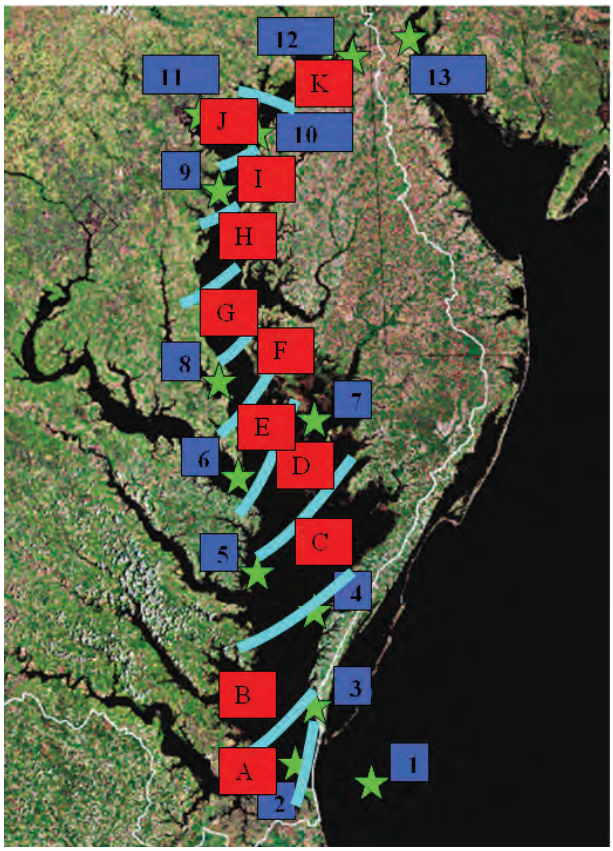

Figure 13. Subarea map

Table 8. Tidal prism calculation using cubature method

Subarea	Area Fraction	Phase Range Contour 1	Phase Range Contour 2	Phase Range	Volume Entering or Leaving (km^3)
A	0.10	0.61	0.62	0.62	0.71
B	0.12	0.62	0.17	0.40	0.55
C	0.16	0.17	0.06	0.12	0.21
D	0.12	0.06	-0.14	-0.04	-0.06
E	0.12	-0.14	-0.08	-0.11	-0.15
F	0.08	-0.08	-0.26	-0.17	-0.16
G	0.06	-0.26	-0.15	-0.21	-0.14
H	0.06	-0.15	-0.04	-0.10	-0.07
I	0.06	-0.04	0.05	0.01	0.00
J	0.06	0.30	0.15	0.23	0.16
K	0.06	0.35	0.18	0.27	0.18
		Tidal Prism			1.25

Figure 15 represents that an approximate 90º phase difference exists between tidal elevation and current at Chesapeake City due to the effect of standing wave.

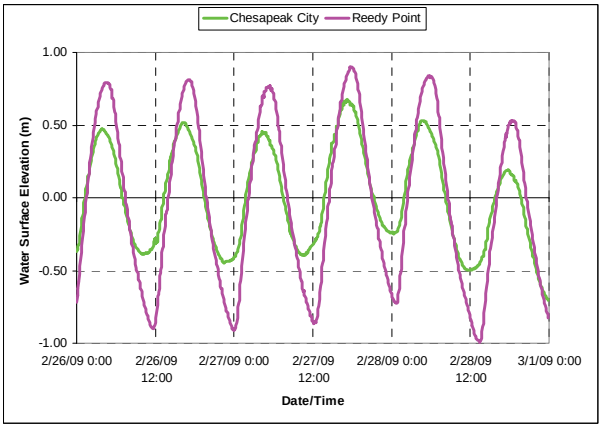

Figure 14. Observed tidal elevations in chesapeake bay & delaware bay canal.

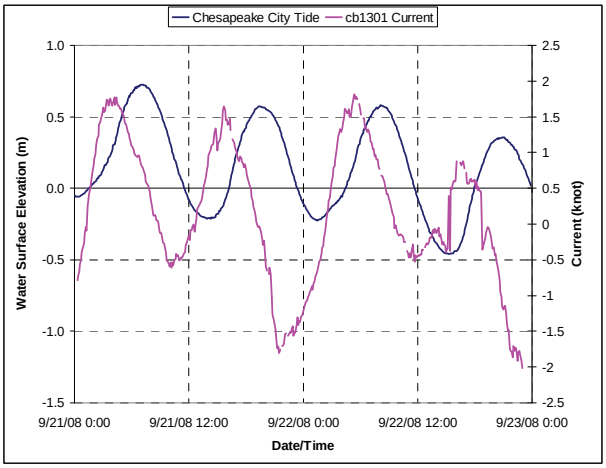

Figure 15. Tide and current at chesapeake city.

Table 9. Progressive wave in C&D canal.

	Canal Tide
Amplitude (m)	0.75
Time Period, T (hour)	12.42
Wavelength, L (m)	457404
Wave Celerity, C (m/s)	10.23
Canal Length, l (m)	22531
Water Depth, h (m)	11.93
h/L	2.61E-05
Wave Type	Long
Wave Number, k	1.37E-05
Wave Frequency, σ	0.00014
Maximum Vel. (m/s)	0.72

3. Conclusions

This paper performs basic tidal analyses of Chesapeake Bay so as to represent a basic tidal analysis approach and provide tidal information for the understanding of tide, sediment transport, and other processes in Chesapeake Bay.

The general distributions of tidal and current ranges, salinity probably result from deep channel, earth rotation, and freshwater discharge. A brief description of general sediment distribution in Chesapeake Bay was represented in this paper in accordance with tidal characteristics and Langland and Cronin [3]. Wind has a significant impact on the tides in Chesapeake Bay.

Taking friction into considered, dominant semidiurnal M_2 constituent tidal elevations within Chesapeake Bay were computed to compare against the actual M_2 amplitudes, and they are found in good agreement. Higher M_2 amplitude was observed at Chesapeake City due to standing wave and the narrowing of C&D Canal.

Removing the effect of wind, mainly progressive wave at the entrance and mainly standing waves are at upper Chesapeake Bay were observed.

The changes of the tidal amplitudes are the consequence of the interaction between the tide and the bay morphology as well as the wave reflection.

4. References

[1] G. Walters and F. Klein, "Modeling Tides in the Chesapeake Bay," Project Report.

[2] R. Patrick, "Rivers of the United States: Estuaries," John Wiley and Sons, 1994.

[3] M. Langland and T. Cronin, "A Summary Report of Sediment Processes in Chesapeake Bay and Watershed," Water-Resources Investigations Report 03-4123, U.S. Department of the Interior & U.S. Geological Survey, 2003.

[4] P. D. Curtin, G. S. Brush and G. W. Fisher, "Discovering the Chesapeake: The History of An Ecosystem," JHU Press, Baltimore, 2001.

[5] National Research Council (USA), Committee on Nonnative Oysters in the Chesapeake Bay, United States, 2004.

[6] L. Zhong and M. Li, "Tidal Energy Fluxes and Dissipation in the Chesapeake Bay," *Continental Shelf Research*, Vol. 26, No. 6, 2006, pp. 752-770.

[7] H. V. Wang and S. Chao, "Intensification of Subtidal Surface Currents over a Deep Channel in the Upper Chesapeake Bay," *Estuarine, Coastal and Shelf Science*, Vol. 42, No. 6, 1996, pp. 771-785.

[8] D. J. Whirford, "Observations of Current Flow through the Mouth of the Chesapeake Bay," *Estuarine, Coastal and Shelf Science*, Vol. 49, No. 2, 1999, pp. 209-220.

[9] H. V. Wang and B. H. Johnson, "Validation and Application of the Second Generation Three Dimensional Hydrodynamic Model of Chesapeake Bay," *Water Quality and Ecosystems Modeling*, Vol. 1, No. 1-4, 2000, pp. 51-90.

[10] S. Huang, H. Lou, Y. Xie and J. Hu, "Hydrodynamic Environment and is Effects in the Xiangshan Bay," *International Conference on Estuaries and Coasts*, Hangzhou, 9-11 November 2003.

[11] D. Salas-Monreal and A. Valle-Levinson, "Sea-Level Slopes and Volume Fluxes Produced by Atmospheric Forcing in Estuaries: Chesapeake Bay Case Study," *Journal of Coastal Research*, Vol. 24, No. sp2, 2008, pp. 208-217.

[12] D. T. Pugh, "Changing Sea Levels," Cambridge University Press, Cambridge, 2004.

[13] M. L. Schwartz, "Encyclopedia of Coastal Science," Springer, Berlin, 2005.

[14] A. T. Ippen, "Estuary and Coastline Hydrodynamics," McGraw-Hill Book Company, Inc., New York, 1966.

[15] J. D. C. Boon, "Secrets of the Tide: Tide and Tidal Current Analysis and Applications, Storm Surges and Sea Level Trends." Horwood Publishing, Chichester, 2004.

[16] S. Canhanga and J. M. Dias, "Tidal Characteristics of Maputo Bay, Mozambique," *Journal of Marine Systems*, Vol. 58, No. 3-4, 2005, pp. 83-97.

[17] Z. Ji, "Estuary Hydrodynamics and Water Quality: Modeling Rivers, Lakes, and Estuaries," John Wiley & Sons, Inc., Hoboken, 2008.

[18] P. Wang, L. C. Linker, R. Batiuk and C. Cerco, "Surface Analysis of Chesapeake Bay Water Quality Response to Different Nutrient and Sediment Loads," *Journal of Environmental Engineering*, Vol. 132, No. 3, 2006, pp. 377-383.

J. Water Resource and Protection, **2010, 2, 629-635**
doi:10.4236/jwarp.2010.27072 Published Online July 2010 (http://www.SciRP.org/journal/jwarp)

Evaluating Raw and Treated Water Quality of Tigris River within Baghdad by Index Analysis

Abdul Hameed M. Jawad Alobaidy[1], Bahram K. Maulood[2], Abass J. Kadhem[1]
[1]*Environmental Research Center, University of Technology, Baghdad, Iraq*
[2]*Twin Rivers Institute, American University of Iraq-Sulaimani, Sulaimani, Iraq*
E-mail: *jawaddhy@yahoo.co.in, Bahram.Khider@auis.org, aik_mik@yahoo.com*
Received April 1, 2010; *revised May* 12, 2010; *accepted May* 24, 2010

Abstract

A water quality index (WQI) is a single value indicator of the water quality determined through summarizing multiple parameters of water test results into simple terms for management and decission makers. In this paper, thirteen parameters were considered. On the basis of these data, raw and treated drinking water from Tigris River within Baghdad were analyzed. Cluster analysis conducted on the WQI data in this area was applied to detect the fluctuation of water quality. In this study, WQI showed that Tigris water never reached "Excellent" levels nor fallen to "Unsuitable" condition, except in occasional untreated water samples. Effects of various sources of pollution were evident and the needs for intensive studies on WQI became evident.

Keywords: Water Quality Index, Tigris River, Drinking Water, Nature Iraq

1. Introduction

Globally, there is an increasing awareness that water will be one of the most critical natural resources in future. Water scarcity is increasing worldwide and pressure on the existing water recourses is increasing due to the growing demands in several sectors such as, domestic, industrial, agriculture, hydropower generation, etc. Therefore, the evaluation of water quality in various countries has become a critical research topic in the recent years [1].

The quality of water is defined in terms of its physical, chemical and biological parameters, and ascertaining its quality is important before use for various intended purposes such as potable, agricultural, recreational and industrial water usages, etc. [2]. It is assessed with the help of various parameters to indicate their pollution level. It is quite likely that any sample of water will exhibit various levels of contamination with respect to the different parameters tested [3].

In monitoring programs, generally relevant chemical, physical, and biological factors are annually (or with less intervals) sampled and analyzed to sort out governing factors for the water quality variations. Generally, such monitoring gives a clue about the status of water quality that might be valid for a limited time and pre-specified objectives. However, these data may not give the indication of trends in water quality over time and across geographic areas. Traditional approaches to assessing water quality are frequently based on a comparison of experimentally determined parameter values with existing guidelines. In many cases, monitoring allows proper identification of contamination sources and may face legal compliance. However, it does not easily give an overall vision of the spatial and temporal trends in the overall water quality in a watershed [4]. Many attempts were made to present the water quality data in understandable and acceptable ways using the water quality index (WQI) [5].

WQI is an arithmetical tool used to transform large quantities of water quality data into a single cumulatively derived number. It represents a certain level of water quality while eliminating the subjective assessments of such quality [5-7]. It is intended as a simple, readily understandable tool for managers and decision makers to convey information on the quality and potential uses of a given water body, based on various criteria [6]. Furthermore it turns complex water quality data into information that is understandable and usable by the public. It gives the public a general idea of the water quality in a particular region.

The advantage of this approach, besides getting the information and data necessary, is also determined the general health or status of the system of concern. In this

way, the index can be used to assess water quality relative to its desirable state (as defined by water quality objectives) and to provide insight into the degree to which water quality is affected by human activity [8].

To summarize the vast amount of analytical data regarding water quality into useful, easy to understand and convenient management tools for the assessment of water quality, the concept of WQI was developed and proposed first by Horten [9]. It is a single number like a grade that expresses the overall water quality at a certain area and time based on several water quality parameters. It is also defined as a rating reflecting a composite influence, on overall quality of water, of a number of water quality parameters. WQI value makes information more easily and rapidly understood rather than a long list of numerical values for a large variety of parameters. Additionally, WQI's also facilitate comparison between different sampling sites and/or events. Thus, they are considered better for transmitting information to general audiences [6]. When their specific characteristics and limitations are considered [10-12], WQI's can be quite useful for the purpose of management and decision-making. Nevertheless, many different methods for the calculation of WQI's have been developed. In general, they all consider similar physical and chemical parameters but differ in the way the parameter values are statistically integrated and interpreted [5].

Water quality indices are generally calculated in two steps. The selected water quality characteristics having different units of measurement are transformed into sub index values. These sub indices are then aggregated to give a water quality index value. Various water quality indices were reviewed by many researchers; [5,7,10-20]. WQI approach has been applied in many countries to assess the overall status of their water bodies, such as United States [21], United Kingdom [22], Canada [23], India [24] and Egypt [25]. The concept is similar, where a few important parameters are selected and compounded into numerical rating for the evaluation of the water quality. However, in Iraq such studies are in a preliminary stage or not existing, therefore this paper may be regarded as the first attempt to be applied in this country that possibly will lead to several investigations in the future. The present study is a part of Nature Iraq Indices Project undertaken to highlight the physico-chemical drinking water quality index and the status of Tigris River water quality which have been used as raw water for the Water Treatment Plant (WTPs) within Baghdad, the capital of Iraq.

2. Materials and Methods

2.1. Study Area

The study area (Tigris River within Baghdad City) is located in the Mesopotamian alluvial plain between latitudes 33°14'-33°25' N and longitudes 44°31'-44°17' E, 30.5 to 34.85 m a.s.l. The River divides the city into a right (Karkh) and left (Risafa) sections with a flow direction from north to south. The area is characterized by arid to semi arid climate with dry hot summers and cold winters; the mean annual rainfall is about 151.8 mm [26].

2.2. Application of the WQI

The data used in this paper were provided by Baghdad Mayoralty (Amanat Baghdad) and cover the period from February 2002 to December 2008. Raw water samples were collected using clean polyethylene containers from sites in the river just close to the WTPs that represent the stations of this study. While treated water samples were collected from the treatment plants just before the distribution of potable water to the houses through the water supply network. Samples were analyzed for chemical and physical properties immediately after collection. The data were merged (monthly average values for each parameters) to obtain a data set covering seven years of data for seven raw (Tigris river before treatment) and seven drinking water (after treatment) stations, (**Figure 1**). For calculating the Water Quality Index, a set of thirteen water quality parameters have been selected based on both importance of the parameters and availability of data. These thirteen parameters are pH value, Alkalinity, Turbidity, Total Dissolved Solids, Hardness, Calcium, Magnesium, Chloride, Sulphate, Ammonia, Fluoride, Iron and Aluminum.

2.3. Calculations of the WQI

For calculating WQI, the following steps were used:

In the first step, unit weight (W_i) for various parameters is inversely proportional to the recommended standard ($V_{standard}$) for the corresponding parameter. W_i values were calculated by using the following formula proposed by Tiwari and Mishra [24],

$$W_i = \frac{K}{V_{standard}} \tag{1}$$

where, K = proportionality constant, $V_{Standard}$ = worldwidely accepted drinking water quality standard prescribed by WHO [27].

The constant of proportionality K in the above equation can be determined from the following condition,

$$\sum W_i = K \sum \left(\frac{1}{V_{standard}} \right) \tag{2}$$

In the second step, Quality rating (Q_i) is calculated as,

$$Q_i = 100 \left[\frac{V_{actual}}{V_{standard}} \right] \tag{3}$$

While, the quality rating for pH (Q_{pH}) was calculated on the basis of,

$$Q_{pH} = 100\left[\frac{(V_{actual} - V_{ideal})}{(V_{standard} - V_{ideal})}\right] \quad (4)$$

where, V_{actual} = value of the water quality parameter obtained from the laboratory analysis.

V_{ideal} = the ideal value of pH considered as equal to (7.00).

$V_{standard}$ = value of the water quality parameter obtained from recommended WHO standard of corresponding parameter.

This equation ensures that $Q_i = 0$ when a pollutant is totally absent in the water sample and $Q_i = 100$ when the value of this parameter is just equal to its permissible value. Thus the higher the value of Q_i is, the more polluted is the water.

Then, the overall WQI was calculated using the method proposed by Ott [10] and Harkins [28] on the basis of weighting and rating of the different physico-chemical parameters, as follows:

$$WQI = \sum_{i=1}^{i=n} W_i Q_i \quad (5)$$

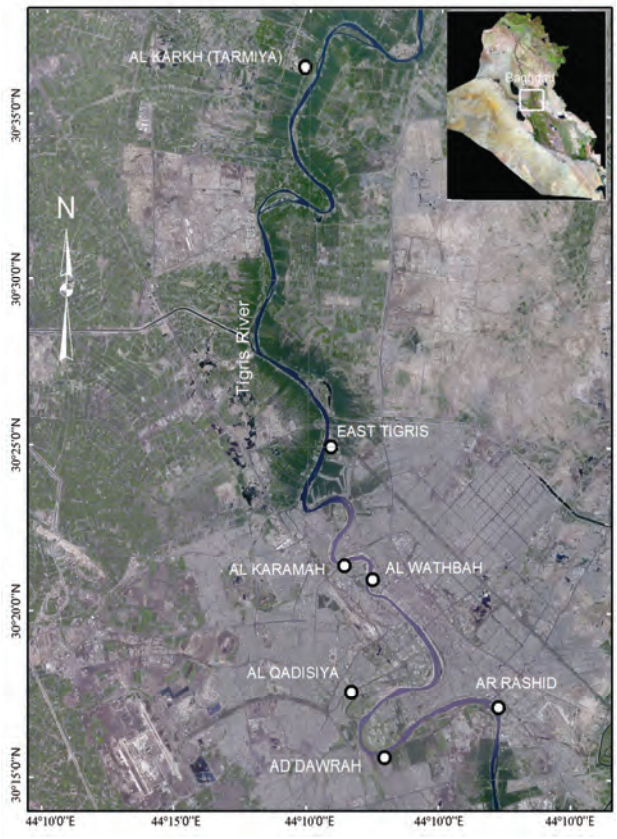

Figure 1. Sampling locations across Tigris River, Baghdad City.

Based on the calculated WQI, the classification of water quality types is given according to [24] as shown in **Table 1**.

2.4. Quality Rating and Weighting

Water quality parameters were studied in respect to their suitability for human consumption. The 'standards' (permissible values of various pollutants) for the drinking water, recommended by the World Health Organization [27], and unit weights are given in **Table 2**.

3. Results and Discussion

3.1. Annual WQI

Applying the former equations on the results of water analysis data of Tigris River, annual WQI (Raw and Treated) have been plotted in **Figure 2**. Spatial profiles of the results showed that, for raw water, none of the samples are coming neither under "Excellent" (range 0-25) nor "Good" (range 26-50) water quality, indicating that the Tigris River water is generally "Poor" (range 51-75) at the upstream and is either "Poor", "Very poor" (range 75-100) or "Unsuitable" (above 100) at the mid and downstream. This may reflect the effect of pollution from urban wastes and anthropogenic activities. On temporal basis, the WQI values for raw water for all sites were highly increased in the last three years (2006-2008).

Table 1. Water quality index scale.

WQI	0-25	26-50	51-75	76-100	>100
Water quality	Excellent	Good	Poor	Very poor	Unsuitable

Table 2. Drinking water standards and unit weights.

Water quality parameters	Standards	Unit Weights (W_n)
pH value (pH unit)	6.5-8.5	0.007990
Alkalinity (mg/L)	100	0.000679
Turbidity (NTU)	5.0	0.013583
Dissolved Solids (mg/L)	500	0.000136
Hardness (mg/L)	100	0.000679
Calcium (mg/L)	100	0.000679
Magnesium (mg/L)	30	0.002264
Chloride (mg/L)	250	0.000272
Sulphate (mg/L)	250	0.000272
Ammonia (mg/L)	0.2	0.339574
Fluoride (mg/L)	1.0	0.067915
Iron (mg/L)	0.3	0.226383
Aluminum (mg/L)	0.2	0.339574

The effect of dryness in the area in the last three years might be behind the clearly observed depletion of WQI throughout this period, especially in the upstream stations where there is no high intervention between the effects of dryness and those of human activities.

Nevertheless, for spatial profiles of treated water, none of the samples are classified as "Excellent" or "Unsuitable". The results showed "Poor" to "Good" quality in all stations. As for temporal trend, water quality was generally "Good" at the upstream throughout the study period (WQI range: 25.24-43.11) for AL KARKH and EAST TIGRIS WTPs. With few exceptions the results of WQI showed generally "Poor" but not "Unsuitable" quality at the midstream and downstream. This might be due to increasing pollution of raw water from urban wastes and anthropogenic activities [20]. Generally, the peak year of degradation of water quality was 2008 in all stations.

For both raw and treated water, the phenomenon of water quality degradation along Tigris was generally evident throughout the seven years results. Therefore, the authorities should practice more efforts in controlling various activities along the river bank. The urgent water management rules should be applied, enforcing wastewater treatment systems among the factories and other activities.

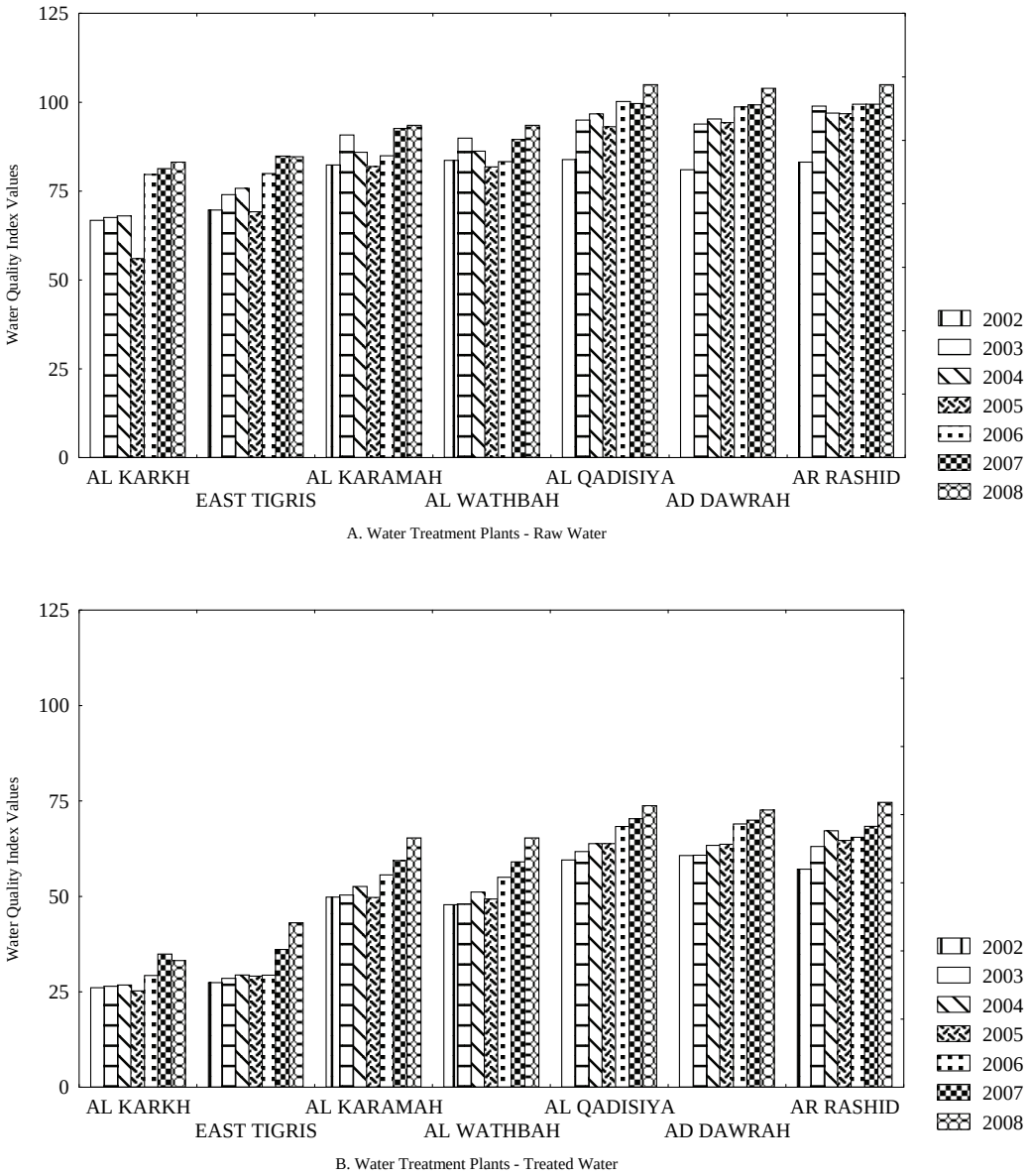

Figure 2. Annual water quality index.

3.2. Cluster Analysis

Cluster analysis was applied to find different classes (sub clusters) within the WQI data that might help us to show how the water quality is affected by the course of the river through the city. The raw and treated WQI data for all sites was processed by SPSS statistical software. The cluster analysis was carried out on the data applying Ward's method, using Squared Euclidean Distance as a measure of similarity. Ward's hierarchical clustering method was chosen for this purpose as it aims to minimize the loss of information at each step in the clustering process [29].

The results of cluster analysis for WQI of raw water are illustrated with a tree dendrogram (**Figure 3**). It is clear that WQI results divided the stations on Tigris into three separate sub clusters: AL KARKH (TARMIYA) at upstream, EAST TIGRIS, ALWATHBAH and ALKARAMAH at midstream, and AR RASHID, ALQADISIYA and AD DAWRAH at downstream. WQI values of raw water deteriorated from "Poor" to "Very poor" to "Unsuitable" along the stretch of the river. However, the major reasons of deteriorating water quality are the discharge from drainage tributaries, city wastewater and other forms of intensives human activities which are increasing in trend from north to south. This comes in accordance with the findings of Fulazzaky [20] and Ouyang [30] who referred to these factors as main reasons for deteriorated water quality.

The results of cluster analysis of WQI for treated water were distributed in three sub clusters as illustrated with a tree dendrogram (**Figure 4**). The first sub-cluster gathers AL KARKH and EAST TIGRIS WTPs, with WQI values reflecting "Good" to "Poor" water. While, ALKARAMAH and AL WATHBAH WTPs were in a second sub-cluster and AD DAWRAH, AR RASHID and AL QADISIYA WTPs were in a third sub cluster. Water quality for both of these sub clusters was "Poor" in general.

It is very important to establish an index showing the information of the river water quality and providing the warning alarm to take pollution control actions. This investigation might be regarded as a pioneer attempt for water quality indices in Baghdad as well as whole Iraq in general. Undoubtedly, this may lead to more intensive detailed studies on WQI in the area in order to fulfil the existing gap of information about this subject in Iraq. The results indicate the need for more consideration of the WTPs along Tigris for years to come.

3.3. Efficiency of the Water Treatment Plants

Efficiency (E%) of the Water Treatment Plants situated at Tigris River was calculated by determining the WQI of the raw water and treated (Tap) water supplied by using the formula given below:

$$E\% = \frac{WQI\ of\ raw\ water - WQI\ of\ treated\ water}{WQI\ of\ raw\ water} \times 100 \quad (6)$$

The water treatment plants of Baghdad Mayoralty have a capacity to treat 2,272,100 cubic meters per day of raw water pumped from Tigris River, from which 2,082,000 cubic meters of water is supplied. The water treatment plants follow the traditional treatment process, in which raw water after aeration is treated with coagulant (alum and lime) and pre-chlorination as required. After flocculation, it is carried over to the sand bed filter for filtration. After this, bleaching powder or chlorine gas is added for disinfection to ensure the Residual Chlorine at the tail end is in the range of 0.2 to 0.5 mg/L.

Table 3 represents the efficiency of the water treatment plant situated at Baghdad City. From **Table 3** it has been concluded that the raw water is poorest in quality throughout the year as the efficiency of WTPs range from 25.07 to 63.30 in the whole period of study. Ultimately, reconsideration of the WTPs system is needed since these stations were designed to provide physical and biological treatment rather than chemical treatment of raw water. This will surely have more consequences if combined with the already high levels of chemical pollution of raw water that we have shown in our results above. Strict measures should be applied in order to control the levels of pollutants discharged into Tigris from different kinds of point and nonpoint sources.

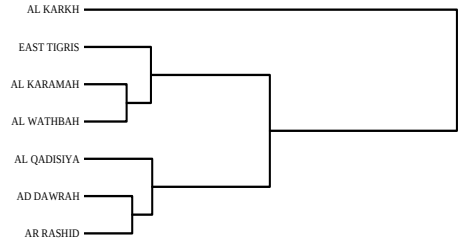

Figure 3. Dendrogram obtained using ward's method for raw water quality index.

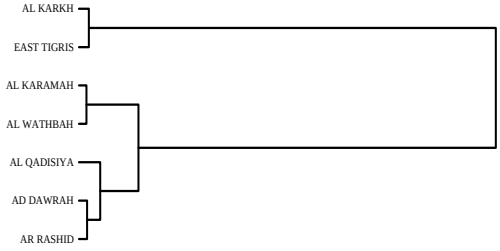

Figure 4. Dendrogram obtained using ward's method for treated water quality index.

Table 3. Efficiency of the water treatment plants.

WTPs	Efficiency%						
	2002	2003	2004	2005	2006	2007	2008
AL KARKH	60.97	60.86	60.57	54.93	63.20	57.07	60.06
EAST TIGRIS	60.62	61.45	61.19	57.86	63.30	57.43	49.08
AL KARAMAH	39.47	44.52	38.79	39.30	34.50	35.87	30.14
AL WATHBAH	42.85	46.56	40.69	39.67	33.87	34.07	30.17
AL QADISIYA	29.03	34.96	33.99	31.46	31.86	29.36	29.69
AD DAWRAH	25.07	35.22	33.49	32.47	30.10	29.52	30.07
AR RASHID	31.26	36.22	30.66	33.18	34.16	31.26	28.84

4. Acknowledgements

Many thanks to Nature Iraq, without their support and encouragement the work would have not been done. Our special gratitude is forwarded to "Nature Iraq Indices" project manager Mr. Haider Abid for his efforts. However, our thanks are also extended to Baghdad Mayoralty for supplying the raw data.

5. References

[1] E. D. Ongley, "Modernization of Water Quality Programs in Developing Countries Issues of Relevancy and Cost Efficiency," *Water Quality International*, September -October 1998, pp. 37-42.

[2] A. Sargaonkar and V. Deshpande, "Development of an Overall Index of Pollution for Surface Water Based on a General Classification Scheme in Indian Context," *Environmental Monitoring and Assessment*, Vol. 89, No. 1, 2003, pp. 43-67.

[3] S. A. Abbasi, "Water Quality Indices: State-of-the-Art," Centre for Pollution Control & Energy Technology, Pondicherry University, Pondicherry, 1999.

[4] P. Debels, R. Figueroa, R. Urrutia, R. Barra and X. Niell, "Evaluation of Water Quality in the Chilla´n River (Central Chile) Using Physicochemical Parameters and a Modified Water Quality Index," *Environmental Monitoring and Assessment*, Vol. 110, No. 1/3, 2005, pp. 301-322.

[5] N. Štambuk-Giljanović, "Water Quality Evaluation by Index in Dalmatia," *Water Research*, Vol. 33, No. 16, 1999, pp. 3423-3440.

[6] N. Štambuk-Giljanović, "Comparison of Dalmatian Water Evaluation Indices," *Water Environment Research*, Vol. 75, No. 5, 2003, pp. 388-405.

[7] W. W. Miller, H. M. Joung, C. N. Mahannah and J. R. Garrett, "Identification of Water Quality Differences in Nevada through Index Application," *Journal of Environmental Quality*, Vol. 15, 1986, pp. 265-272.

[8] N. Radwn, "Evaluation of Different Water Quality Parameters for the Nile River and the Different Drains," 9*th International Water Technology Conference*, Sharm El-Sheikh, Egypt, 2005.

[9] R. K. Horton, "An Index Number System for Rating Water Quality," *Journal of Water Pollution Control Federation*, Vol. 37, No. 3, 1965, pp. 300-306.

[10] W. R. Ott, "Environmental Indices: Theory and Practice," Ann Arbor Science Publishers Inc., Ann Arbor, Michigan, USA, 1978.

[11] D. Hallock, "A Water Quality Index for Ecology's Stream Monitoring Program," Technical Report, Washington Department of Ecology, Environmental Assessment Program, Olympia, 2002.

[12] S. F. Pesce and D. A. Wunderlin, "Use of Water Quality Indices to Verify the Impact of Córdoba City (Argentina) on Suquìa River," *Water Research*, Vol. 34, No. 11, 2000, pp. 2915-2926.

[13] R. M. Brown, N. I. McClelland, R. A. Deininger and R. G. Tozer "A Water Quality Index: Do We Dare?" *Water Sewage Works*, Vol. 117, No. 10, 1970, pp. 339-343.

[14] A. A. Bordalo, W. Nilsumranchit and K. Chalermwat, "Water Quality and Uses of the Bangpakonk River (Eastern Thailand)," *Water Research*, Vol. 35, No. 15, 2001, pp. 3635-3642.

[15] C. Cude, "Oregon Water Quality Index: A Tool for Evaluating Water Quality Management Effectiveness," *Journal of American Water Resource Association*, Vol. 37, No. 1, 2001, pp. 125-137.

[16] S. M. Liou, S. L. Lo and S. H. Wang, "A Generalized Water Quality Index for Taiwan," *Environmental Monitoring and Assessment*, Vol. 96, No. 1-3, 2004, pp. 35-52.

[17] M. N. El-Gafy, A. Faria, A. El-Bahrawy, A. Khalifa, E. El-Basiony and M. Abdelmotaleb, "Decision Support System for Evaluation the Groundwater Quality," *Emirates Journal for Engineering Research*," Vol. 10, No. 1, 2005, pp. 69-78.

[18] D. K. Sinha and A. Saxena, "Statistical Assessment of Underground Drinking Water Contamination and Effect of Monsoon at Hasanpur, J.P.Nagar (Uttar Pradesh, India)," *Journal of Environmental Science and Engineering*, Vol. 48, No. 3, 2006, pp. 157-164.

[19] S. E. Gómez, R. C. Menni, J. G. Naya and L. Ramirez, "The Physical-Chemical Habitat of the Buenos Aires Pejerrey, *Odontesthes bonariensis* (Teleostei, Atherinopsi-

dae), with a Proposal of a Water Quality Index," *Environmental Biology of Fishes*, Vol. 78, No. 2, 2007, pp. 161-171.

[20] M. A. Fulazzaky, "Water Quality Evaluation System to Assess the Brantas River Water," *Water Resource Management*, Vol. 23, No. 14, 2009, pp. 3019-3033.

[21] L. W. Canter, "Environmental Impact Assessment," 2nd Edition, McGraw-Hill Inc., New York, USA, 1996.

[22] M. A. House, "A Water Quality Index for River Management," *Water and Environment Journal*, Vol. 3, No. 4, 1989, pp. 336-344.

[23] Canadian Council of Ministries of the Environment (CCMC), "Canadian Water Quality Index 1.0 Technical Report and User's Manual," *Canadian Environmental Quality Guidelines*, Technical Subcommittee, Gatineau, 2001.

[24] T. N. Tiwari and M. Mishra, "A Preliminary Assignment of Water Quality Index of Major Indian Rivers," *Indian Journal of Environmental Protection*, Vol. 5, No. 4, 1985, pp. 276-279.

[25] UNEP "Development of Water Quality Indices for Sustainable Development: A Case Study," *Proceeding of the Expert Group Meeting on the Implication of Agenda Region*, Amman, 2-5 October 1995.

[26] A. S. Al-Adili, "Geotechnical Evaluation of Baghdad Soil Subsidence and their Treatments," Ph.D. Thesis, University of Baghdad, Iraq, 1998.

[27] World Health Organization (WHO), "Guidelines for Drinking Water Quality," 3rd Edition, Geneva, 2004.

[28] R. D. Harkins, "An Objective Water Quality Index," *Journal of Water Pollution Control Federation*, Vol. 46, No. 5, 1974, pp. 588-591.

[29] J. H. Ward, "Hierarchical Grouping to Optimize an Objective Function," *Journal of the American Statistical Association*, Vol. 58, No. 301, 1963, pp. 236-244.

[30] T. Ouyang, Z. Zhu and Y. Kuang, "Assessing Impact of Urbanization on River Water Quality in the Pearl River Delta Economic Zone, China," *Environmental Monitoring and Assessment*, Vol. 120, No. 1-3, 2006, pp. 313-325.

J. Water Resource and Protection, **2010, 2, 636-643**
doi:10.4236/jwarp.2010.27073 Published Online July 2010 (http://www.SciRP.org/journal/jwarp)

Estimation of Melt Contribution to Total Streamflow in River Bhagirathi and River DhauliGanga at Loharinag Pala and Tapovan Vishnugad Project Sites

Manohar Arora[1], D S Rathore[1], R D Singh[1], Rakesh Kumar[1], Amit Kumar[2]
[1]*Scientist, National Institute of Hydrology, Roorkee, India*
[2]*Research Associate, Centre for Glaciology, Dehradun, India*
E-mail: *arora@nih.ernet.in*
Received September 1, 2009; *revised September* 23, 2009; *accepted September* 30, 2009

Abstract

Many of the major rivers in India originate from the Himalayas. These rivers have significant contribution from snow and ice which makes these rivers perennial. Due to steep slopes, all such streams have potential sites for hydropower generation. There is a requirement of estimation of the contribution from snow and glacier melt, rainfall contribution and sub surface contribution in the total runoff for sustainable supply of water to the hydropower plants. Considering this aspects, in this study a snowmelt runoff simulation model SNOWMOD suitable for Himalayan basins developed earlier has been modified and applied for simulation of flows. Input to the model such as glacier cover, permanent snow cover, seasonal snow cover generated through remote sensing techniques were used in conjunction with daily maximum and minimum temperature, rainfall and discharge. Two hydropower dam sites on major tributaries (Bhagirathi and DhauliGanga) of River Ganga have been selected for determination of different runoff components. However, though the data available was for a very limited period but the results indicate that these tributaries have significant contribution from snow and ice for long term sustainability of flows to these schemes.

Keywords: Himalayas, Snow and Ice, SNOWMOD, Modeling, Hydropower Schemes

1. Introduction

The Himalayan Mountain, system is the source of one of the world's largest supplies of fresh water. All the major south Asian rivers originate in the Himalayan and their upper catchments are covered with snow and glaciers. The Indus, the Ganga and the Brahmaputra river systems originating from the Himalayan region receive substantial amount of precipitation in the form of snow and glaciers. The perennial nature of Himalayan Rivers and appropriate topographic setting of the region provide a substantial exploitable hydropower in this area. In the Himalayan range there are more than > 10,000 glaciers [1] and feed a number of Himalayan rivers. This ice exposed surface of the glacier increases with time resulting in higher quantum of runoff. As the melt season advances, the melt water contribution from the glaciers increases. By the end of melt season, the melt runoff is reduced due to increases in air temperature and fresh snowfall on the higher reaches. Evidently, runoff generated from the glaciers in the Himalayan basins has a significant influence on the streamflow of the river. The melt rate of the glacier is deter- mined by the prevailing climatic conditions and, therefore, varies from year to year. The physical changes in the glacier, like trend of exposition of glacier surface, influence the melting and runoff pattern of the glacier. Further, contribution of snow and ice melt to the total increase with altitude, but variation in the different components of runoff with season has not been quantified for any Himalayan rivers.

In glaciated areas, much of the precipitation falls in solid form of throughout the year, so that it contributes to mass storage rather than directly to runoff. For example in the Alps, a minimum variation in annual runoff was observed from the river basin with 30-40% glacier cover [2]. The contribution of snow and glacier- melt runoff to Himalayan Rivers is significant and an estimation of the amount is necessary for the development, planning, and management of water resources. Singh *et al.* [3] estimated the average contribution of snow and glacier-melt runoff

in the annual streamflow of the Chenab River at Akhnoor using a water balance approach for a period of 10 years (October 1982-September 1992). The average snow and glacier runoff contribution to the annual flow of the Chenab River at Akhnoor is estimated to be about 49 percent. Further Singh and Jain [4] have used this approach to estimate snow and glacier contribution in the Satluj River at Bhakra. It was found that average contribution of snow and glacier runoff in the annual flow of Satluj River at Bhakra is about 59%. Kumar *et al.* [5] have estimated the average contribution of snow- and glacier-melt runoff in the annual flow of the Beas River at Pandoh Dam using 15 years of flow data (1990-2004). The results of the analysis show that the snow- and glacier-melt runoff contributes about 35% to the annual flow of the Beas River at Pandoh Dam.

Streamflow in the Himalayan Rivers is generated from rainfall, snow and ice. The distribution of runoff produced from these sources is such that the streamflow may be observed in these rivers throughout the year, *i.e.* they are perennial in nature. Snow and glacier melt runoff contributes substantially to the annual flows in these rivers and its estimation is required for the planning, development and management of the water resources of this region. Keeping in view the importance of melt contributions to the total streamflow in the Himalayan Rivers, a study has been carried out on two major rivers of the great Ganga river system. Simulation on a daily scale of the melt runoff for the melt season was done using the snowmelt model SNOWMOD. The model, designated primarily for mountainous basins, conceptualizes the basin as a number of elevation zones depending upon topographic relief. The basic inputs to the model are temperature, precipitation and snow-covered area. The snowmelt is computed using the degree-day approach and rain induced melting is also considered. The degree day provides a reasonably good estimate of snowmelt as compared with detailed evaluation of the various com- ponents in the energy balance approach [6,7]. An early application of a degree-day approach was made by Finsterwalder & Schunk (1987) in the Alps and since then this approach has been used widely all over the world for the estimation of snowmelt [8-10].

2. Materials and Methods Study Area

The proglacial melt-water stream emerging from the snout of the Gangotri Glacier at an elevation of 4000 m is known as river Bhagirathi.

The Project site is near Loharinag-Pala, upstream of Uttarkashi. It is about 200 km from the nearest railhead at Rishikesh. The catchment of river Bhagirathi extends from latitude 30° 30' N to 31° 30' N and longitude 78° 30' E to 79° 30' E . It is completely mountainous, part of which is covered by snow. The catchment of river Bhagirathi up to Loharinag experiences snow in winter and remains covered with green vegetation in summer.

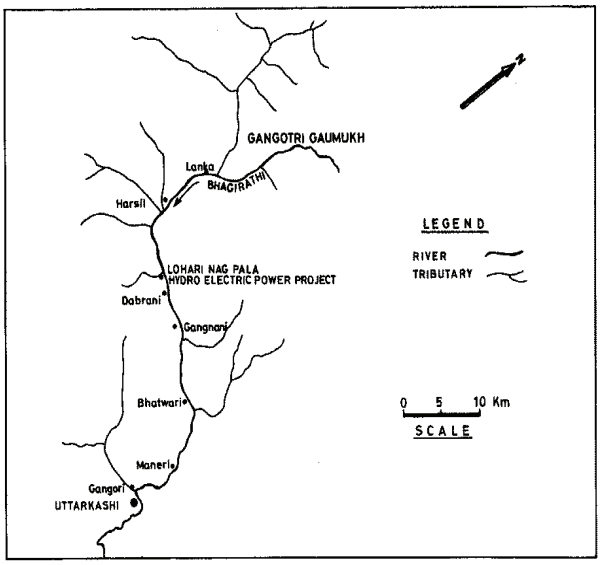

Figure 1. Location map of Lohaninag Pala hydro−power project.

The Dhauliganga River rises from the Nitti Pass in outer Himalayan ranges at a height of about 5070 m. The basin ridge is at an average elevation of 5000m. The average slope of the river from origin to the project site is 34.3 m/km. The catchment of river Dhauliganga extends from latitude 30°15' N to 31°00' N and longitude 79°30´ E to 80°15' E. Total catchment area is 2962.10 sq km.

2.1. Data Availability

No direct records of streamflow are available at Loharagpala site. The transposed data of streamflow have been generated at the Loharinag pala site utilizing the available streamflow data at Maneri site. The rainfall data of Jhala and Bhojwasa has been used for the analyis. Temperature data of Mukhim station and Bhojwasa near Gangotri glacier is used in this study. The daily snow cover over of the Bhagirathi basin upto Loharinag pala have been estimated from IRS derived LISS-III data during the year 2004. The Survey of India topographic sheet no. 53 I (12,15,16), 53 J (9,13), 53 M (3,4,8), 53 N (1,2,5,6) on 1:50,000 scales are used to delineate the catchment boundary. Contours, snow covered and snow free area, drainage, glacier, and stream networks and the benchmarks are digitized using GIS software ILWIS 3.3 and IMAGINE ERDAS 8.6. LANDSAT images were downloaded for the georeferencing of the study area.

For the analysis of the Tapovan site the transposed data of streamflow have been generated at the Tapovan site utilizing the available streamflow data at Joshimath site. The temperature data of Joshimath has been used for

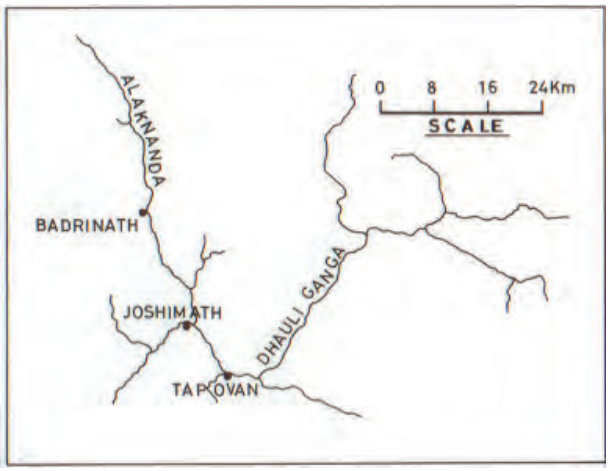

Figure 2. Location map of tapovan vishnugad project.

the analysis. The daily snow cover over of the Dhauliganga basin upto Tapovan-Vishnugad has been estimated from IRS derived LISS-III and AWiFs data during the year 2005.

3.1. Preparation of Digital Elevation Model(DEM)

Digital Elevation Model (DEM) of the catchment area of Bhagirathi River and River Dhauli Ganga is developed using DEM from SRTM, GLOBE DEM in IMAGINE ERDAS 8.6 (**Figures 3** and **4**). The DEM of the study area is quite helpful in defining the catchments boundary, identifying the stream network, estimating the average slope etc. The satellite remote sensing data provide a synoptic view of the catchments area and can provide the details about the physiographic features present in the catchments area. In the present study, IRS-LISS III data were used for determining the snow covered area of the catchments.

3.2. Mapping of Glacier Cover

The study region falls in the Higher or Greater Himalayas and constitutes of crystalline throughout. Topographic maps at scale 1:25000 and 1:50,000 scales have been used for georeferencing of remote sensing images. The glacier cover boundary and area were also estimated. The percentage wise elevation zones with respect to catchment area for Bhagirathi and DhauliGanga basin is given in **Figures 5** and **6** respectively and the zone wise Glaciated area is given in **Tables 1** and **2** (such evaluation data should be given in the results section, here just tell the readers how do you get the percentage wise elevation zones).

Determination of snow cover area:

The snow cover area is determined using IRS LISS III satellite images. The daily snow cover area values are extrapolated from the depletion curves prepared from the available data.

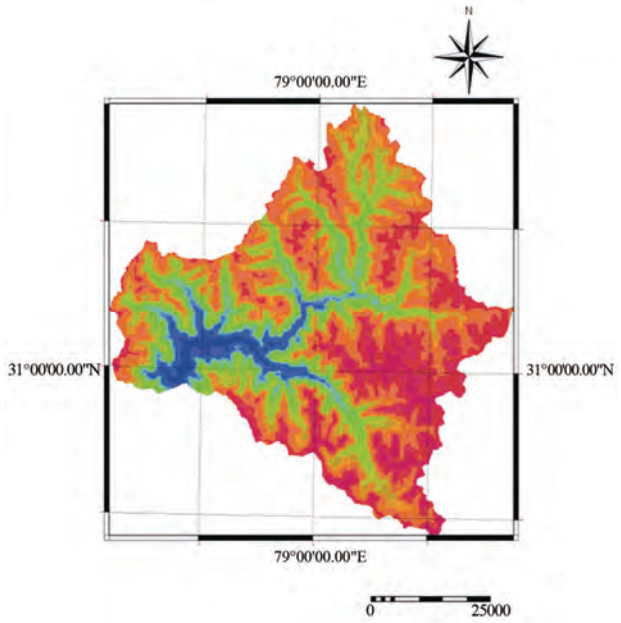

Figure 3. Digital Elevation Model (DEM) of the Bhagirathi basin upto Loharinag Pala H.E. Project study area.

3.3. Simulation of Flows

The conceptual snow melt model SNOWMOD is used for the simulation of flows. The description of model is given in Singh and Jain [11] Model variables are to be derived from actual observations of temperature, precipitation and snow covered area.

4. Results

4.1. Modeling of Streamflow of Bhagirathi River.

The SNOWMOD model has been applied for simulating the daily flows for the ablation season for Loharinag Pala site in the River Bhagirathi four years. The flow data for the year 1999 has been considered for calibrating the model whereas the year 2000, 2001, and 2002 have been considered for validating the model. The efficiency of the model has been computed based on the daily simulated and observed flow values for four years. The values of the model efficiencies are 88%, 80%, 93% and 83% respectively for the years 1999, 2000, 2001 and 2002. The performance of the model in preserving the runoff volume of entire ablation season has been tested based on the criteria computed as percentage difference in ob served and simulated runoff (D_v) during the ablation season. Their values computed for the year 1999, 2000, 2001 and 2002 are –19.12%, –14.33%, –18.76% and –8.55% respectively. The comparison of the daily year is shown in **Figure 7(a)**, **Figure 7(b)**, **Figure 7(c)** and **Figure 7(d)** the model has capability to separate out the simu lated and observed flow hydrographs for the all contributions of rainfall, snow and glacier melt and base

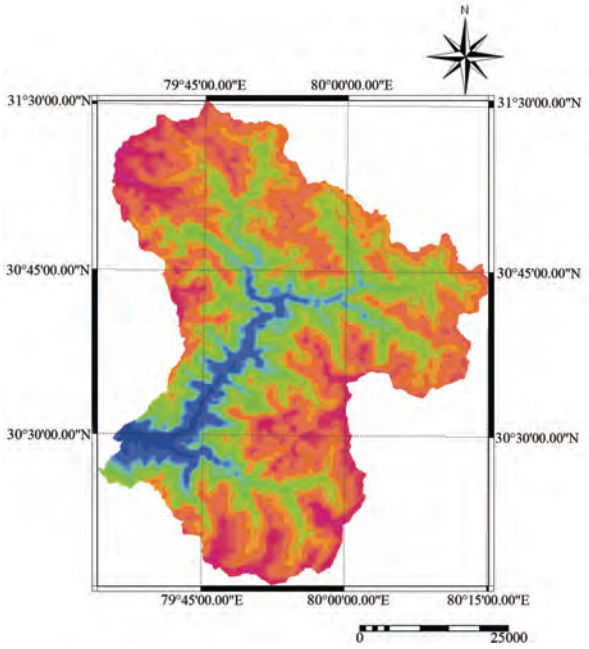

Figure 4. Digital Elevation Model (DEM) of the Dhauli Ganga basin up to Tapovan Vishnugad Project site.

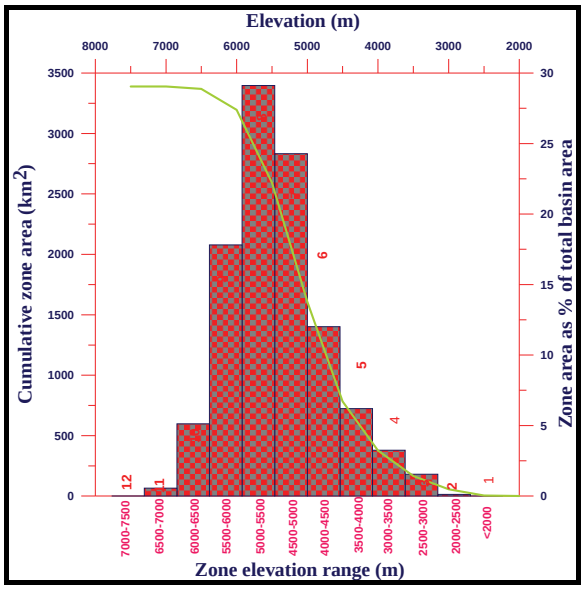

Figure 5. Area of different elevation zones as percentage of total basin area and area-elevation curve for the Bhagirathi basin upto Loharinag sites.

flow from the simulated flows. From these figures, it has been observed that the model has simulated also the daily flows reasonably well showing generally a good matching with the daily observed flows. The trends and peaks of the daily flow hydrographs for the ablation period are very well simulated by the model. Percentage difference in volume, model efficiency and contributions of rain snow and base flow computed by the model are summaized in **Table 3** for the four years. Most of the high peaks observed in the daily flow hydrographs are generly during the months of July and August attributed to the glacier melt. Thus these months are considered as the peak melting season in the western Himalayan region. However, sometimes the flow resulting due to high ineity rainfall also reflects the peaks in the daily flow hyroaphs. The simulation of baseflow indicates that the baseflow contribution to the streamflow increases as the season advances, being at maximum during the peak season and then starts decreasing.

The model has been applied to simulate the daily flow hydrographs considering the records of four ablation seasons together. It has been found that the overall efiiency of the model for the study period of four years is about 0.86% and overall percentage difference in volume of simulated and observed flows (D_v) is about –15.19%. It is also observed that the model is capable of simulating the daily flows very well except few peaks. It may be attributed to some factors which have not been consiered in the model. Thus it requires further investigations to understand the reason and suitably modify the structure of the model to cater such an event.

4.2. Modelling of Streamflow of DhauliGanga River

The flow data for the year 1983 has been considered for calibrating the model whereas the year 1984, and 1987 have been considered for validating the model for simulating the daily flows. The efficiency of the model has

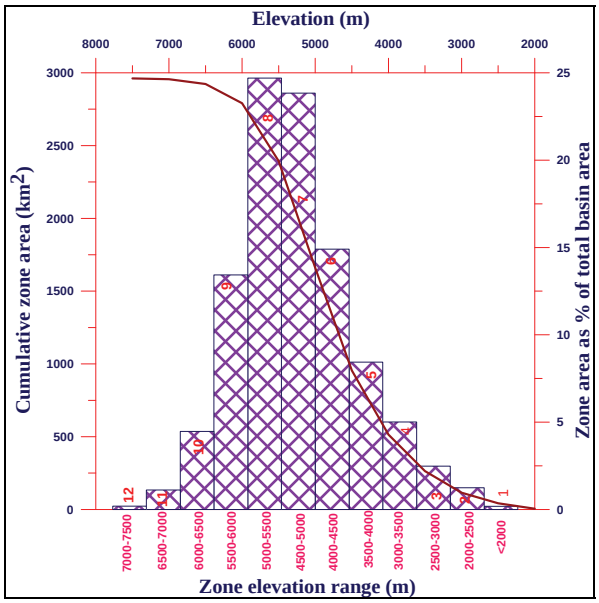

Figure 6. Area of different elevation zones as percentage of total basin area and area-elevation curve for the Dhauliganga basin up to Tapovan.

Table 1. Zone wise Glacier cover area of the Bhagirathi basin upto Loharinag-Pala.

Elevation Range	Zones	Zones	Zone Area (sq.km)	Glacierized Area (Sq.km)	Non Glacierized Area (Sq.km)	Glacierized Area (%)
>2000	2000	Zone1	0	0.00	0.00	0.00
2000-2500	2500	Zone2	3.76	0.00	3.76	0.00
2500-3000	3000	Zone3	52.46	0.00	52.46	0.00
3000-3500	3500	Zone4	109.94	0.00	109.94	0.00
3500-4000	4000	Zone5	210.07	0.16	209.91	0.00
4000-4500	4500	Zone6	407.00	15.92	391.08	0.47
4500-5000	5000	Zone7	822.81	105.41	717.40	3.11
5000-5500	5500	Zone8	986.44	278.97	707.47	8.23
5500-6000	6000	Zone9	603.40	284.72	318.69	8.40
6000-6500	6500	Zone10	173.50	124.26	49.24	3.67
6500-7000	7000	Zone11	18.91	13.89	5.02	0.41
7000-7500	7500	Zone12	0.02	0.00	0.02	0.00
Total			3388.32	823.33	2564.99	24.30

Table 2. Zone wise Glacier cover area of the Dhauliganga basin upto Tapovan.

Elevation Range	Zones	Zones	Zone Area (Sq.km)	Glacierized Area (Sq.km)	Non Glacierized Area (Sq.km)	%Glacierized Area
2000	2000	Zone1	5.33	0.00	5.33	0.00
2000-2500	2500	Zone2	36.95	0.00	36.95	0.00
2500-3000	3000	Zone3	73.39	0.00	73.39	0.00
3000-3500	3500	one4	148.33	0.00	148.33	0.00
3500-4000	4000	Zone5	249.76	0.52	249.25	0.02
4000-4500	4500	Zone6	441.64	22.91	418.72	0.77
4500-5000	5000	Zone7	705.92	128.36	577.56	4.33
5000-5500	5500	Zone8	731.69	287.85	443.84	9.72
5500-6000	6000	Zone9	397.94	246.75	151.19	8.33
6000-6500	6500	Zone10	132.27	111.62	20.66	3.77
6500-7000	7000	Zone11	33.09	28.76	4.33	0.97
7000-7500	7500	Zone12	5.78	5.39	0.39	0.18
Total			**2962.10**	**832.17**	**2129.93**	**28.09**

been computed based on the daily simulated and observed flow values for three years. The values of the model efficiencies are 69%, 73%, 86% respectively for the years 1983, 1984, and 1987. The performance of the model in preserving the runoff volume of entire ablation season has been tested based on the criteria computed as percentage difference in observed and simulated runoff (D_v) during the ablation season. Their values computed for the year 1983, 1984 and 1987 are –18.36, –25.59 and –5.35 respectively. The comparison of the daily simulated and observed flow hydrographs for all the three years is shown in **Figure 8(a), Figure 8(b)** and **Figure 8(c)**. The model has capability to separate out the contributions of rainfall, snow and glacier melt and base flow from the simulated flows. From these figures, it has been observed that the model has simulated the daily flows reasonably well showing generally a good matching with the daily observed flows.

The trends and peaks of the daily flow hydrographs forthe ablation period are very well simulated by the model. Percentage difference in volume, model efficiency and contributions of rain snow and base flow

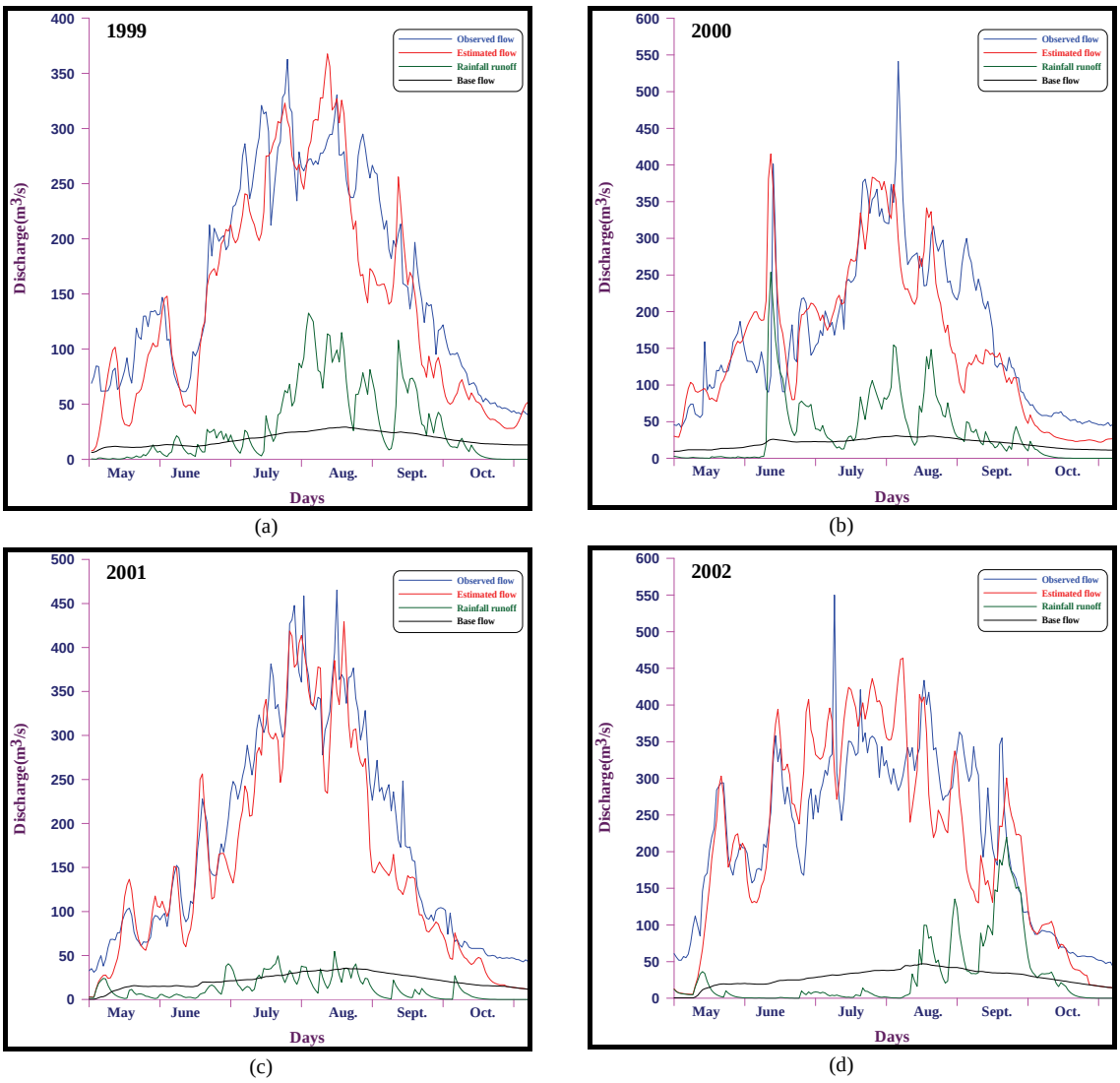

Figure 7. (a) Different Components of simulated runoff for summer season 1999 for the Bhagirathi basin upto Loharinag Pala; (b) Different Components of simulated runoff for summer season 2000 for the Bhagirathi basin basin upto Loharinag Pala; (c) Different Components of simulated runoff for summer season 2001 for the Bhagirathi basin basin upto Loharinag Pala; (d) Different Components of simulated runoff for summer season 2002 for the Bhagirathi basin basin upto Loharinag Pala.

Table 3. Percentage difference in volume, model efficiency and contributions of rain snow and base flow computed by the model.

Year	Model	Percentage Diff. in Vol.	Model efficiency (%)	Rain (%)	Snow (%)	Base flow (%)
1999	SNOW MOD	-19.12%	88%	20.5	66.71	12.73
2000	SNOW MOD	-14.33%	80%	23.06	63.81	13.12
2001	SNOW MOD	-18.76%	93%	8.14	77.95	13.90
2002	SNOW MOD	-8.55%	83%	13.50	73.67	12.82

computed by the model are summarized in **Table 4** all the years. Most of the high peaks observed in the daily flow hydro graphs are generally during the months of July and August attributed to the glacier melt. Thus these months are considered as the peak melting season in the western Himalayan region. However, sometimes the flow resulting due to high intensity rainfall also reflects the peaks in the daily flow hydrographs. The simulation of base flow indicates that the baseflow contribution to the streamflow increases as the season advances, being

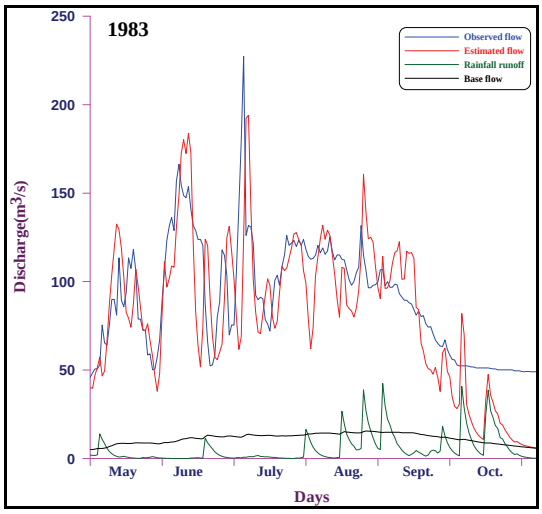

(a)

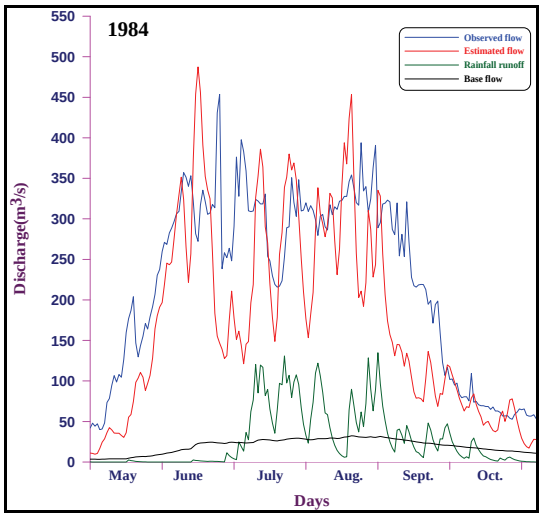

(b)

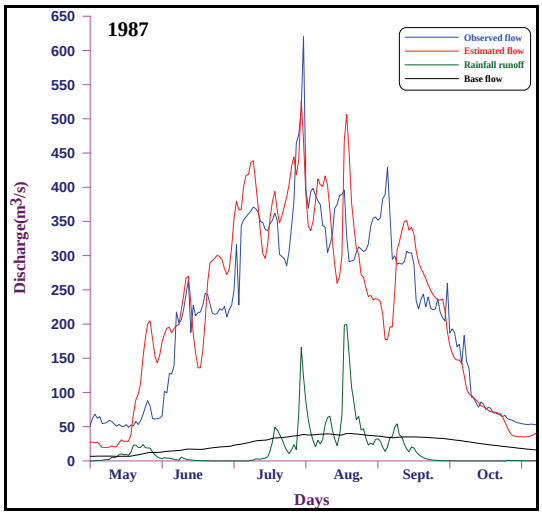

(c)

Figure 8. (a) Different Components of simulated runoff for summer season 1983 for the Dhauliganga basin; (b) Different Components of simulated runoff for summer season 1984 for the Dhauliganga basin; (c) Different Components of simulated runoff for summer season 1987 for the Dhauliganga basin.

Table 4. Percentage difference in volume, model efficiency and contributions of rain snow and base flow computed by the model

Year	Model	Per-centage Diff. in Vol.	Model effi-ciency (%)	Rain (%)	Snow (%)	Base flow (%)
1983	Snowmod	–18.36%	69%	6.91	79.23	13.95
1984	Snowmod	–25.59%	73%	16.17	72.22	11.62
1987	Snowmod	–5.35%	86%	7.98	80.61	11.40

at maximum during the peak season and then starts decreasing.

5. Conclusions

1) The model simulated daily streamflow of River Bhagirathi satisfactorily for all the three years, providing coefficient of determination (R^2) above average 0.85, and average volume difference (D_v) about –15.19 %. There is need to test the model using a longer hydro meteorological database. To improve the model, a better representation of melt rate in the accumulation and ablation zones and its variation with time, has to be incorporated. Results also strengthen the view of strong storage and drainage characteristics of the glacier, which need further investigation. Rain contributions, snow contribution and base flow to stream discharge, have been computed using snowmod model. In the total discharge the maximum snow/ice contribution has been found out to be 63.81% to 77.95% whereas the rainfall contribution was in the range 8.14% and 23.06% and the baseflow contribution in the range 12.73% to 13.90% of the total discharge. The average contribution of the snowmelt, rainfall runoff and base flow during the study period 1999, 2000, 2001 and 2002 were found to be 70.54%, 16.30%, and 13.14% respectively.

2) The model simulated daily streamflow of Dhauli-Ganga river satisfactorily for all the three years, providing coefficient of determination (R^2) above average 0.76, and average volume difference (D_v) about –16.43%. The maximum contribution has been found for the snow component 79.23% to 80.61% of the total discharge, the rainfall component occurred to be 6.91% to 17.67% and the base flow contributed 11.40% to 13.95% of the total discharge. The average contribution of the snowmelt, rainfall runoff and base flow during the study period 1983, 1984 and 1987 were found to be 77.35%, 10.35% and 12.32% respectively.

6. References

[1] V. K. Raina and D. Srivastava, "Glacier Atlas of India," Geological Society of India, Bangalore, 2008, p. 315.

[2] P. Kasser, "Fluctuation of Glaciers (1959-1965)," United Nations Educational, Scientific and Cultural Organization, Paris, 1967.

[3] P. Singh, S. K. Jain and N. Kumar, "Estimation of Snow and Glacier-Melt Contribution to the Chenab River, Western Himalaya," *Mountain Research Development*, Vol. 17, No. 1, 1997, pp. 49-56.

[4] P. Singh and S. K. Jain, "Snow and Glacier Melt in the Satluj River at Bhakra Dam in the Western Himalayan Region," *Hydrological Sciences*, Vol. 47, No. 1, 2002, pp. 93-106.

[5] V. Kumar, P. Singh and V. Singh, "Snow and Glacier Melt Contribution in the Beas River at Pandoh Dam, Himachal Pradesh, India," *Hydrological Sciences Journal*, Vol. 52, No. 2, 2007, pp. 376-388.

[6] "Runoff Evaluation and Streamflow Simulation by Computer," Part II, US Army of Engineers, North Pacific Division, Portland, 1971.

[7] E. A. C. Anderson, "The National Weather Service River Forecast System — Snow Accumulation and Ablation Model," National Oceanic and Atmospheric Administration, Washington, D.C., 1973.

[8] S. Finsterwalder and H. Schunk, "Der Suldenferner," *Oesterreichischer Alpenverein*, Vol. 18, 1987, pp. 72-89.

[9] J. Martinec, A. Rango and R. Roberts, "Snowmelt Runoff Model (SRM) User's Manual (Version 3.0)," In: M. Baumgartner, Ed., Department of Geography, University of Bern, Switzerland, 1994.

[10] M. C. Quick and A. Pipes, "UBC Watershed Model Manual (Version 4.0)," University of British Columbia, Vancouver, 1995.

[11] P. Singh and V. P. Singh, "Snow and Glacier Hydrology," Kluwer, Dordrecht, 2001.

[12] P. Singh and S. K. Jain, "Modelling of Streamflow and its Components for a Large Himalayan Basin with Predominant Snowmelt Yield," *Hydrological Sciences*, Vol. 48, No. 2, 2003, pp. 257-276.

J. Water Resource and Protection, **2010, 2, 644-650**
doi:10.4236/jwarp.2010.27074 Published Online July 2010 (http://www.SciRP.org/journal/jwarp)

Photocatalysis of Naphthenic Acids in Water

Sabyasachi Mishra[1,2*], Venkatesh Meda[2], Ajay K. Dalai[2], Dena W. McMartin[3], John V. Headley[4], Kerry M. Peru[4]
[1]*College of Agricultural Engineering and Post Harvest Technology, Central Agricultural University, Ranipool, Gangtok, Sikkim, India*
[2]*College of Engineering, University of Saskatchewan, Saskatoon, Canada*
[3]*Environmental Systems Engineering, University of Regina, Regina, Canada*
[4]*Water Science and Technology Directorate, Environment Canada, Saskatoon, Canada*
E-mail: *s.mishra@usask.ca*
Received April 23, 2010; *revised May* 24, 2010; *accepted May* 30, 2010

Abstract

Naphthenic acids (NAs) are soluble in water and are concentrated in oil sand process water (OSPW) as a result of caustic oil sands extraction processes. Significant environmental and regulatory attention has been focused on the naphthenic acids. A laboratory scale photocatalysis system was developed using UV_{254} florescent lamps. Experiments were conducted to determine the NA degradation efficiency of this system in presence of TiO_2 catalyst. Degradation kinetics for total NAs as well as individual z-families was calculated. The developed treatment system was able to degrade OSPW NAs with half life values ranging between 1.55 and 4.80 h. This system also completely reduced the acute toxicity associated with NAs (up to 5 min. IC_{50} v/v > 90%) based on Microtox assays.

Keywords: Photocatalysis, Naphthenic Acids, Treatment, Kinetics, Toxicity

1. Introduction

Naphthenic acids (NAs) are natural constituents of bitumen and the oxidative product of petroleum hydrocarbons. NAs are solubilized and concentrated in oil sand process water (OSPW) during oil sands extraction and enter surface and subsequently ground water systems through mixing and/or erosion of riverbank adjacent to oil sands deposits [1]. Clemente *et al.* [2] reported that OSPW in the Athabasca Oil Sands (AOS) north of Fort McMurray (Alberta, Canada) may contain NAs as high as 110mg/L. NA contaminated water can cause gastrointestinal disturbances, effects on the formation of blood platelets, cell proliferation, and respiration [3].

In addition to contributing to OSPW toxicity, NAs cause corrosion in the oil sands refining processes. Most natural NAs occur in their sulfide form, mainly responsible for corrosivity. Availability of carboxylic groups in the NA structure to react with metal ions contributes to this property [4] and also determines the extent of corrosiveness [2]. Corrosion due to NAs is a major concern for petroleum refineries, which limits the choice of materials used in equipment and supply chain.

To address these concerns, many methods have been reported to date, having potential to be used for treating water contaminated with naphthenic acids, including: chemical [5,6], bio-remediation [1,7-11], and photolysis/ photocatalysis treatment [12-14]. These processes, in their present forms, invariably use expensive chemicals, require long retention times, and have large annual operating costs. Among all these treatment methods cited above, photocatalysis, with all its variations and improvements, is considered to bring a revolutionary approach to address the current environmental problems. In this regard, McMartin [12,13] reported that photolysis in presence of sunlight is effective for selective degradation of NAs. Application of UV radiation increased the NAs degradation rate. Photolysis not only degrades NAs, but can also increase their bioavailability. Headley *et al.* [14] reported that photodegradation of NAs on TiO_2 surface is efficient under natural sunlight. Further research is necessary to modify this treatment method for better environmental adaptability.

Photocatalysis in presence of UV light and a catalyst have not been reported for either degradation or increased bioavailability of NAs. To study this potential remediation method, a laboratory scale photocatalysis system is described in the work reported herein. The

ability of the system to degrade NAs and reduce toxicity was evaluated. The main objectives of this research were to develop and evaluate a laboratory scale photocatalysis system for the treatment of naphthenic acids in water and to conduct feasibility study for degradation and detoxification of naphthenic acid mixtures in water.

2. Materials and Methods

2.1. Experimental Design and Setup

A photocatalysis system (**Figure 1**) was designed using UV fluorescent tubes (Philips Ltd., Saskatoon, SK, 8W) and concentric shell water jacketed quartz photo cells. This double-jacketed quartz reactor for photocatalysis was fabricated at the scientific glass blowing facility at the University of Victoria, BC, Canada. Cooling water was circulated through the outer shell to reduce heating load due to the UV source.

Three variables, NAs, water and TiO_2, were chosen based on 1 × 2 × 2 × 2 full factorial design with one treatment method, two types of NAs, two water sources, and two TiO_2 conditions. Both Fluka and OSPW NAs were used; deionized (Milli-Q) water and water from South Saskatchewan River at Saskatoon, SK, were tested in the presence as well as absence of particulate TiO_2 catalyst with a concentration of 0.3 g/L. Therefore, eight treatment combinations for the treatment system were tested (**Table 1)**. Four initial concentrations (40, 60, 80, and 100 ppm) were evaluated in triplicate. Samples were collected every 30 min. for 5 h.

Figure 1. Photocatalysis setup with UV lamps.

Table 1. Photocatalysis experiment combinations.

Combinations	Explanation
Fluka-DI	Fluka NAs with deionized water
Fluka-DI-TiO_2	Fluka NAs with deionized water and TiO_2
Fluka-RW	Fluka NAs with river water
Fluka-RW-TiO_2	Fluka NAs with river water and TiO_2
OSPW-DI	OSPW NAs with deionized water
OSPW-DI-TiO_2	OSPW NAs with deionized water and TiO_2
OSPW-RW	OSPW NAs with river water
OSPW-RW-TiO_2	OSPW NAs with river water and TiO_2

2.2. Extraction of OSPW Naphthenic Acids

OSPW was collected from an oil sands extraction operation (Fort McMurray, AB, Canada) to produce the authentic NAs mixture. The NAs were extracted from OSPW using an adapted liquid-liquid extraction method described by Janfada *et al*. [15]. The final concentration of the NAs extract was determined by serial dilution and comparison to an aliquot of the oil sands NA extract produced by Rogers *et al*. [16] and was found to be 6,800 mg/L. A five-point linear regression curve was created for quantification of the NA extract used herein and further verified by integrated area comparison of LC-MS results for both the OSPW NAs extract and those for the commercially available Fluka NAs. The two methods were correlated confirming the OSPW NAs extract concentrations. OSPW NAs solutions were prepared by the dilution method (**Table 2**).

2.3. Sample Preparation

Commercially available Fluka NAs (Sigma-Aldrich, Oakville, ON) and an authentic OSPW NA extract were used in experiments to determine degradation kinetics of NAs in water with or without TiO_2 catalyst under UV_{254}. A 4000 ppm stock solution of NAs was prepared in methanol to produce desired concentrations for experimentation (**Table 2**). For environmental relevance, samples were prepared at concentrations ranging between 40 and 100 ppm at 20 ppm intervals.

2.4. Quantification and Analysis of NAs

Electrospray ionization mass spectrometry (ESI-MS) in negative mode was used to quantify and characterize naphthenic acid concentration in the samples using method described by Headley *et al*. [17]. This method allowed for a detection limit of 0.01 mg/L [12,17,18].

Kinetic analysis of the degradation of NAs in water was done considering a pseudo first order reaction

Table 2. Sample preparation with naphthenic acids.

Concentration (ppm)	Sample (mL)	NA (mg)	Fluka NA Stock (µL)	OSPW NA Stock (µL)
40	100	4	1000	1500
60	100	6	1500	2000
80	100	8	2000	2500
100	100	10	2500	3000

mechanism [12,13], with the rate constant and the half-life period calculated by Integrated Rate Law.

SPSS 14.0 for Windows (SPSS Inc., Chicago, IL) was used to analyze data statistically. Error bars were plotted for each treatment. SPSS was also used to perform univariate analysis of variance (ANOVA) and Tukey's HSD test. Tukey's HSD test examines all pair wise comparisons among means. ANOVA was performed to analyze treatment means and Tukey's HSD test was done to compare the treatment means.

Toxicity of the samples before and after treatment was determined using Microtox assay at ALS Labs (Saskatoon, SK). Microtox Analyzer (Model #500, Strategic Diagnostics Inc., Newark, DE) with test organism *Vibrio fischeri* was used following the reference method proposed by Environment Canada (ERS1/RM/24). IC_{50} value (max 100%), the half maximal (50%) inhibitory concentration (IC) of a substance, was measured at residence times of 5, 15 and 30 mins. for each of the sample before and after treatment.

3. Results and Discussion

The NA standards were analyzed at room temperature

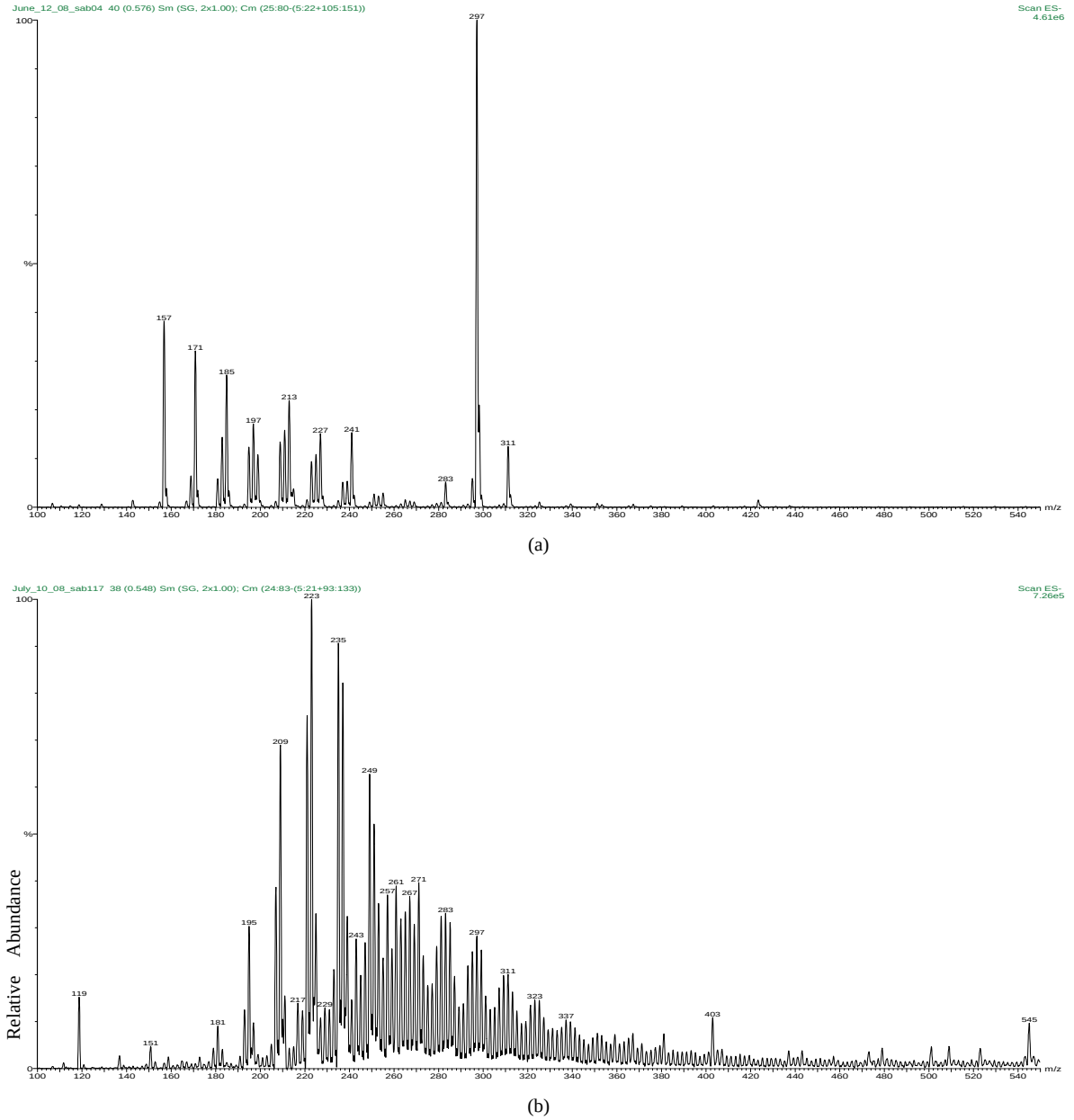

(b)

Figure 2. Mass spectra of (a) Fluka NAs and (b) OSPW NAs standards.

(22 ± 2)˚C. The percentage relative abundance of individual species of NAs is shown in **Figure 2**. Comparison of carbon number and z-family distribution are given in **Figure 3**. Components with lower mass to charge (m/z) ratio (157-297 m/z) are predominant in Fluka NAs. OSPW NAs constituents have comparatively higher m/z ratios (195-325 m/z). This composition difference affects the photodegradation and toxicity of NAs mixtures.

Rate constant values for each of the treatments can be seen in **Figure 4**. Results (R^2 = 0.944) indicate that initial concentration of the sample has no effect on the reaction kinetics of the NA degradation. Keeping other variables, such as type of water and TiO_2, constant; the system took less time to degrade OSPW NAs than Fluka NAs. This difference in degradation rates may be due to the presence of NA-like compounds present in OSPW NAs.

Frank *et al*. [19] suggested that OSPW NAs extracts contain multi-carboxylic groups in their structures. Such dicarboxylic acids are susceptible to photo-oxidation on the surface of TiO_2. Presence of other components containing aromatic functional groups, sulphur, nitrogen, and unsaturated groups likely contribute to the difference in rates observed [20]. Thus, photocatalysis degraded OSPW NAs more rapidly than the commercial NAs. The use of TiO_2 increased the reaction rate and made the de gradation process faster with shorter half-life period because of the catalytic effect of TiO_2. Similarly, the type of water has significant effect on the degradation process of NAs.

The use of river water made the degradation process slower as compared to deionized water for both Fluka and OSPW NAs extract. This can be attributed to the matrix effect of others salts and materials present in the river water [21]. For applied photocatalysis, NAs degradation was more rapid for the combination of OSPW NAs in deionized water and with TiO_2 compared to river water. Comparative chromatograms of the results before treatment and after 5 h of treatment are also provided (**Figure 5**). The chromatograms suggest that the lower molecular weight NAs are more readily degraded compared to higher molecular weight NAs.

The distribution of carbon number and z-family data of the NAs sample prior to and after treatment indicates selective degradation of lower molecular weight NAs (**Figure 6**). NAs in the z = –4 and –6 (two and three-ring NAs) families with carbon numbers ranging from 12 to 15 displayed the greatest concentration reduction after treatment. Similar results were observed for NAs with higher z values (z = –12, six ring NAs). This might be due to the presence of NA-like compounds with multi-carboxylic groups in their structures, which degrade faster as compared to classical NAs. This contributes to the higher overall degradation rate of NAs. Further investigation, using ultra high resolution MS, is necessary to study the influence of these NA co-extracts on the degradation kinetics.

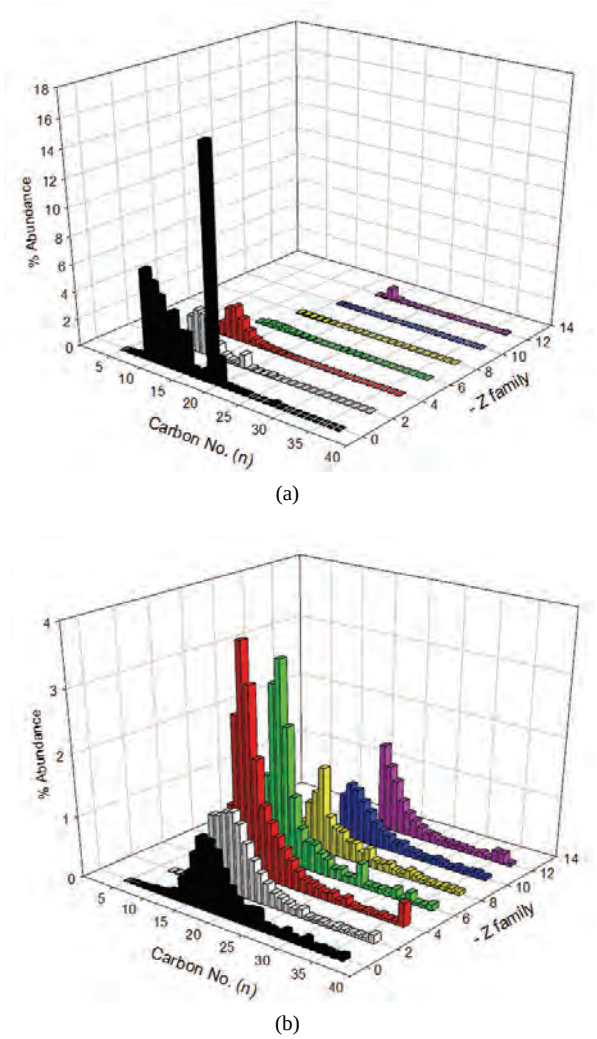

Figure 3. Comparison of carbon no. and z-family distribution for (a) Fluka NAs; (b) OSPW NAs.

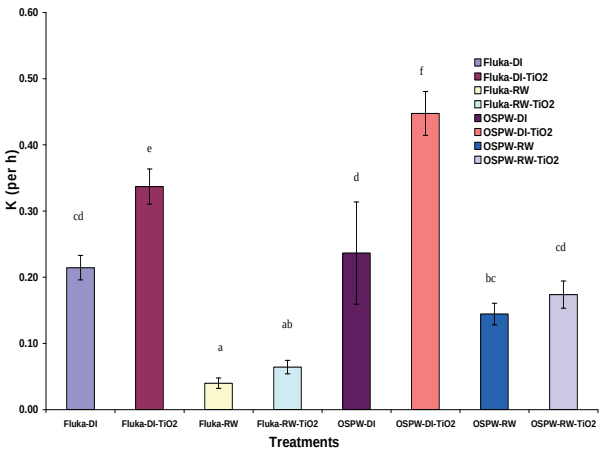

Figure 4. Rate constants (k) for different treatment combinations (R^2 = 0.944); means with the same letter designation are not different (P = 0.05) by Tukey's HSD test.

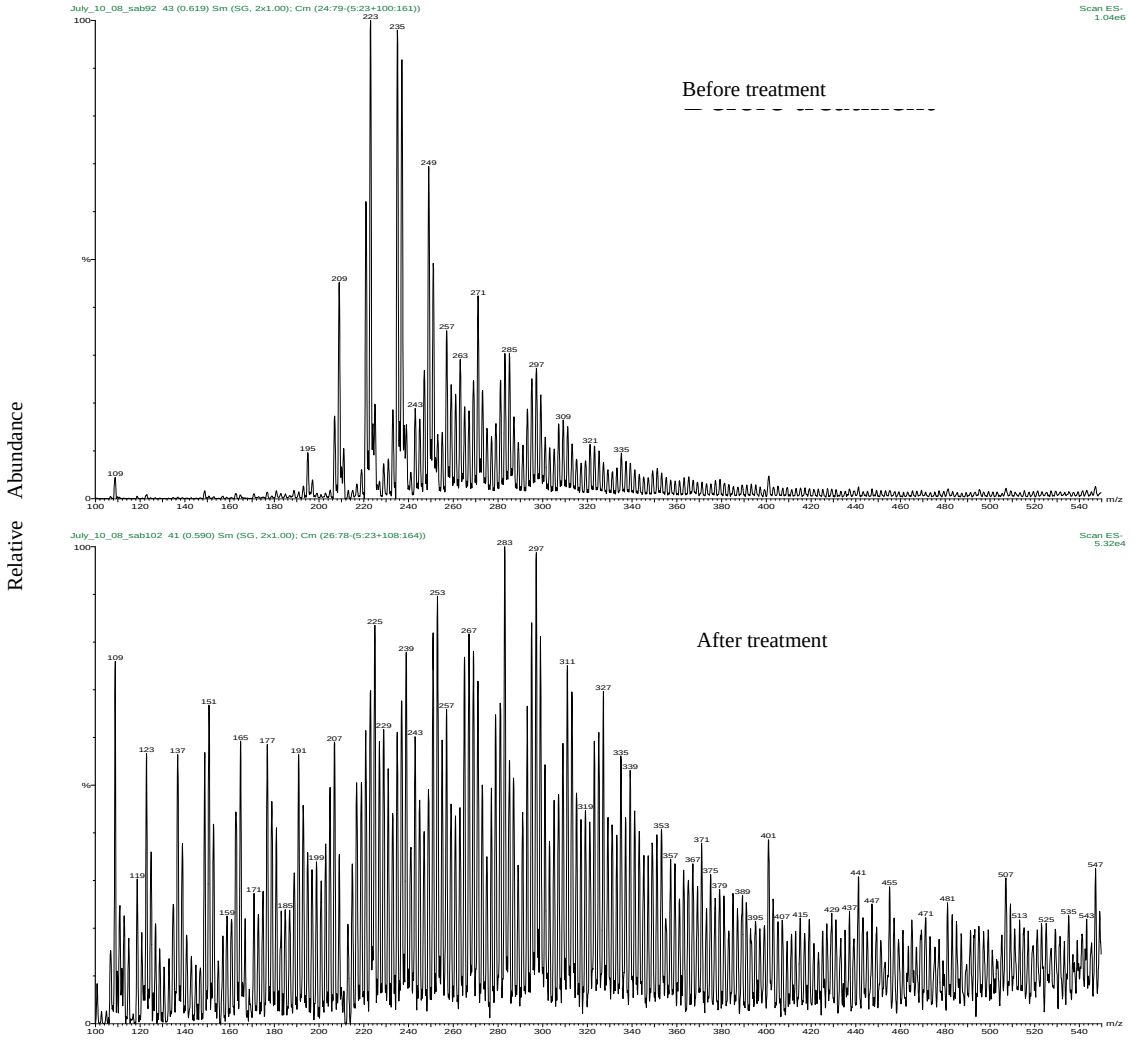

Figure 5. Mass spectral comparison of the OSPW NA extract before and after treatment for 5 h at 24°C.

The results from univariate analysis of variance, clearly show that the source of NAs, type of water, and presence of TiO_2, all have contributed significantly to rate constant of the degradation process (at P = 0.05). Also, the interaction between the type of water and use of TiO_2 had significant effect on the rate constant. The optimal pseudo-first order rate constant (k) and half-life value under the conditions investigated were 0.447 (h^{-1}) and 1.55 h, respectively.

Apparent distribution of concentrations of individual NAs according to z value was determined after further data mining. Corresponding degradation rate constants for individual z series were calculated (**Figure 7**). The results show that NAs with z = –4 and –6 were more rapidly degraded than rest of the z-series. Furthermore, NAs with higher z values degraded faster than linear and single ring NAs. This may be due to the presence of unsaturated NA-like compounds [4,19] with higher cyclization, which both degrade faster and contribute to faster degradation reaction kinetics of NAs with higher z. It is also possible that the results are due to the use of low resolution ESI-MS for NAs analysis, which has been reported to indicate substantial false-positive detections and misclassification of OSPW NAs [20], thereby overestimating the NA concentration in the sample. There is a valid need of further data mining using high and ultra high resolution MS to support these findings.

Microtox toxicity tests were completed using the pre- and post-treatment samples exhibiting the highest rate of degradation reaction (OSPW NAs in deionized water with TiO_2). The Mictrotox results are provided in **Table 3**. High toxicity of the sample with 30 min. IC_{50} v/v (%) as 15.65% could be treated and detoxified completely with final 30 min. IC_{50} v/v (%) as more than 90%. Similar

results were found for the OSPW NAs in river water with TiO_2 (**Table 4**). Moderate to high toxicity of the sample with 30 min. IC_{50} v/v (%) as 20.11% could be treated and detoxified completely with final 30 min. IC_{50} v/v (%) value as more than 90 %. This decrease in toxicity can be attributed to the selective degradation of lower molecular weight NAs (with z = –4 and –6), which are generally considered responsible for the majority of NAs toxicity.

4. Conclusions

The developed system is effective in degrading both commercial NAs and OSPW NA extracts rapidly, with half life values ranging between 1.55 and 17.37 h for the various treatments investigated. The apparent rate constants of degradation of NAs according to their z values were also determined. The photocatalytic system was also shown effective for completely removing toxicity of NAs as confirmed using Microtox tests. Since the results are based on ESI-MS analysis that is not optimal for distinguishing between classical NAs and other NA-like compounds in the sample, further investigation using high and ultra high resolution MS is recommended.

Table 3. Microtox toxicity results for OSPW NA extract in deionized water with TiO_2.

Parameters	Before Treatment	After Treatment
5 min. IC_{50} v/v (%)	25.92	> 90%
95% Confidence Interval v/v (%)	23.54 to 28.54	N/A
15 min. IC_{50} v/v (%)	18.34	> 90%
95% Confidence Interval v/v (%)	16.92 to 19.88	N/A
30 min. IC_{50} v/v (%)	15.65	> 90%
95% Confidence Interval v/v (%)	14.20 to 17.24	N/A
Temperature (ºC)	6.0	6.0
pH	9.67	7.66
Toxicity	High toxicity	No toxicity

Table 4. Microtox toxicity results for OSPW NA extract in river water with TiO_2.

Parameters	Before Treatment	After Treatment
5 min. IC_{50} v/v (%)	30.84	> 90%
95% Confidence Interval v/v (%)	28.61 to 33.24	N/A
15 min. IC_{50} v/v (%)	22.92	> 90%
95% Confidence Interval v/v (%)	21.75 to 24.15	N/A
30 min. IC_{50} v/v (%)	20.11	> 90%
95% Confidence Interval v/v (%)	19.05 to 21.22	N/A
Temperature (ºC)	15.0	15.0
pH	8.86	8.31
Toxicity	Moderate toxicity	No toxicity

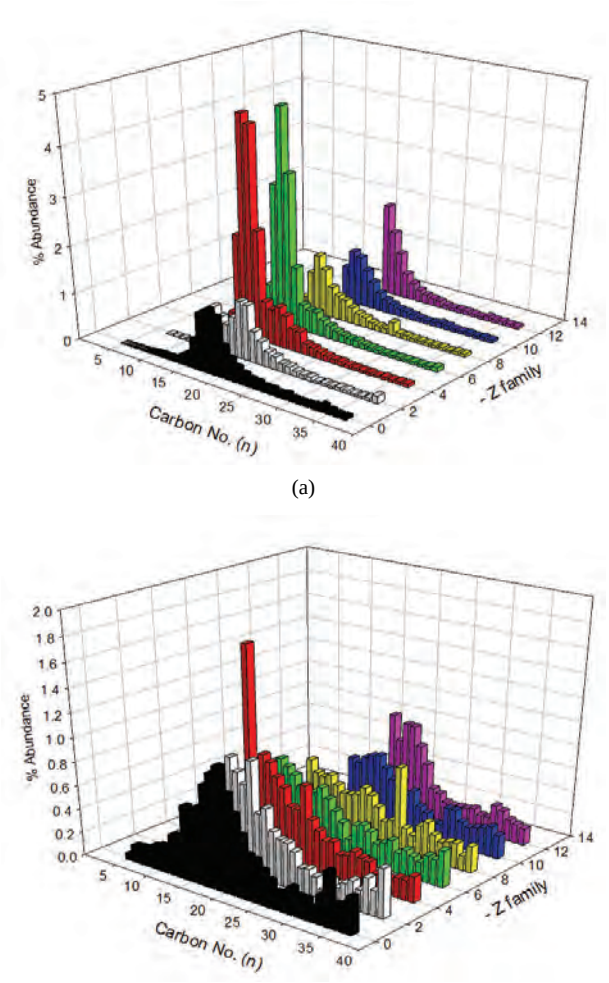

Figure 6. OSPW NA extract (a) before and (b) after treament with respect to carbon No. and z-family.

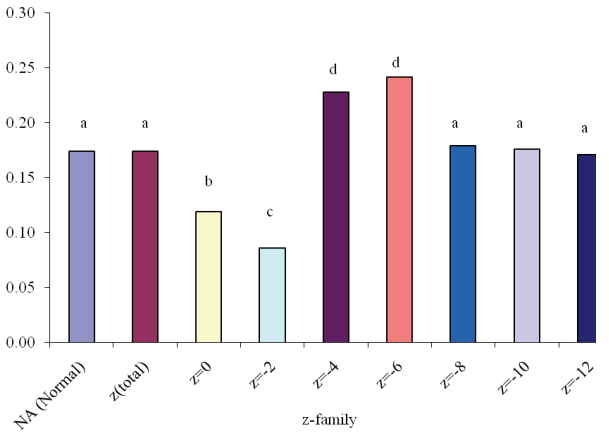

Figure 7. Variation of rate constant "k" with z-family of OSPW NAs in river water due to photocatalysis for 5 h.

5. Acknowledgements

The authors thank Communities of Tomorrow (CT), Natural Science and Engineering Research Council (NSERC) and Science Horizons Youth Award for funding this work and, Central Agricultural University, India for providing facilities to prepare the manuscript.

6. References

[1] J. V. Headley and D. W. McMartin, "A Review of the Occurrence and Fate of Naphthenic Acids in Aquatic Environments," *Journal of Environmental Science and Health*, Part A, Vol. 39, No. 8, 2004, pp. 1989-2010.

[2] J. S. Clemente and P. M. Fedorak, "A Review of the Occurrence, Analyses, Toxicity and Biodegradation of Naphthenic Acids," *Chemosphere*, Vol. 60, No. 5, 2005, pp. 585-600.

[3] L. E. J. Lee, K. Haberstroh, D. G. Dixon and N. C. Bols, "Salinity Effects on the Toxicity of Naphthenic Acids to Rainbow Trout Cell Lines," *Proceedings of the* 27*th Aquatic Toxicity Workshop*, Halifax, October 2000.

[4] R. A. Frank, K. Fischer, R. Kavanagh, B. K. Burnison, G. Arsenault, J. V. Headley, K. M. Peru, G. V. D. Kraak and K. R. Solomon, "Effect of Carboxylic Acid Content on the Acute Toxicity of Oil Sands Naphthenic Acids," *Environmental Science and Technology*, Vol. 43, No. 2, 2009, pp. 266-271.

[5] M. D. MacKinnon and H. Boerger, "Description of Two Treatment Methods for Detoxifying Oil Sands Tailings Pond Water," *Water Pollution Research Journal of Canada*, Vol. 21, No. 4, 1986, pp. 496-512.

[6] A. C. Scott, W. Zubot, M. D. MacKinnon, D. W. Smith and P. M. Fedorak, "Ozonation of Oil Sands Process Water Removes Naphthenic Acids and Toxicity-Technical Note," *Chemosphere*, Vol. 71, No. 1, 2008, pp. 156-160.

[7] E. K. Quagraine, H. G. Peterson and J. V. Headley, "In Situ Bioremediation of Naphthenic Acids Contaminated Tailing Pond Waters in the Athabasca Oil Sands Region —Demonstrated Field Studies and Plausible Options: A Review," *Journal of Environmental Science and Health*, Part A, Vol. 40, No. 3, 2005, pp. 685-722.

[8] A. C. Scott, M. D. MacKinnon and P. M. Fedorak, "Naphthenic Acids in Athabasca Oil Sands Tailings Waters are Less Biodegradable Than Commercial Naphthenic Acids," *Environmental Science and Technology*, Vol. 39, 2005, pp. 8388-8394.

[9] O. V. Biryukova, P. M. Fedorak and A. Q. Sylvie, "Biodegradation of Naphthenic Acids by Rhizosphere Microorganisms," *Chemosphere*, Vol. 67, No. 10, 2007, pp. 2058-2064.

[10] S. A. Armstrong, "Dissipation and Phytotoxicity of Oil Sands Naphthenic Acids in Wetland Plants," Ph.D. Dissertation, University of Saskatchewan, Saskatoon, 2008.

[11] X. Han, A. C. Scott, P. M. Fedorak, M. Bataineh and J. W. Martin, "Influence of Molecular Structure on the Biodegradability of Naphthenic Acids," *Environmental Science and Technology*, Vol. 42, No. 4, 2008, pp. 1290-1295.

[12] D. W. McMartin, "Persistence and Fate of Acidic Hydrocarbons in Aquatic Environments: Naphthenic Acids and Resin Acids," Ph.D. Dissertation, University of Saskatchewan, Saskatoon, 2003.

[13] D. W. McMartin, J. V. Headley, D. A. Friesen, K. M. Peru and J. A. Gillies, "Photolysis of Naphthenic Acids in Natural Surface Water," *Journal of Environmental Science and Health*, Part A, Vol. 39, No. 6, 2004, pp. 1361-1383.

[14] J. V. Headley, J. Du, K. M. Peru, D. W. McMartin, "Electrospray Ionization Mass Spectrometry of the Photodegradation of Naphthenic Acids Mixtures Irradiated with Titanium Dioxide," *Journal of Environmental Science and Health*, Part A, Vol. 44, No. 6, 2009, pp. 591-597.

[15] A. Janfada, J. V. Headley, K. M. Peru and S. L. Barbour, "A Laboratory Evaluation of The Sorption of Oil Sands Naphthenic Acids on Organic Rich Soils," *Journal of Environmental Science and Health*, Part A, Vol. 41, No. 6, 2006, pp. 985-997.

[16] V. V. Rogers, K. Liber and M. D. MacKinnon, "Isolation and Characterization of Naphthenic Acids from Athabasca Oil Sands Tailings Pond Water," *Chemosphere*, Vol. 48, No. 5, 2002, pp. 519-527.

[17] J. V. Headley, K. M. Peru, D. W. McMartin and M. Winkler, "Determination of Dissolved Naphthenic Acids in Natural Waters Using Negative-Ion Electrospray Mass Spectrometry," *Journal of the AOAC International*, Vol. 85, No. 1, 2002, pp. 182-187.

[18] J. V. Headley, K. M. Peru, M. P. Barrow and P. J. Derrik, "Characterization of Naphthenic Acids from Athabasca Oil Sands Using Electrospray Ionization: The Significant Influence of Solvents," *Analytical Chemistry*, Vol. 79, No. 16, 2007, pp. 6222-6229.

[19] R. A. Frank, R. Kavanagh, B. K. Burnison, G. Arsenault, J. V. Headley, K. M. Peru, G. V. D. Kraak and K. R. Solomon, "Toxicity Assessment of Collected Fractions from an Extracted Naphthenic Acid Mixture," *Chemospere*, Vol. 72, No. 9, 2008, pp. 1309-1314.

[20] J. W. Martin, X. Han, K. M. Peru and J. V. Headley, "Comparison of High- and Low-Resolution Electrospray Ionization Mass Spectrometry for the Analysis of Naphthenic Acid Mixtures in Oil Sands Process Water," *Rapid Communication in Mass Spectrometry*, Vol. 22, No. 12, 2008, pp. 1919-1924.

[21] S. Mishra, "Microwave Assisted Photocatalytic Treatment of Naphthenic Acids in Water," Ph.D. Dissertation, University of Saskatchewan, Saskatoon, 2009.

J. Water Resource and Protection, **2010, 2, 651-659**
doi:10.4236/jwarp.2010.27075 Published Online July 2010 (http://www.SciRP.org/journal/jwarp)

The Influence of Seawater on a Coastal Aquifer in an International Protected Area, Göksu Delta Turkey

Zeynel Demirel
Mersin University Engineering Faculty, Environmental Engineering Department, Mersin, Turkey
E-mail: *zdemirel@mersin.edu.tr*
Received March 22, 2010; *revised June* 8, 2010; *accepted June* 15, 2010

Abstract

Göksu Delta is an important wetland where the Göksu River reaches the sea in the eastern part of the town of Tasucu-Ice1. The delta is classified as a Wetland of International Importance according to the Ramsar Convention. In the Göksu Delta area, urban and agricultural expansions have caused an ever-growing need for fresh water. High groundwater pumping rates and overexploitation of the aquifers, leading to seawater mixing in the Göksu coastal aquifers. The chemical types of groundwater from alluvial aquifer are Ca-Mg-HCO_3, but in the region where sea water mixing is occurred it changes and the Na and Cl ions are added to groundwater. The similar occurrence can be observed in the groundwater from the limestone aquifer. The chemical types of groundwater are Ca-HCO_3 or Ca-Mg-HCO_3 and they change to Ca-Na-Mg-HCO_3-Cl in the vicinity of seawater mixing regions. A statistical comparative analysis also shows that some of the samples are affected by sea water mixing. The extent of seawater intrusion is reflected by the distribution of salinity and electrical conductivity as an equiconcentration map.

Keywords: Göksu Delta-Turkey, Ramsar Convention, Sea Water Intrusion, Statistical Comparative Analysis, Geographic Information System

1. Introduction

The Göksu Delta is formed by the Goksu River near the Southern part of Silifke, a town in Turkey's Mediterranean region. Göksu Delta is an important wetland (15000 ha) where the Göksu River reaches the sea in the eastern of the town Tasucu-Ice1 [1].

The Mediterranean coastline stretching from the city of Taşucu to the Susanoğlu region is heavily populated due to urban developments (villas, apartments, complexes, and multi-storey buildings) in the last fifteen years, though most of these structures are occupied only in the summer season for vacation purposes. Because of an increased population influx from the surrounding cities, especially during the peak season (May to September), the population of this region has increased several times.

The Göksu Delta is not only an urban area but it is also surrounded by densely cultivated orchards (mostly citrus), traditional vegetable farms and greenhouse cultivations, where farming activities continue all year long due to the favorable climate.

In the Göksu Delta area, urban and agricultural expansions have caused an ever-growing need for fresh water. In this region, water supply for most municipalities, domestic use water for urban developments and irrigated water for agricultural activities are almost exclusively provided through hand dug or drilled wells. Therefore, water resources in the Göksu Delta area are subjected to intensive demands, stresses and pollution risks [2]. The expansion of irrigated agriculture induces the risk of groundwater quality degradation through high groundwater pumping rates and overexploitation of the aquifers, leading to seawater intrusion in the coastal aquifers.

Göksu Delta is an internationally important wetland due to its location being on a bird migration route. The Environmental Protection Department of the Ministry of Environment has declared the Göksu Delta as a Special Environmental Protection Zone to protect the area against pollution and exploitation, and to ensure that natural resources and cultural assets have a future. The delta is classified as a Wetland of International Importance according to the Ramsar Convention on Wetlands of International Importance. The Goksu Delta has also a special significance for being one of the few remaining areas in the world where sea turtles (Caretta caretta, Chelonia mydas) and blue crabs (Callinectes sapidus) lay their eggs [1,3].

Under steady-state conditions, a state of equilibrium is

established between seawater and freshwater in Göksu coastal alluvial aquifer. However, owing to increasing demand for water, groundwater may be subjected to over-exploitation and the natural equilibrium is thus disturbed. This results in aggressive seawater mixing, which may even reach the inland aquifer.

The purpose of this study is to understand the seawater intrusion into groundwater, to investigate the pollution of groundwater by sea water and pictorially represent it using the geographic information system (GIS).

2. Site Description

The Göksu Delta is situated in the Mediterranean Sea region of the southeastern part of Turkey and extends from 36°15-36°25 of latitude north to 33°55-34°05 of longitude west. The Göksu Delta area is bounded by the Taurus Mountains on the northern side and by the Mediterranean Sea on the southern and eastern side. The southern portion of the Göksu Delta area is a delta plain made up of sediments from Göksu River. The Goksu River flow regime is strongly dependent on the seasonal rains and temperature. The average flow of Goksu River is 130 m^3/s where it reaches the highest value during May.

In the Göksu Delta area, climate is characterized by hot and dry periods in the summer and by warm and wet periods in the winter, which is typical for the coastal zones around the Mediterranean Sea. The mean annual temperature in this area is 19°C. Showers start in October, and continue until mid April and the maximum rainfall occurs in December. The Göksu Delta area receives slightly higher than 607 mm of precipitation annually, and extended periods (*i.e.*, 3-4 months) without precipitation are common

The study area was located in the southern part of Miocene carbonate rocks of the Taurus Mountains Belt.

The oldest rock unit of the Göksu Delta is the Akdere Formation from the Paleozoic Age, which consists of marble, schist and quartzite. The Akdere Formation (middle-upper Devonian) is generally found in the northern part of the study area. Kusyuvası Formation (Middle Trias) consists of limestone. The Tokmar Formation (upper Jura-lower Cretaceous) is found in the western part of delta and contains dolomite and limestone.

Tertiary units are composed of lower-middle Miocene Karaisali formation and middle-upper Miocene Kuzgun formation (**Figure 1**). Tertiary rocks consist of a succession of marine, lacustrine and fluvial deposits, which display transitional characteristics both vertically and areally in the study area.

The Quaternary basin-fill deposits are a heterogeneous mixture of metamorphic and sedimentary rock detritus ranging from clay to boulder size. The mixture includes stream alluvium, stream-terrace deposits, fan deposits, delta deposits, shore deposits. The basin-fill deposits vary greatly in lithology and grain-size, both vertically and areally. Accordingly, the hydraulic properties of these deposits can differ greatly over short distances, both laterally and vertically.

The alluvial aquifer consists of a heterogeneous mixture of gravel, sand, silt, clay and sandy-clay. Conceptually the aquifer system in the delta is an unconfined aquifer and more than 500 m thick. Recharge occurs by means of precipitation and infiltration at the top of the delta. The recharge rate is determined as 35.23 mm by using Visual HELP model [4].

3. Materials and Methods

Salty water can be detected directly in observation wells by electrical electrodes or by sampling, or indirectly by geoelectrical methods [5]. In this study, the direct method by sampling is used. AquaChem software is used and it allows comparing a sample (Sea water sample) to another multiple samples (all groundwater samples). This comparation uses a linear regression algorithm to generate the correlation coefficient and the Euclidean distance between Sea water and all other samples.

For chemical analysis, a total of 16 water samples from the Göksu Delta (9 from alluvial aquifer, 4 from limestone aquifer, 1 from Paradeniz Lake, 1 from Akgöl and 1 from Mediterranean Sea) were obtained from 2006 to 2008 by four separate sampling campaigns at the sampling points shown in **Figure 1**. **Table 1** summarizes the chemical analysis results for water samples collected from the Göksu Delta and the **Table 2** shows the chemical characters of waters. The pH, temperature (T), electrical conductivity (EC) and salinity (sal) were measured at 25 sampling points in four different periods between 2006 and 2008 (**Table 3**).

Water samples obtained from the wells are from various depths because the wells in the area vary greatly in depth. Average well depth is 5 m for hand dug wells (showed with DSI) and 30-35 m for drilled wells (shown with ME). Electrical conductivity (EC), temperature (T), salinity (sal) and pH were monitored during pumping, and samples were collected only when values were stabilized or after at least three well volumes had been purged. Measurements of EC and pH were made in the field using a pH/Cond 340i WTW meter. For the pH measurements the electrode was calibrated against pH buffers at each location.

Cations were analyzed by inductively coupled plasma (ICP) and anions by ion chromatography (IC). SiO_2 was analyzed mainly by visible spectrophotometer. Bicarbonates were determined by titration in the laboratory. Samples were analyzed in the laboratory of General Directorate of Mineral Research and Exploration (MTA) of Turkey in Ankara.

Followed by water quality analysis, a vector-based GIS software package MapInfo was used to map, query, and analyze the data in this study. GIS is an effective tool for storing large volumes of data that can be correlated spatially and retrieved for the spatial analysis and integration to produce the desirable output. GIS has been used by scientists of various disciplines for spatial queries, analysis and integration for the last three decades [6]. GIS is a powerful tool and has great promise for use in environmental problem solving. Most environmental problems have an obvious spatial dimension and spatially distributed models can interact with GIS [7]. Troge [8] reported that this computer-based tool has allowed successful integration of water quality variables into a comprehensible format.

4. Results and Discussion

The groundwater samples collected from the Göksu Delta are colorless, odorless and free from turbidity. In **Table 1**, the results of ion concentrations of groundwater for July 2006 are presented. The **Table 2** shows the chemical types of groundwater from different aquifers and places.

Paradeniz Lake is a saltwater lagoon connected to the sea and the chemistry of Paradeniz water is similar to the Mediterranean Seawater. The EC values of sea water and lake water are 53000 µS/cm and 48000 µS/cm, respectively.

The types of groundwater from alluvial aquifer are Ca-Mg-HCO_3, but in the region where sea water intrusion occurs it changes and the Na and Cl ions are added in the types of groundwater (**Table 2**). The similar occurrence can be observed in the groundwater from the limestone aquifer. The chemical types of groundwater are Ca-HCO_3 or Ca-Mg-HCO_3 and they change to Ca-Na-Mg-HCO_3-Cl in the vicinity of seawater mixing regions.

Table 1. Results of the chemical analyses. Concentrations are in milligram per liter

Sampling	ME-1	ME-12	ME-20	ME-23	ME-24	ME-26	ME-28	ME-3	ME-18	ME-14	ME-15	ME-16	ME-21	Akgöl	Paradeniz	Sea water
	Alluvial aquifer									Limestone aquifer				Surface water		
pH	7.39	7.56	7.76	8.12	8.4	7.84	7.45	7.42	7.17	6.94	7.17	7.2	7.29	8.3	8.05	7.91
T	23.4	21.3	21.5	22	21.6	26	21.5	23.2	21.5	22.3	20.1	21.2	22.1	33.9	31	29.2
EC	1220	1988	925	2810	1031	711	598	756	719	1025	997	558	893	439	45300	53500
sal	0.4	0.9	0.2	1.3	0.3	0.1	0	0.1	0.1	0.3	0.3	0	0.2	0	29.6	35.5
DO	5.2	6.6	6.7	6.9	7.2	7.5	7.2	6.9	6.6	7	8.1	6.9	7.2	5.5	4.9	4.7
NO_2	0.1	0	0	0.26	0	0	0	0.26	0	0	0	0	0	0	0	0
NO_3	15	1.8	15.9	10.6	5.3	9.3	11.9	9.7	14.2	9.74	6.2	12.4	32.34	6.64	0	6.64
NH_3	0.13	0	0.07	0	0.43	0	0	0	0.02	0	0	0.012	0.012	0.34	4.01	4.01
PO_4	1.35	0.21	0.23	0.45	0.24	0.13	0.42	0.61	1.86	0.28	0.54	0.13	0.35	0.88	0.39	0.2
P	1	0.6	0.2	0.5	0.3	0.2	1.2	0.6	1.1	0.4	0.6	0.1	0.4	1.4	0.2	0.7
Br	1.05	0.47	0.5	1.93	0.47	2.64	3.38	0.53	1.63	0.64	0.59	1.54	0.58	0.72	0.42	0.58
I	0.1	0.5	0.3	0.3	0.1	0	0.5	0.1	0.1	0.1	0.1	0.2	0.2	0.2	3	0.2
F	0.93	0.46	0	1.97	1.16	0.21	0.3	0.22	0.08	0	0.56	0.34	0.45	0.83	0.81	1.96
Na	150	361	121	535	213	70.9	16.8	42.2	29.6	73.6	-	10.4	48.4	21.7	9556	10934
K	6.54	21.9	3.25	20	4.26	4.98	1.97	2.79	2.38	2.89	-	1.43	3.42	1.86	396	485
Ca	66.7	32.8	33.5	17.1	18.3	31.3	52.6	64.9	74.9	118	-	64.1	61.9	36.5	350	373
Mg	42.8	25.2	26.9	18.3	5.69	25.8	41.6	40.4	22.7	14	-	24.6	40.9	23.8	717	822
HCO_3	546	340	261	255	255	194	219	407	267	370	-	285	279	213	128	140
Cl	78.4	418	149	696	157	102	51.7	29	54.2	136	-	15	94.2	22.5	15177	17929
SO4	125	100	40.3	91.4	40.7	21.7	47.6	58	32.2	21	-	27.4	41.3	34.4	2470	2915
KOI	21	22	1	28	3	3	10	2	2	19	-	2	12	16	1050	1000
Mn	0	0	0	0	0	0	0	0	0	0	0	0	0	0	0	0
Fe	7.5	0.2	3.41	5.5	5.5	5.5	4.16	0.8	2.07	0	0	0.03	5.5	0.5	0.5	0.06
Cu	0.27	0.37	0.41	0.14	0.35	0.26	0.17	0.29	0.24	0	0	0	0.21	0.9	0.4	0.77
SiO_2	48	12	20.6	2.8	5.5	17.7	28	11	10	2.6	2.8	8.2	29	17.4	7	0.14
Mo	0.3	0	0	0	0	0	0.1	0	0	0.6	0	0	0	0	0	0
Cr	0.047	0.026	0	0	0	0	0	0.08	0	0	0	0	0	0	0	0.048

Table 2. The chemical characters of ground waters in the Göksu delta.

Sample number	Aquifer	Chemical character
ME-1	Alluvial	Na-Mg-Ca-HCO3
ME-12	Alluvial	Na-Cl-HCO3
ME-18	Alluvial	Ca-Mg-HCO3-Cl
ME-20	Alluvial	Na-Mg-HCO3-Cl
ME-23	Alluvial	Na-Cl
ME-24	Alluvial	Na-Cl-HCO3
ME-26	Alluvial	Na-Mg-Ca-HCO3-Cl
ME-28	Alluvial	Mg-Ca-HCO3-Cl
ME-3	Alluvial	Mg-Ca-Na-HCO3
ME-14	Limestone	Ca-Na-HCO3-Cl
ME-16	Limestone	Ca-Mg-HCO3
ME-21	Limestone	Mg-Ca-Na-HCO3-Cl

With very few exceptions, sample points fall within the mixing field of the Piper diagram (**Figure 2**). Three regions are distinguished in the diagram. First region where the samples ME3 and ME 28 are placed show the aquifer region where the seawater intrusion does not occurred. The second place, the central of the Piper diagram where the samples ME1 and ME 20 are shows the aquifer region where the sea water impact begins. The third place is very close to the Sea water sample, where the samples ME 12 and ME 23 are shows the aquifer region where the sea water mixing with sea water occurs. The samples ME12 and ME23 are very close to the Sea and Paradeniz waters.

The other indicators for the detection of sea water influence are T, EC and sal values. **Table 3** contains the results of pH, T, EC and sal measurements for four periods between 2006 and 2008. By using MapInfo, many

Table 3. The values of electrical conductivity and salinity between 2006 and 2008.

Kuyu No	Date	pH	T (^{o}C)	EC (µS/cm)	sal
DSI-2	07/2006	6.85	28.4	598	0
	06/2007	6.80	27.9	641	0.1
DSI-20	07/2006	7.34	28.2	437	0
	06/2007	7.83	26.9	459	0
	01/2008	7.93	12.7	448	0
	04/2008	8.60	20.5	667	0.1
DSI-35	07/2006	7.47	24.7	657	0.1
	06/2007	7.18	24.0	762	0.1
	01/2008	8.02	16.1	1295	0.4
	04/2008	8.00	17.8	1308	0.4
DSI-38	07/2006	7.40	21.1	920	0.2
	06/2007	7.96	21.8	856	0.2
	01/2008	7.90	19.1	864	0.2
	04/2008	8.30	19.5	930	0.2
DSI-4	07/2006	7.32	25.9	531	0
	06/2007	7.10	27.8	481	0
	01/2008	7.90	14.3	620	0
	04/2008	8.20	19.8	987	0.3
ME-10	07/2006	7.40	20.2	802	0.2
	06/2007	7.93	27.0	453	0
	01/2008	7.70	15.0	465	0
	04/2008	8.80	20.8	684	0.1
ME-11	07/2006	7.80	23.2	1416	0.5
	06/2007	7.85	22.1	1425	0.5
	01/2008	8.20	12.3	1576	0.6
	04/2008	8.40	21.8	1825	0.8
ME-13	07/2006	7.06	25.5	850	0.2
	06/2007	6.90	25.0	904	0.2
	01/2008	7.30	14.8	866	0.2
	04/2008	7.48	20.6	1024	0.3
ME-2	07/2006	8.10	23.7	1085	0.3
	06/2007	7.90	26.6	1058	0.3
	01/2008	8.31	8.8	1132	0.3
	04/2008	8.70	27.1	1247	0.4
ME-25	07/2006	7.94	20.7	434	0

	06/2007	8.13	21.7	435	0
	01/2008	8.50	19.4	699	0.1
	04/2008	8.38	20.5	527	0
	07/2006	7.20	21.4	788	0.1
ME-27	06/2007	6.87	22.1	914	0.2
	01/2008	7.80	18.6	1212	0.4
	04/2008	7.48	21.4	843	0.2
	07/2006	7.72	21.4	1510	0.6
ME-4	06/2007	7.30	22.6	970	0.3
	01/2008	7.85	20.0	2030	0.9
	04/2008	8.13	21.1	2080	0.9
	07/2006	7.54	22.8	2260	1.0
ME-5	06/2007	7.43	26.6	1430	0.5
	01/2008	7.73	18.8	2930	1.4
	04/2008	8.04	21.5	1575	0.6
	07/2006	8.48	20.8	716	0.1
ME-9	06/2007	7.93	23.3	837	0.2
	01/2008	8.70	16.0	814	0.2
	04/2008	9.03	20.3	1075	0.3
	07/2006	8.10	21.5	1476	0.6
ME-8-A	06/2007	8.45	21.0	1490	0.6
	01/2008	8.19	18.5	1546	0.6
	04/2008	8.50	21.2	1755	0.7
	07/2006	7.39	23.4	1220	0.4
ME-1	06/2007	7.55	23.9	1146	0.4
	01/2008	7.67	20.1	1412	0.5
	04/2008	7.80	22.6	1710	0.6
	07/2006	7.56	21.3	1988	0.9
ME-12	06/2007	7.62	22.9	1894	0.8
	01/2008	7.90	18.7	1404	0.5
	04/2008	8.50	20.1	1470	0.5
	07/2006	7.76	21.5	925	0.2
ME-20	06/2007	7.73	23.1	751	0.1
	01/2008	7.92	19.1	925	0.2
	04/2008	8.27	20.5	728	0.1
	07/2006	8.12	22.0	2810	1.3
ME-23	06/2007	8.16	22.9	2830	1.4
	01/2008	8.80	19.2	3460	1.7
	04/2008	8.30	22.0	3420	1.7
ME-24	07/2006	8.40	21.6	1031	0.3
	07/2006	7.84	26.0	711	0.1
ME-26	06/2007	7.57	28.0	780	0.1
	01/2008	8.50	14.5	1004	0.3
	04/2008	8.13	21.4	3420	1.7
	07/2006	7.45	21.5	598	0
ME-28	06/2007	7.07	21.7	601	0
	01/2008	8.90	18.5	3050	1.5
	04/2008	7.73	21.1	2830	1.3
	07/2006	7.42	23.2	756	0.1
ME-3	06/2007	7.20	24.3	739	0.1
	01/2008	7.60	15.2	712	0.1
	04/2008	7.65	26.8	1091	0.3
	07/2006	7.17	21.5	719	0.1
ME-18	06/2007	6.95	30.9	753	0.1
	01/2008	7.90	11.7	932	0.2
	04/2008	8.03	20.3	1003	0.3

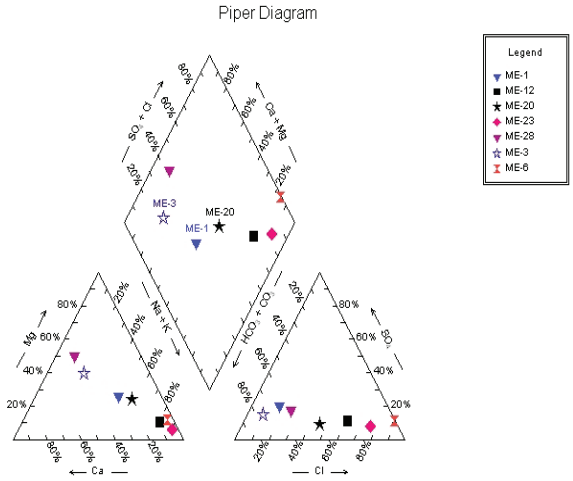

Figure 2. Piper diagram.

thematic maps are produced and by overlaying these maps sea water affected areas are determined.

The extent of saltwater affect is reflected by the distribution of salinity and electrical conductivity as an equiconcentration map (**Figures 4-9**). The periodical sal and EC measurements are used to show the development of saltwater mixing in space for four selected times.

The thematic map of groundwater temperature shows that in the region the temperature is increased in the places where the sea water mixing occurs. These regions are the southern part of Delta and in the vicinity of Sultanoğlu and Altınkum towns. In these regions the groundwater temperature increased until to 25-26˚C (**Figure 3**).

EC values vary between 434 and 3460 µS/cm and sal values between 0-1.7.

Table 4. The results of statistical (comparation) analyses.

Main Sample: ME-6, 17.07.2006				
Index	Sample	Corr Coeff	Euclidean distance	
32	ME-6,	1.0	0.0	7
31	ME-22,	1.0	3112.905	7
14	ME-23,	0.941	20349.32	7
34	ME-8,	0.882	20773.57	7
9	ME-12,	0.76	20672.79	7
15	ME-24,	0.486	20978.22	7
13	ME-20,	0.319	21031.26	7
22	ME-26,	0.239	21098.99	7
25	ME-14,	–0.006	21069.52	7
33	ME-7,	–0.014	21082.51	7
28	ME-21,	–0.069	21113.98	7
6	ME-1,	–0.169	21067.24	7
11	ME-18,	–0.223	21159.15	7
24	ME-28,	–0.244	21165.09	7
30	ME-19,	–0.297	21189.85	7
23	ME-3,	–0.315	21171.34	7
27	ME-16,	–0.362	21203.06	7
29	ME-17,	–0.384	21209.38	7

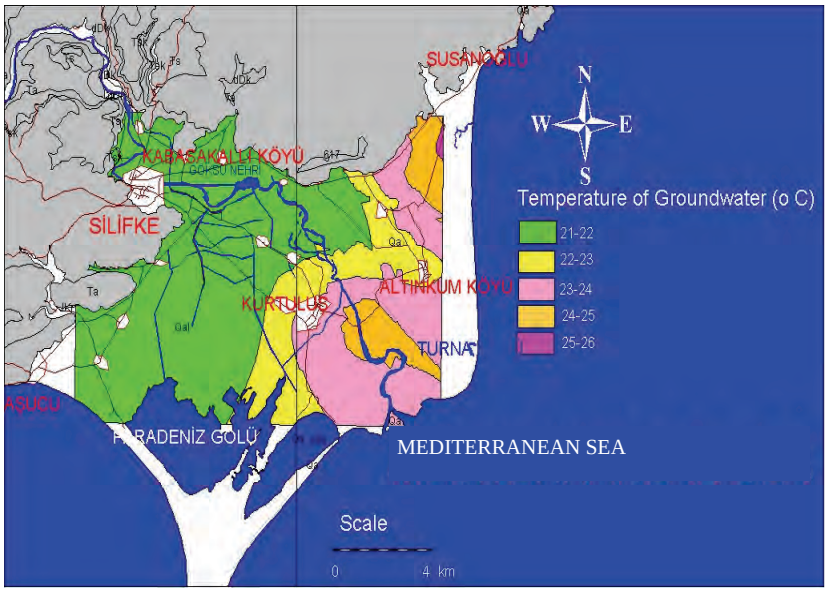

Figure 3. Temperature of groundwater for 2006.

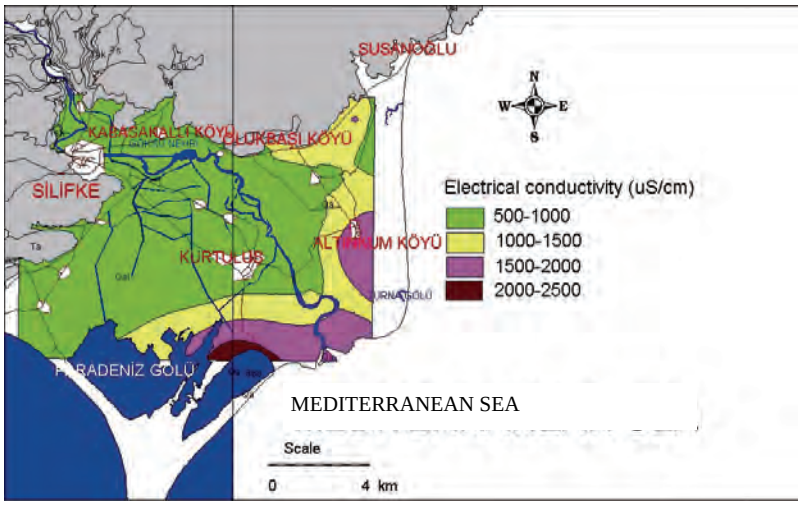

Figure 4. Thematic map for electrical conductivity (2006).

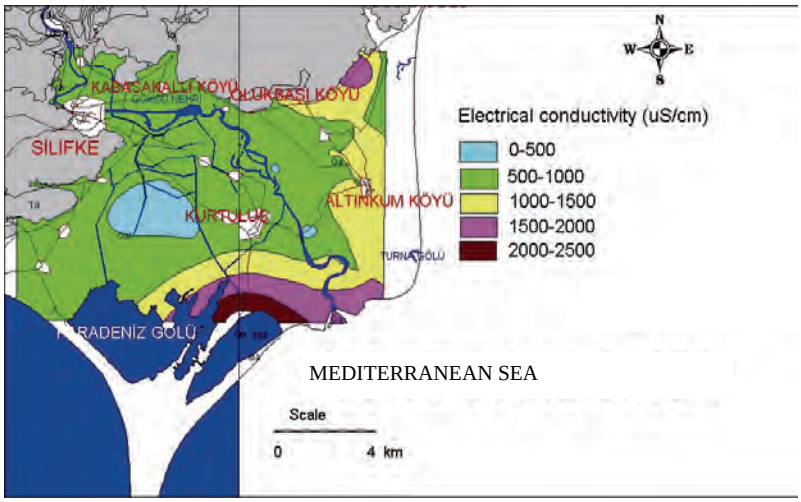

Figure 5. Thematic map for electrical conductivity (2007).

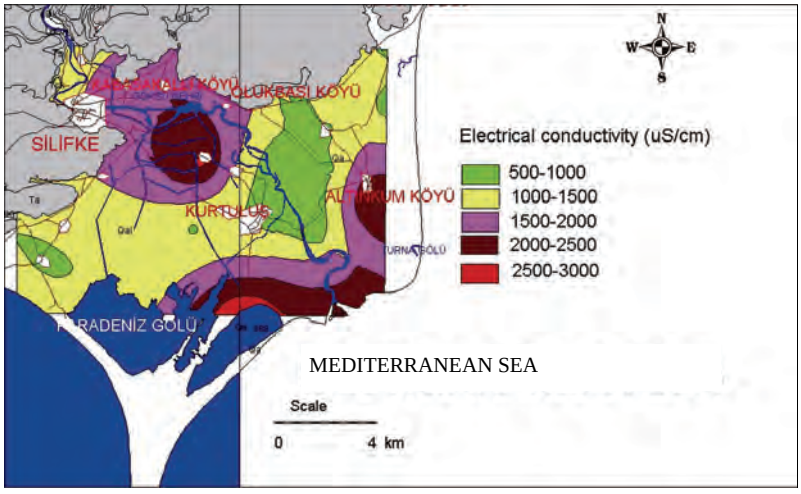

Figure 6. Thematic map for electrical conductivity (2008).

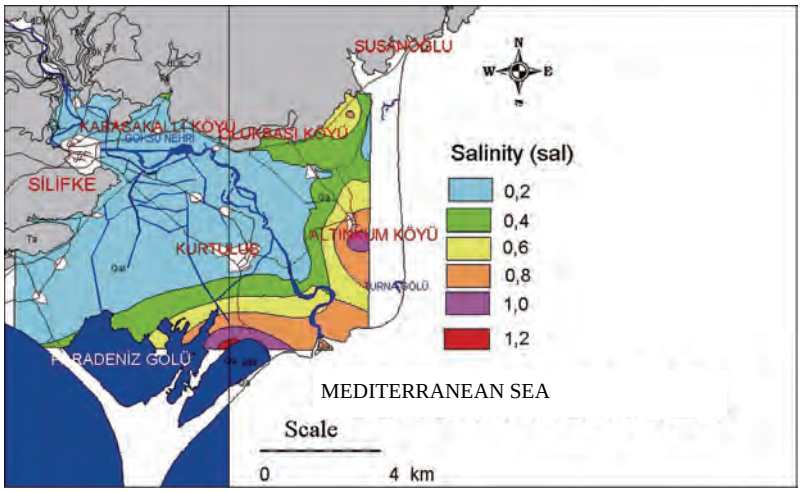

Figure 7. Thematic map for salinity (2006).

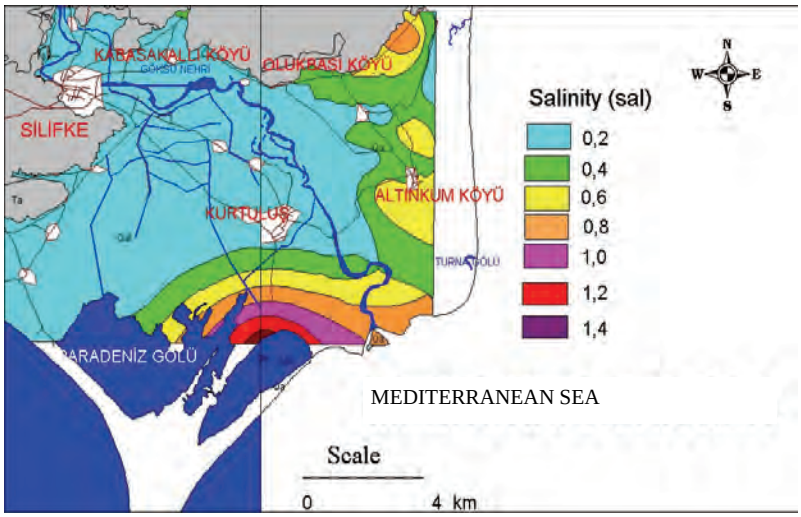

Figure 8. Thematic map for salinity (2007).

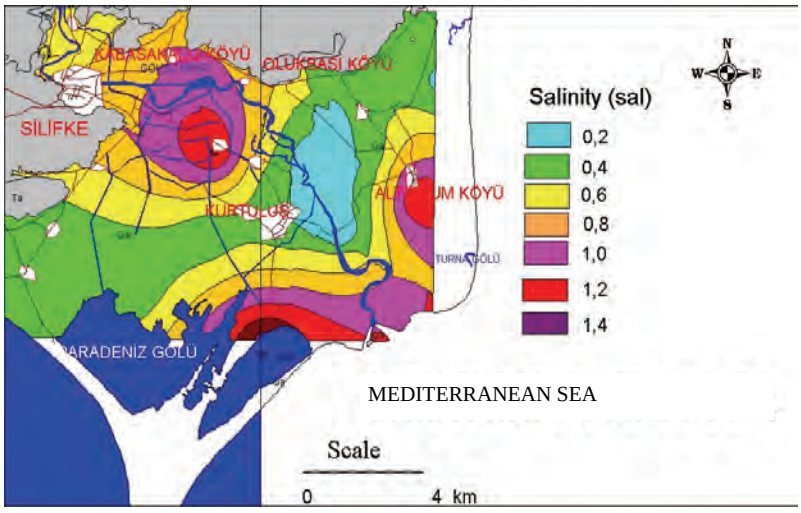

Figure 9. Thematic map for salinity (2008).

EC and sal contours prevailing in the delta, for 2006, 2007 and 2008, are presented in **Figures 4-9,** respectively. The EC and sal thematic maps give almost the same picture for all periods. The affect of seawater is reflected in a high value of EC (over 1500 µS/cm) and sal (over 0.6) of groundwater. It is obvious that groundwater quality is seriously degradated in the region. These thematic maps indicate that sea water is affected almost more than 2 km in inland.

The natural recharge of the aquifer seems not to be quantitative adequate to improve significantly the water quality.

Owing to increasing demand for water, groundwater has been pumped to over-exploitation and natural equilibrium has thus been disturbed. This has resulted in seawater mixing reaching inland aquifers.

5. Conclusions

Groundwater is an indispensable resource for water supply for the towns on Göksu Delta, for the urban and for sources has seriously impeded the development of industry, agriculture and the improvement of the people's living standards in this internationally protected region.

The chemistry and the chemical types of groundwater indicate the sea water intrusion in Göksu delta. The chemical characters of waters in the region affected by the sea water are changed. The statistical comparation analysis supports also this event.

With the equi-concentration mapping of EC and sal the extent of the seawater pollution in the aquifer was determined. The seawater mixing reached more than 2 km inland in the north and east direction. The salinity and electrical conductivity measurements and the thematic maps indicate that the origin of groundwater salinity in Göksu Delta is due to seawater intrusion which resulted from intensive pumping.

6. Acknowledgements

The author would like to acknowledge the Scientific and Technological Research Council of Turkey, (TUBITAK) Ankara, for financing this project (105Y285).

7. References

[1] Z. Ayas, N. Barlas Emir and D. Kolankaya, "Determination of Organochlorine Pesticide Residues in Various Environments and Organisms in Göksu Delta, Turkey," *Aquatic Toxicology*, Vol. 39, No. 2, 1997, pp. 171-181.

[2] Z. Demirel, "Monitoring of Heavy Metal Pollution of Groundwater in a Phreatic Aquifer in Mersin-Turkey," *Environmental Monitoring and Assessment*, Vol. 132, No. 1-3, 2007, pp. 15-23.

[3] F. B. J. Glen, A. K. Godley and A. C. Broderick, "Marine Turtle Nesting in the Goksu Delta, Turkey, 1996," *Mar Turtle Newsl*, Vol. 77, 1997, pp. 17-19.

[4] Z. Demirel, "Göksu Deltası Yeraltısuyu Kalitesinin Fotometrik Ölçümler İle Belirlenmesi ve Su Kalitesi-Coğrafi Bilgi Sisteminin Oluşturulması," TUBITAK Project, No. 105Y285, 2008.

[5] A. J. Melloul and L. C. Goldenberg, "Monitoring of Seawater Mixing in Coastal Aquifers: Basic and Local Concerns," *Journal of Environmental Management*, Vol. 51, No. 1, 1997, pp. 73-86.

[6] P. A. Burrough and R. A. McDonnell, "Principles of Geographical Information Systems," Oxford University Press, Oxford, 1998, p. 333.

[7] M. F. Goodchild, B. O. Parks and L. T. Steyaert, "Environmental Modeling with GIS," Oxford University Press, Oxford, 1993, p. 520.

[8] M. F. Troge, "A GIS Strategy for Lake Management Issues," *National Conference on Environmental Problem-Solving with Geographic Information Systems*, Cincinnati, 1994.

J. Water Resource and Protection, **2010, 2, 660-664**
doi:10.4236/jwarp.2010.27076 Published Online July 2010 (http://www.SciRP.org/journal/jwarp)

Investigation on Microorganisms and their Degradation Efficiency in Paper and Pulp Mill Effluent

Radhakrishnan Saraswathi[1*], Manghatai Kesavan Saseetharan[2]
[1]*Coimbatore Institute of Technology, Coimbatore, India*
[2]*Government College of Technology, Coimbatore, India*
E-mail: *saraswathi*70*@rediffmail.com*
Received April 16, 2010; *revised June* 11, 2010; *accepted June* 20, 2010

Abstract

Paper and pulp mill is a source of major pollution generating industry leaving huge amount of intensely colored effluent to the receiving end. Rapid increase of population and the increased demand for industrial establishments to meet human needs have created problems such as over exploitation of available resources, increased pollution taking place on land, air and water environment. The intention of this research paper is to identify predominant bacteria and fungi in paper and pulp mill effluent in addition to evaluate the degradation efficiency of individual isolates and combination of isolates. Treatment efficiency of individual isolates and combination of isolates are evaluated by shake flask method. Combination of Pseudomonas Alkaligenes, Bacillus subtilis along with Trichoderma reesei shows higher BOD, COD reduction of 99% and 85% respectively. As individual isolates Pseudomonas Alkaligenes show 92% BOD reduction and 77% COD reduction over other bacterial isolates and Trichoderma reesei removed 99% BOD and 80% COD respectively.

Keywords: Water Resource and Protection, Microorganisms, Degradation, Bacteria, Fungi, BOD, COD, Treatment Efficiency

1. Introduction

Paper and pulp mill is a large industrial enterprise that generates a significant amount of wastewater containing high concentration of lignin causing brown color and high Chemical Oxygen Demand. There has been considerable organic matter in pulp mill effluents on the environment. Some members of this family are known to be toxic, mutagenic, persist ant and bioaccumulating and are thought to cause numerous harmful disturbances in biological systems. There is no industry which does not add wastes into the environment. The introduction of contaminants through effluent and sludge to different environmental compartments can often overhelm the self cleansing capacity of recipient ecosystems and thus result in the accumulation of pollutants to problematic or even harmful levels. Prabu and Udayasoorian [1] reported that white rot fungus isolated from soil samples enriched by continuous pulp and paper mill effluent irrigation and identified as Phanerochaete chrysosporium was capable of 84% effluent decolourization along with 79% COD reduction.

Over several decades attempts have been made to remove the dark color from the effluents. Of late industry follows either chemical oxidation/precipitation methods or biological methods for color removal. Chemical oxidation/precipitation methods are tedious, provide an additional environmental load. Biological methods are often preferred since it has many advantages like rapid biodegradation rates, low sludge yield and excellent process stability. Biological methods are of particular interest because they can also reduce chemical and biological demands (COD, BOD), which are also significant problem in pulp wastewater and so reduce holding times in aeration and sedimentation ponds prior to wastewater discharge into the environment [2-4].

A number of research studies have discovered that a group of extracellular isoenzymes called ligninases which are lignin peroxidase (LiP), manganese-dependent peroxidase (MnP) and laccase produced by some microorganisms are capable of degrading lignin present in the paper and pulp mill effluent. de Oliveria *et al*. [5] evaluated the ability of these bacterias to remove color and COD from paper mill effluent. Bacillus pumilus CBMAI 0008 isolated from wood decomposition and Paenibacillus sp CBMAI 868 isolated from paper mill wastewater

are able to produce alkaline enzymes under thermophilic conditions, including xylanases and manganese dependent peroxidase.

Some investigators have made an attempt to treat pulp and paper mill wastewater by the thermophilic temperature at which they are discharged to reduce energy cost for treatment. Reddy *et al*. [6] treated the pulp and paper mill effluent by using thermophilic microorganisms in batch systems. They compared the aerobic treatment of pulp and paper mill effluent at the temperatures of 40°C, 50°C and 60°C. Maximum removal efficiency of 55.2% was achieved at 40ºC. However once degradation is obtained the degradation rate decreases significantly as temperature increases. Ruiz-Ordaz *et al*. [7] investigated on phenol biodegradation using repeated batch culture of Candida tropicalis in a multistage bubble column. The phenol removal efficiency of 98.7% was achieved. Marihal *et al*. [8] utilized Rhizobacteria isolated from pentachlorophenol-tolerant crop species for biodegradation of pentachlorophenol. 90% phenol reduction was achieved using these bacteria. Pentachlorophenol (PCP) is a polychlorinated aromatic compound that is widespread in industrial effluents and is considered to be a serious pollutant. PCP is also formed unintentionally in effluents of paper and pulp industries. A number of plant species were evaluated for their ability to tolerate different concentrations of Pentachlorophenol (PCP) in the soil. An important strategy for effluent treatment is the isolation and characterization of genetically significant microorganisms together with designing and optimization of process parameters to deal with specific environment pollutants. Nagarathnama *et al*. [9] successfully treated kraft mill effluent using Rhizopus oryzae. Rhizopus oryzae, a zygomycete, decolorize, dechlorinate and detoxify bleach plant effluent at lower cosubstrate concentration. With glucose at g/L, this fungus removed 92-95% of the color, 50% of the chemical oxygen demand, 72% of the adsorbable organic halide and 37% of the extractable organic halide in 24 hour at temperatures of 25-45ºC and a pH of 3-5. The aim of this research study is to begin with isolating the predominant fungi and bacteria present in pulp and paper mill effluent and evaluating the degradation efficiency of individual isolates and combination of isolates in laboratory scale.

2. Materials and Methods

2.1. Effluent Source

The effluent was obtained from SESHASAYEE PAPER MILL, Erode, Tamilnadu, a South Indian based Integrated Pulp and Paper Industry. The paper pulp effluent from the inlet, outlet of primary settling tank was used for investigation. The sample was collected using a sterile plastic container and transported to the RND Softech Private Limited research laboratory situated in Coimbatore within 4 hours. The effluent was stored at 4ºC until required.

2.2. Methods

All the testing was performed according to Standard Microbiological methods for the Examination of Water and Wastewater as described [10]. Shake flask method was used to evaluate the treatment efficiency of individual isolates and combination of isolates.

2.3. Isolation and Identification of Predominant Microorganisms

The sample was serially diluted using sterile pipettes from 10^{-1} to 10^{-8} dilution. **Figure 1** shows bacterial and fungal strain capable of growing on Nutrient agar and PDA agar medium. Five different types of bacteria were predominant in the raw effluent; single type of fungi was found to be present. For enumeration of bacteria nutrient agar medium containing peptone (5 g/L), yeast extract (1.5 g/L), sodium chloride (5 g/L), agar (15 g/L) and for enumeration of fungi Potato dextrose agar containing potato (200 gm), dextrose (20 gm, agar-15 gm, distilled water (1000 mL) at pH 5.6 was used. To obtain pure culture the cultures were repeatedly streaked nutrient agar medium and incubated at 37°C for 24 hrs. The isolated bacteria were identified by colony morphology, gram staining, microscopic observation and confirmation test. The identified bacteria were Pseudomonas alkaligenes, Bacillus pumilus, Bacillus subtilis, Klebsielle sp, Proteus sp. The isolated fungal culture was identified as Trichoderma reesei using Lactophenol cotton blue staining method.

3. Microbial Treatment of Effluent

The raw effluent physiochemical parameters are given in **Table 1**. The raw effluent was treated using the isolated bacteria and fungi. The treatment efficiency was validated by calculating the percentage reduction of physiochemical parameters.

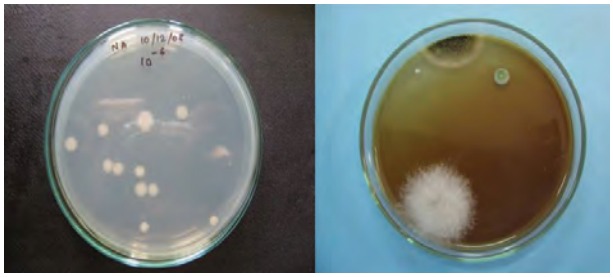

Figure 1. Bacterial and fungal strain growing on nutrient agar and PDA agar medium.

Table 1. Physiochemical analysis of raw effluent (Inlet of Primary Clarifier).

Parameter	Raw effluent
pH	7.5
Color – Hazen	117
Total dissolved solids (mg/l)	900
Total suspended solids (mg/l)	590
Biochemical oxygen demand (mg/l)	286
Chemical oxygen demand (mg/l)	1164
Hardness (mg/l)	56
Chlorides (mg/l)	40

Table 2 gives the treatment efficiency of the five isolates for comparison and the isolates Klebsielle sp, Proteus sp, are excluded from further study as their percentage reduction of parameters are low compared to other three isolates.

3.1. Different Combinatorial to Improve the Treatment Efficiency

To improve the efficacy of the bacterial treatment, the three isolates found good are combined in possible ways as shown in **Table 3** and the validation of the test is performed based on the same physio chemical parameters.

Combination 1 – Pseudomonas alkaligenes + Bacillus pumilus

Combination 2 – Pseudomonas alkaligenes + Bacillus subtilis.

Combination 3 – Bacillus pumilus + Bacillus subtilis.

Combination 4 – Pseudomonas alkaligenes + Bacillus pumilus + Bacillus subtilis.

Table 3. Efficiency of treatment using different combinational.

Parameters studied	% reduction			
	Comb.1	Comb.2	Comb.3	Comb.4
pH *	7.3	7.3	8	7.7
TDS	11	12	0	11
TSS	49	58	42	49
BOD	77	98	69	62
COD	59	77	66	69
Hardness	39	45	40	40
Chlorides	36	36	36	36
Floc size	0*	1.2 mm	0*	1.1 mm

pH *—Not in Percentage, 0 *—No floc formation

It was evident from **Table 3** that combination 2 and combination 4 was found to be efficient compared to other combinations. Thus combination 2 and 4 are being used for further study.

Trichoderma reesei showed increased reduction of parameters and was found to be efficient in treatment of paper mill effluent. The efficient bacterial combination 2 (Pseudomonas alkaligenes + Bacillus subtilis) and combination 4 (Pseudomonas alkaligenes + Bacillus pumilus + Bacillus subtilis) shown in **Table 3** and Trichoderma reesei shown in **Table 4** were combined to enhance the treatment efficiency. It was evident from **Table 5** that combination 2 + Trichoderma reesei was competent compared with combination 4 + Trichoderma reesei and the derived consortia was used for validation and standardization of process parameters.

Table 2. Treatment of effluent using the bacterial isolates.

Parameters studied	% reduction				
	Pseudomonas alkaligenes	Bacillus pumilus	Bacillus subtilis.	Klebsielle sp	Proteus sp
pH *	7.3	7.5	7.5	7.1	7.8
TDS	11	12	12	0	11
TSS	58	60	59	35	20
BOD	92	79	85	60	55
COD	77	69	72	65	50
Hardness	40	58	47	23	0
Chlorides	36	32	29	11	11
Floc size	1 mm	2 mm	1.3 mm	0 *	0 *

pH *—Not in Percentage, 0 *—No floc formation

Table 4. Treatment of effluent using trichoderma reesei.

Parameter studied	% reduction
pH *	6.2
TDS	22
TSS	45
BOD	99
COD	80
Hardness	56
Chlorides	39
Floc size	1.7 mm

pH *—Not in Percentage

Table 5. Treatment of effluent using the bacterial isolates and fungus.

Parameters studied	% reduction Comb.2 + T.reesei	% reduction Comb.4 + T.reesei
pH *	7.2	6.9
TDS	22	12
TSS	59	52
BOD	99	82
COD	85	72
Hardness	56	40
Chlorides	40	36
Floc size	1.7 mm	1.2 mm

pH *—Not in Percentage

4. Results and Discussion

It is implicitly known from **Figure 2** that the percentage reduction of TSS, BOD, COD and Hardness seems higher but varying in all the combinations; Chlorides reduction was identical in all the four combinations, whereas there was no TDS reduction in combination 3. Effective floc formation was attained in combination 2 and combination 4 which enhance settling process. **Figure 3** signifies that the treatment using Trichoderma reesei as individual isolate proved to be more efficient for the reduction of the parameters in paper and pulp mill effluent. Likewise **Figure 4** be an evidence that the combination 2 + Trichoderma reesei was superior in reducing paper and pulp mill effluent parameters. **Figure 5** reveals the validation of treatment efficiency of combination 2 and Trichoderma reesei based on the research investigation.

5. Concluding Remarks

Pseusodomonas Alkaligenes, Bacillus pumilus, Bacillus subtilis proved to degrade paper and pulp mill waste effectively. The degradation rates achieved by these

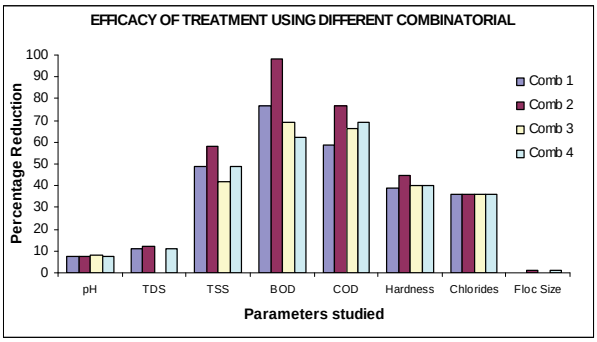

Figure 2. Treatment efficiency of different combinatorial.

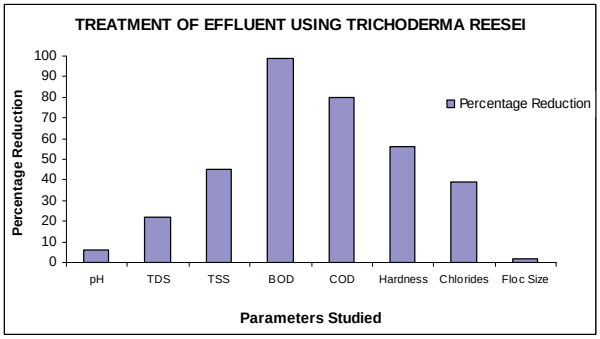

Figure 3. Effluent treatment using Trichoderma reesei.

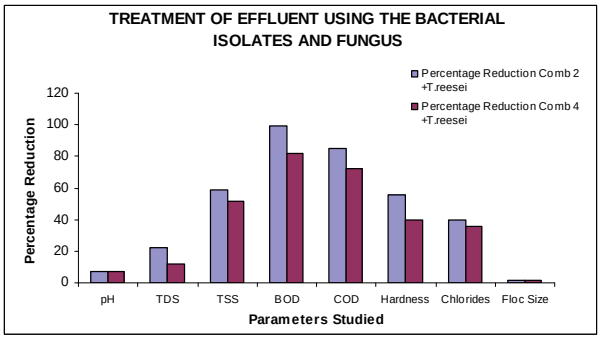

Figure 4. Effluent treatment using the bacterial isolates and fungus.

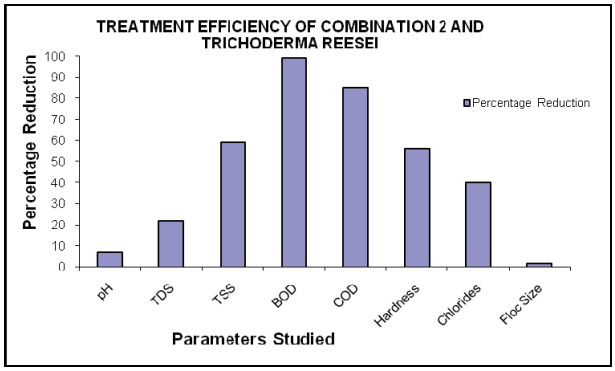

Figure 5. Treatment efficiency of combination 2 and Trichoderma reesei.

isolates were 92%, 79%, 85% of BOD and 77%, 69%, 72% COD respectively. Furthermore Pseusodomonas Alkaligenes kept higher degradation rate than other isolates. In combination of isolates, Combination 2 (Pseusodomonas Alkaligenes, Bacillus subtilis) showed 98% of BOD, 77% COD removal and Combination 4 (Pseusodomonas Alkaligenes, Bacillus subtilis, Bacillus pumilus) showed 79% of BOD, 69% COD removal. Trichoderma reesei exhibited higher degradation activity on paper and pulp waste when used individually. 99% of BOD, 80% COD was achieved by this fungi. When bacteria and fungi were combined and used in treatment, 99% BOD and 85% COD reduction was achieved. The maximum COD reduction rate of 85% was observed when Bacillus subtilis was used individually and in the Combination of 2 along with Trichoderma reesei (Pseusodomonas Alkaligenes, Bacillus subtilis). Three isolates Pseusodomonas Alkaligenes, Bacillus pumilus, Trichoderma reesei both as individual isolates and in their combination proved to have more treatment efficiency rather than other isolates.

6. References

[1] P. C. Prabu and C. Udayasoorian, "Decolorization and Degradation of Phenolic Paper Mill Effluent by Native White Rot Fungus Phanerochaete Chyysosporium," *Asian Journal of Plant Sciences*, Vol. 4, No. 1, 2005, pp. 60-63.

[2] S. Prasongsuk, P. Lotrakul, T. Imai and H. Punnapayak, "Decolourization of Pulp Mill Wastewater Using Thermotolerant White Rot Fungi," *Science Asia*, Vol. 35, 2009, pp. 37-41.

[3] A. P. Buzzini, M. A. Nolasco, A. M. Springer and E. C. Pires, "Evaluation of Aerobic and Anaerobic Treatment of Kraft Pulp Mill Effluent for Organochlorines Removal," *Water Practice & Technology*, Vol. 1, No. 3, 2006.

[4] P. Singh and I. S. Thakur, "Removal of Color and Detoxification of Pulp Mill Effluent by Microorganisms in Two Step Bioreactor," *Journal of Scientific & Industrial Research*, Vol. 63, No. 11, 2004, pp. 944-948.

[5] P. L. de Oliveira, C. T. D. Marta, A. N. Ponezi, L. R. Durrant, "Use of Bacillus Pumilus CBMAI 0008 and Paenibacillus SP.CBMAI 868 for Color Removal from Paper Mill Effluent," *Brazilian Journal of Microbiology*, Vol. 40, No. 2, 2009, pp. 354-357.

[6] P. Reddy, V. L. Pillay and A. K. S. Singh, "Degradation of Paper and Pulp Mill Effluent by Thermophilic Microorganisms Using Batch Systems," *Water SA*, Vol. 31, No. 4, 2005.

[7] N. Ruiz-ORDAZ, J. C. Ruiz-Lagunez, J. H. Castanon-Gonzalez, E. Hernandez-Manzano, E. Cristiani-Urbina and J. Galindez-Mayer, "Phenol Biodegradation Using a Repeated Batch Culture of Candida Tropicalis in a Multistage Bubble Column," *Reviate Latinoamericana de Microbiologia*, Vol. 43, 2001, pp. 19-25.

[8] K. Avita, Marihal, K. S. Jagadeesh and S. Sinha, "Biodegradation of PCP by the Rhizobacteria Isolated from Pentachlorophenol-Tolerant Crop Species," *International Journal of Environmental Science and Engineering*, Vol. 1, No. 4, 2009, pp. 189-193.

[9] R. Nagarathnama and P. Bajpai, "Decolorization and Detoxification of Extraction-Stage Effluent from Chlorine Bleaching of Kraft Pulp by Rhizopus Oryzae," *Applied and Environmental Microbiology*, Vol. 65, No. 3, 1999, pp. 1078-1082.

[10] APHA, AWWA, WPCF, "Standard Methods for the Examination of Water and Wastewater", 20th Edition, American Public Health Association, Washington, D.C., 1995.

[11] P. Sharma, L. Singh and N. Dilbaghi, "Biodegradation of Orange II Dye by Phanerochaete Chrysosporium in Simulated Wastewater," *Journal of Scientific & Industrial Research*, Vol. 68, 2009, pp. 157-161.

J. Water Resource and Protection, **2010, 2, 665-674**
doi:10.4236/jwarp.2010.27077 Published Online July 2010 (http://www.SciRP.org/journal/jwarp)

Hydrochemical Peculiarities of Bog Ecosystems in the North-Siberian Lowland

Tamara Efremova, Stanislav Efremov
V.N.Sukachev Institute of Forest, Siberian Branch of the Russian Academy of Sciences, Academgorodok, Krasnoyarsk, Russia
E-mail: *efr2@ksc.krasn.ru*
Received April 8, 2010; *revised May* 20, 2010; *accepted May* 22, 2010

Abstract

Surface waters of eutrophic bogs (fens) in the North-Siberian (Taimyr) lowland are characterized by hydrocarbonate, sulfate as well as hydro carbonate-sulfate calcium-magnesium composition. They relate to the type of oxygen waters, mainly, to the class of neutral weakly alkaline and to the family of ultrafresh and fresh waters and to the kind of waters poor with dissolved organic matter. Natural hydrochemical background of bog ecosystems makes in heavy metals in the first approximation: Co–0.16, Pb–0.57, Ni–4.67 and Cu–5.94 mkg/L. In most cases the surface waters are not polluted by heavy metals. Bog waters located in immediate closeness from Norilsk mining and smelting industrial complex are polluted by nickel at mid-level.

Keywords: Bogs, Hydrochemical Characteristics, Heavy Metals, Pollution

1. Introduction

The North-Siberian (Taimyr) lowland stretches out from the Yenisei river to the Khatanga gulf and borders in the north on the Byrranga mountains and in the south – on the Putoran mountains which is an extreme northern part of the Middle-Siberian plateau. The larger part of its area has a height less than 100 m above sea level (asl), and in the lesser one the hilly-glacial topography prevails up to the height 200-250 m asl. The lowland is rich in rivers and lakes of various origin (glacial-tectonic, glacial thermokarst, lagoon, floodplain one) and is characterized by a strong paludification. Cryogenic geological processes and such phenomena as thermokarst, solifluction, cryogenic heaving, cryogenic cracking, ice formation, ablation, subsurface erosion (erosive leakage) etc. which result in reconstruction of surface, also in soil and plant cover and in active paludification of the area are characteristic of natural complexes of the North-Siberian lowland. Thermokarst on frozen organogenic and porous mineral rocks connected with the destruction of ice in ground (segregation and deposit forming ice) is the result of formation of collapse shapes of topography. In combination with cryogenic heaving it results in that the surface of bog massifs obtains a complex morphostructural look. The different hypsometric hierarchy of small and middle forms of topography is clearly observed here. Peat mounds (palsas) of different height with mineral core alternate with secondary pools and lakes which have sometimes peaty sometimes peaty-mineral or mineral bottoms.

According to bog zoning the studies were performed at the turn of two bog provinces: Middle Siberian province of tundra, larch open forests and flat-raised bogs as well as Middle Siberian province of northern and middle taiga forests and palsa mires [1,2]. Total feature for all peatlands of this type is an interchange of frost peat mounds 1-5 m high and melted depressions (bog hollows). Mounds are residual outcrops of very old peatlands from the warmer epoch of Quaternary period destroyed by erosion and thermokarst [3]. Bog hollows between mounds are contemporary bogs with a strongly pronounced peat accumulation process. The area of depressions, as a rule, considerably exceeds the extension of elevated areas. Mounds are usually covered by moss-shrub and tree groups consisting of pine, larch and birch tree species; depressions are occupied by sedge-hypnum and sedge-sphagnum associations or pools. The water regime of bog hollows, as a rule heavily watered, has a running character. Run-off from the neighboring slopes of peat mounds proceeds in bog hollows. The flow of subpermafrost waters which accelerates degradation of permafrost in mounds is also observed here. Thickness of peat enveloping bedding of bog hollows makes from 0.8

to 3 meters. Low mire peat deposits prevail in assigned bog provinces, it means the sedge and hypnum deposits take about 70% but sphagnum ones take approximately 30%.

Wide development of sulfide-copper-nickel mineralization is a characteristic feature of natural-territorial complexes in the Priyeniseisky trans-polar region [4]. Unique copper-nickel fields of the Norilsk ore region are related to the Priyeniseisky megablock. Alkaline, alkaline-basite, then basite and hyper basite-basite as well as toleite (trapps), alkaline-hyper basite, also kimberlite products of magmatism which are the certain chains in the lateral and age series of magmatism and endogenic ore formation are developed within this megablock successively (from the west to the east).

Natural waters, having a contact with different chemical variations of rocks, inevitably gain a specific composition which sufficiently shows in time and space the initial natural mosaic structure of conditions for their formation. In addition to natural factors the hydrogeological and hydrochemical situation in the studied region is determined also by emission of sulfur and heavy metals into the atmosphere by enterprises of non-ferrous metallurgy of the Norilsk mining and smelting industrial complex. Aerosol technogenic (man-caused) emissions are differently accumulated in the catchment area depending on their type, remoteness from the emission source, also on component and aggregate composition of technogenic fluxes, geomorphology of the territory, prevailing wind rose, weather, season and other factors. The processes of intralandscape migration of chemical elements are also developed ambiguously. Geomorphologically subordinate peat and bog ecosystems can play the positive role in accumulation and in "damping" of ecologically hazardous technogenic fluxes. Peatlands are a combined geochemical barrier-mechanic, oxygen, biogenic and sorption one where many chemical elements are accumulated [5]. However the buffer "capacity" of hydromorphic complexes has a certain stability threshold outside of which the degradation of the system itself starts. Therefore under high technogenic loads on environment the problem of protection of natural water resources becomes one of the most important. Meanwhile, bogs in the North-Siberian lowland area are poorly studied from the hydrological point of view.

The aim of this paper was the following: in comparison with waters of rivers and deep lakes of glacial- tectonic genesis a) to determine chemical composition of waters in bog hydrographic network and on this base to make up their classification; b) to analyze the amount of water soluble Cu, Ni, Co, Pb which show the element composition of sulfide ores; c) to assess the pollution level of surface waters by heavy metals and sulfur.

2. Objects and Methods of Study

Paludified basins of Bol'shoi Avam, Norilskaya, Rybnaya, Omuntakh, Ambarnaya rivers, also "hanging" bogs in Khaeralakh mountains, raised peatlands in vicinity of Kayerkan town-Burovoye lake, the route Alykel'-Vologochan as well as the cape Bludnyi (in the region of the lake Melkoye) were covered by studies (**Figure 1**). The first-hand points for water sampling were: organogenic, secondary lakes of thermokarst origin; transit waters of overlying bogs which are accumulated in pools (sized less than 1 ha) on slope (hanging) peatlands; fissure bog waters of frost peat mounds; bog waters of lakes at the different heights toward the foot of a large peat mound (**Table 1**). Water samples were taken simultaneously in rivers, in the lake Melkoye which is of glacial-tectonic origin and in the waterfall "Krasnyye kamni (Red stones)".

Determination of pH, water soluble carbon, calcium, magnesium, chlorine and hydrogen carbonate was performed according to the instruction [6]. Potassium, sodium, water soluble heavy metals and sulfur were determined by methodical instructions [7-9]. Geochemical classification of waters was made according to [10]. The following taxonomic levels were segregated: groups, types, classes, families, genera, and kinds of waters.

3. Chemical Composition and Classification of Surface Waters

Surface waters of the North- Siberian lowland relate to the group of cold and weak thermal as well as to the type of oxygen waters. By alkaline- acidic conditions they, mainly, correspond to the class of neutral and weak alkaline waters (**Table 2**). This is the class of waters (pH 6.5-8.5) to which the majority of natural waters of the land relates. In the water phase of peatlands the medium reaction makes, mainly, pH 6,4-7,4 similar to forest fens

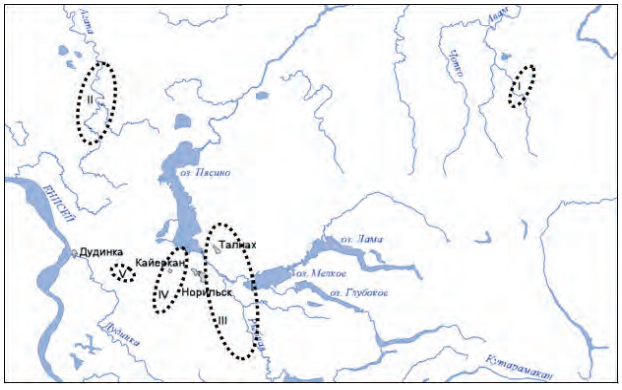

Figure 1. Chart of study regions.

Table 1. Regions and water sampling points of bog, river, waterfall and glacial-tectonic lakes in the North-Siberian lowland (the phase of mean water).

Regions of water sampling	No. of a sample	Points of water sampling
1	2	3
I. The Bol'shoi Avam river valley	1 *r*	The Bol'shoi Avam river bed
	2 *b*	Bog pool in paludified larch forest at the foot of the river bank slope (the right river bank)
II. The Agapa river basin	3 *r*	The Verkhnyaya Agapa river bed
	4 *r*	The Agapa river bed
	5 *r*	The Norilskaya river mouth
	6 *l*	Area of water of the lake Melkoye – of the glacial-tectonic genesis
	7 *b*	The pool* of transitional bog waters on the slope peatland of the cape Bludnyi
	8 *b*	The thermokarst lake on the hilly bog of the cape Bludnyi
		The right bank part of the Norilskaya river valley:
	12 *b*	thermokarst lake in 100 m from the river bank
	13 *b*	thermokarst lake in 200 m from the river bank
		The Khayerlakh mountains:
	14 *b*	the pool of the "hanging" bog with shallow peat deposit (at theheight 650 m)
	15 *w*	The waterfall "Krasnye kamni"
		The large mound peat bog:
	16 *b*	the "lower" lake between frost peat mounds
III. The Norilskaya river Basin	17 *b*	the "upper" lake on the frost peat mound
	18 *b*	fissure bog waters of a frost peat mound
		The left bank part of the Norilskaya river valley:
	19 *r*	the Rybnaya river mouth
	20 *r*	the Yergalakh river mouth
	21 *b*	the bog lake on the peatland of the Omuntakh river left bank
		Thermokarst lakes of the large mound peatland in vicinity of Oganer:
	22 *b*	the pool on the frost peat mound with running fire evidences
	23 *b*	talweg incised into mineral bed of peatland
	24 *b*	the lake at the mineral foot of a peat mound
	25 *b*	the lake at the height 5 m from the foot of a peat mound
	26 *b*	the lake at the height 10 m from the foot of a peat mound
	27 *b*	the lake at the height 15 m from the foot of a peat mound
	28 *r*	The Ambarnaya river bed
IV. The Ambarnaya river valley – the ridge Nadezhda		*Thermokarst lakes of peat bogs:*
	29 *b*	the bog lake on the river bank slope
	30 *b*	the lake on the paludified plateau
	31 *b*	the bog lake in the inter-montane valley
	32 *b*	the bog lake at the height mark 339 m
		Flat mound peatland with thermokarst lakes:
V. Route Alykel' – Vologochan	33 *b*	the big bog lake
	34 *b*	bog pool (micro-depression)
	35 *b*	fissure waters of a frozen peat mound

Legend: *r*—river, *b*—bog, *l*—lake, *w*—waterfall**,** **)* pool—water area less than 1 ha

of boreal forest zone. Waters of other classes are met more seldom. So, the strong-acid waters (pH 3.6-4.0) were found in bog lakes in suburb of Oganer, Kayerkan town (samples 22 *b*, 30 *b*), in fissure water of flat- hilly peatland in the neighborhood of Alykel' airport (35 *b*). Acidity of such water in nature derives usually from oxidation of disulfides what results in H_2SO_4 [10]. However the formation of sulfuric acid in the study region can also have an anthropogenic nature which is connected with emissions of sulfur oxides by enterprises of non- ferrous metallurgy of the Norilsk mining and smelting industrial complex. Heavily alkaline waters with pH 9-10 are also found in vicinity of Oganer suburb. This is a talweg incised into mineral bed of peat land (23 *b*) and a bog lake on mineral foot of a large peat mound (24 *b*). Heavily alkaline medium is determined most likely by the contact with saline bed of relict genesis. It was shown that in Mesozoic the Yenisei-Khatangskaya depression was flooded by a shallow-water sea which was resulted in salification of subaqueous grounds [11]. Ionic com-

Table 2. Chemical composition of waters in bogs, rivers, waterfall and lakes of glacial- tectonic origin in the North- Siberian (the Taimyr) lowland (the mean water phase)

No.of water sample*	Sum of ions, mg/L	pH	C, mg/L	Anions, mg/L			Cations, mg/L			
				HCO_3^-	SO_4^{2-}	Cl^-	Ca^{2+}	Mg^{2+}	Na^+	K^+
1	2	3	4	5	6	7	8	9	10	11
Waters of rivers, waterfall and the lake of glacial- tectonic genesis										
1 *r*	54,06	7,1	2,76	35,38	3,94	2,91	7,12	3,32	1,20	0,19
3 *r*	33,40	7,1	2,53	17,08	3,98	3,78	4,75	2,86	0,70	0,25
4 *r*	41,69	6,9	2,41	14,64	12,38	4,94	5,54	3,32	0,62	0,24
5 *r*	56,51	7,2	1,56	23,18	12,43	5,81	10,30	2,85	1,80	0,14
19 *r*	48,66	6,9	2,56	17,08	12,82	5,52	8,70	2,85	1,59	0,10
20 *r*	119,77	7,3	2,07	41,48	42,00	4,36	22,96	6,17	2,59	0,21
28 *r*	189,13	7,0	0,62	78,08	64,99	2,61	26,14	13,78	3,18	0,34
15 *w*	51,16	7,1	1,12	23,18	10,99	4,07	7,92	3,80	1,02	0,18
6 *l*	47,83	6,4	2,91	17,08	12,38	5,81	7,92	2,85	1,69	0,10
Bog waters										
2 *b*	52,68	6,9	3,76	29,28	5,66	4,94	7,92	3,33	1,50	0,05
7 *b*	136,91	7,0	4,51	71,98	25,39	4,65	23,76	8,55	2,45	0,13
8 *b*	60,56	6,5	2,41	17,08	25,63	3,20	10,30	3,80	0,50	0,05
12 *b*	189,73	7,6	1,42	122,0	22,51	3,49	22,17	13,31	6,20	0,05
13 *b*	112,33	7,4	2,87	63,44	18,38	3,20	15,84	7,60	3,42	0,45
14 *b*	48,06	6,5	2,18	17,08	16,27	3,20	6,34	4,27	0,88	0,06
16 *b*	101,15	7,4	0,62	63,44	10,46	4,07	13,46	7,12	2,12	0,48
17 *b*	200,34	7,3	1,16	134,20	18,10	2,61	25,34	14,73	3,40	1,96
18 *b*	40,39	6,4	1,16	4,88	21,89	2,61	6,33	3,33	1,22	0,13
21 *b*	229,70	6,9	2,72	35,38	132,29	3,20	39,60	14,25	4,60	0,38
22 *b*	84,96	3,6	3,13	No	58,94	3,78	13,46	7,13	0,60	1,05
23 *b*	187,43	9,1	1,39	76,49	58,94	5,81	26,53	14,49	5,12	0,05
24 *b*	927,34	10,0	1,36	225,7	345,60	74,4	53,06	20,74	178,80	29,0
25 *b*	289,83	7,4	1,57	53,68	158,21	6,97	42,77	21,86	4,50	1,84
26 *b*	336,74	7,2	2,15	23,18	214,75	5,81	55,44	28,51	6,80	2,25
27 *b*	226,72	6,1	2,54	10,98	140,74	5,81	34,05	13,78	1,36	20,00
29 *b*	183,02	7,5	0,62	96,38	40,08	2,61	25,34	12,36	5,60	0,65
30 *b*	61,84	4,1	1,60	No	44,88	2,91	12,67	4,22	0,80	0,66

position of bog waters shows just this. In the lake near the mineral foot of the large mound peatland Oganer we have found a considerable amount of sodium 179 mg/L as compared to 0.2-6.8 mg/L in other study objects. This higher sodium amount is, for sure, the result of exchange sorption of calcium waters with sodium in rocks of marine origin. Here the increased amount of Cl^- ion — 74.4mg/L was also found which is not great (2.6-12.2 mg/L) in surface water of Taimyr lowland what is typical of rivers, lakes and bogs of northern areas. Chlorine is as a main anion in seas and salty lakes. At the water contact with saline mineral rocks the chlorine is easily leached and is accumulated in the lake.

In mineralization degree (*i.e.* sum of dissolved ions) the studied surface waters relate to the ultra fresh (< 100 mg/L) and fresh (100-1000 mg/L) water family. Water of almost all rivers, of the lake Melkoye and waterfall "Krasnye kamni" is ultra fresh one. Fresh water is only in rivers Ambarnaya and Yergalakh (189.1 and 119.8 mg/L, respectively). Such results agree with the characteristics of river waters in Siberia: water mineralization in the Yenisei river makes 53.8, in the Ob' river—76.6, in the Lena river—84.6 mg/L, in the Angara river mouth it is 90-100 mg/L [3]. On the average, waters in studied bogs are more mineralized: 41.7% of them relate to the ultra fresh and 58,3%—to fresh waters (101.2-927.3 mg/L, respectively). It is determined by removal of chemical elements from catchment area and by accumulation in hypsometrically lower topography elements. Most mineralized are waters of organogenic lakes in suburb of Oganer which is located near sources of technogenic emissions.

All water categories, including bog waters, contain the small amount of water soluble carbon—0.62-4.51 mg/L and relate to the kind of water which is poor with soluble organic substance. Such a peculiarity is determined, in our opinion, by two conditions: a) transformation of plant debris proceeds in tundra slowly; b) the humification products being formed in neutral and weak alkaline water are easily fixed by cations, forming the organomineral complexes, then they coagulate and precipitate.

Ionic composition of waters defines their important geochemical peculiarities and is assumed as a basis of their dividing into the kinds–the smallest taxon of water classification by Perel'man, Kasimov. The quality of the performed chemical water analysis is confirmed by the value of the definition error: the difference between the sum of anions and cations does not exceed 5% in all the cases (**Table 3**). Water systematization to the kinds was carried out according to prevailing ions and according to the correlation between them [12,13]. In the Middle-Siberian lowland the hydrocarbonate and sulfate waters are noted according to dominating anion $HCO3^-$, Cl^-, SO_4^{2-} at its amount more than 25% mg-equv/L from the anion sum. In the case of exceeding 25% by two anions the combined waters are noted-hydrocarbonate-sulfate and sulfate- hydrocarbonate ones (**Table 3**). Depending on domination of Ca^{2+}, Mg^{2+}, Na^+ the waters are divided into calcium-magnesium, magnesium- calcium and sodium ones.

The sulfate (39%) and hydrocarbonate (35%) waters prevail in bog ecosystems, but the combined waters—hydrocarbonate-sulfate and sulfate-hydrocarbonate ones dominate in rivers. Sulfate amount in river water approaches to the average SO_4^{2-} concentration in the waters of the land as a whole which makes 12 mg/L [14]. Bog waters contain sulfates much more, as a rule. The waters of lakes of the large mound peatland Oganer are most rich in SO_4^{2-} ion, its amount makes 141-345 mg/L (24 *b*-27*b*) which is located in the epicenter of technogenic emissions of the mining and smelting industrial complex "Norilsk nickel". Exceeding relative to the average index for the waters of the land as a whole achieves here an order and more.

Hydrocarbonate waters are characteristic of both river and bog waters, but mostly of last ones. The amount of HCO_3^- ion varies widely within 1-226mg/L. In acid bog waters (pH 3.6-4.1) the hydrocarbonate anion is not met. Calcium (4.0-55.4 mg/L) and magnesium (0,90-28,5 mg/L) are dominating cations. The ratio Ca^{2+}: Mg^{2+} makes, mainly, 2:1 in waters being studied varying in the mouth of the Norilskaya, Rybnaya and Yergalakh rivers up to 3-3.7. Such results agree as a whole with the ratio of dominating cations in fresh natural water [13].

Hydrocarbonate calcium-magnesium waters of bogs, rivers and lakes in cold humid regions are zonal. Sulfate-hydrocarbonate, hydrocarbonate-sulfate and sulfate waters show most likely the regional specificity determined by sulfide fields of ores. Such waters are typical of the rivers Agapa, Norilskaya, Rybnaya, Yergalakh, Ambarnaya, of the lake Melkoye and some bog ecosystems (14 *b*, 23-24 *b*, 29 *b*). Sulfate waters are inherent only in bogs. In tundra landscapes this phenomenon is azonal [10] since geographically they correspond to a greater extent to central and southern parts of the steppe zone. Sulfate ultrafresh and fresh waters of bog ecosystems relate to different classes in their alkaline-acidic properties: neutral and weak alkaline (pH 6.5-8.5) as well as weak acidic ones (pH 3~4-6.5). This relation to different classes was used for preliminary assessment of contribution of potential SO_4^{2-} sources to the water environment.

In our opinion, neutral and weak alkaline sulfate waters of bog ecosystems reflect to a greater extent the subalkaline trend of intra-chamber differentiation of theTalnakh-Norilsk sulfide massif. This trend is due to in tensive alkalinization of initial hyperbasite-basite melt [4]. At the contactwith alkalis the underground sulfide waters are neutralized. Being connected with surface waters in regional deep faults they enrich waters with sulfates: the Norilsk ore region is located under extreme conditions of

Table 3. Classification of surface waters by ionic composition and assessment of definition error at chemical analysis

No.of water sample*	∑ of anions (∑a)	∑ of cations (∑c)	Definition error**, %	mg-equiv/Lof the anion sum, %			Water kind
	mg-equiv/L			HCO_3^-	Cl^-	SO_4^{2-}	
1	2	3	4	5	6	7	8
Waters of rivers, waterfall and lakes of glacial- tectonic genesis							
1 *r*	0,745	0,690	3,8	77,85	11,14	11,0	$C^{Mg\ Ca}$
3 *r*	0,471	0,513	4,3	59,44	22,9	17,62	$C^{Ca\ Mg}$
4 *r*	0,639	0,587	4,2	37,55	22,06	40,37	$CS^{Ca\ Mg}$
5 *r*	0,805	0,857	3,1	47,20	20,62	32,20	$SC^{Mg\ Ca}$
19 *r*	0,704	0,745	2,8	39,77	22,30	37,93	$SC^{Mg\ Ca}$
20 *r*	1,679	1,781	2,9	40,50	7,38	52,11	$SC^{Mg\ Ca}$
28 *r*	2,708	2,602	2,0	47,26	2,73	50,0	$CS^{Ca\ Mg}$
15 *w*	0,725	0,762	2,5	52,27	15,95	31,49	$SC^{Mg\ Ca}$
6 *l*	0,704	0,709	0,04	39,77	23,58	36,64	$SC^{Mg\ Ca}$
Bog waters							
2 *b*	0,739	0,739	0,0	64,95	19,08	15,96	$C^{Mg\ Ca}$
7 *b*	1,841	2,01	4,4	64,09	7,17	28,73	$SC^{Mg\ Ca}$
8 *b*	0,905	0,855	2,8	30,93	10,05	59,0	$SC^{Mg\ Ca}$
12 *b*	2,568	2,488	1,6	77,88	3,85	18,26	$C^{Ca\ Mg}$
13 *b*	1,514	1,586	2,3	68,69	6,01	25,30	$C^{Mg\ Ca}$
14 *b*	0,710	0,712	0,14	39,44	12,68	47,75	$CS^{Ca\ Mg}$
1	2	3	4	5	6	7	8
16 b	1,374	1,371	0,0	75,69	8,44	15,14	CMg Ca
17 b	2,651	2,693	0,8	83,02	2,8	14,22	CMg Ca
18 b	0,610	0,650	3,2	13,11	12,13	74,75	S Mg Ca
21 b	3,427	3,378	0,7	16,92	2,65	80,42	S Mg Ca
22 b	1,336	1,32	0,6	no	8,08	91,96	S Mg Ca
23 b	2,704	2,783	1,4	46,23	6,14	45,41	SCMg Ca
24 b	13,0	12,90	0,4	28,46	16,15	55,38	CSNa
25 b	4,37	4,202	2,0	20,13	4,55	75,28	S Mg Ca
26 b	5,02	5,50	4,5	7,57	3,31	89,04	S Mg Ca
27 b	3,278	3,423	2,2	5,49	5,06	89,44	S Mg Ca
29 b	2,489	2,557	1,3	63,48	2,97	33,54	CS Ca Mg
30 b	1,018	1,042	1,2	no	8,15	91,84	S Mg Ca
31 b	2,952	2,936	0,3	63,68	11,82	24,49	CMg Ca
32 b	3,106	3,052	0,9	72,44	2,67	24,88	CMg Ca
33 b	0,625	0,645	1,6	60,8	23,84	15,36	CMg Ca
34 b	0,326	0,324	0,3	4,91	22,39	72,70	S Mg Ca
35 b	0,274	0,287	2,3	no	22,26	77,34	S Mg Ca

stress relief from the rift-genic (fissure- and ditch-like) structures [3]. Neutral and weak alkaline sulfate waters were found in bog lakes of the Omuntakh river left bank and in those ones of the large mound peatland in Oganer suburb (21 *b*, 25 *b*, 26 *b*).

We assume that formation of acid sulfate waters in bog ecosystems is directly connected with the impact of technogenic sulfur oxide fluxes by enterprises of the Norilsk mining and smelting industrial complex. Acid sulfate waters (pH 3.6-6.1) were found in vicinity of

towns Talnakh, Kayerkan, Oganer suburb and the route Alykel'-Vologachan to the west from Norilsk city (the samples 18 *b*, 22 *b*, 30 *b*, 34 *b*, 35 *b*). Ultrafresh and fresh bog waters, not saturated practically with all mineral compounds, have a great dissolving ability but the deficit of bases does not enable them to neutralize fully the annual setting out SO_3 amount. An active acidification points to the instability of water phase of bogs to technogenic emissions because of lack of mechanisms which support it in stable regime (the low mineralization, high dissolving ability, deficit of bases).

Therefore the transformation of hydrocarbonatic and hydrocarbonate-sulfate waters into sulfate ones is entirely appropriate for typical geochemically subordinated bog landscapes. It is not improbable that acid sulfate waters of bog ecosystems can be the result of natural processes. In frozen regions the sulfide fields have an oxidation zone of sulfate type with formation of sulfuric acid and easily dissolved sulfates of Fe, Cu, Zn and other metals [10]. This version is indirectly supported by the highest Fe amount just in heavy acid (1000-740 mkg/L) sulfate waters in relation to other objects (361-3.6 mkg/L).

4. Amount of Water Soluble Forms of Heavy metals and Assessment of Pollution Level of Surface Waters

Equally with sulfur the solid emissions of Ni, Cu, Co, Pb are present in aerotechnogenic fluxes of the Norilsk mining and smelting industrial complex. Amount of water soluble forms of heavy metals in surface waters of Taimyr lowland greatly varies both in water categories (the bog, river and lake waters) and in study regions (**Tables 4** and **5**).

The low concentration of metals is noted in the "Krasnye kamni" waterfall, also in rivers and lakes located to the north, the north-east and the east from Norilsk city - rivers Verkhnyaya Agapa and Agapa, the mouth of the Norilskaya river, Bol'shoy Avam and the lake Melkoye. The total amount of heavy metals in ultrafresh and fresh waters of rivers and lakes with neutral and alkaline medium reaction doesn't almost exceed 10 mkg/L. In the vicinity of Talnakh town there is also relatively little Cu, Ni, Co, Pb–3-14 mkg/L in surface waters, somewhat more of them—5-19 mkg/L there is in the Kayerkan-Vologochan region, mainly, in waters of bog ecosystems. As an exception here the bog lake with heavy acidic sulfate waters (the left bank of the Ambarnaya river) is where the sum of water soluble metals is enlarged up to 150 mkg/L. However, the highest concentration of heavy metals is revealed in bog ecosystems of the Oganer suburb. In thermokarst lakes, formed at different heights of the large mound peatland, the sum amount of heavy metals ranges from 140 to 800 mkg/L. Their maximum is found in waters of peatland gone by rapid fire.

Based on such an analysis the surface waters were divided into three groups by the amount of accumulated heavy metals: 1) river and lake waters, 2) bog waters with a low amount of Ni, Cu, Co and Pb which, to a first approximation, we consider as a natural background and 3) bog waters which are at maximum enriched by heavy metals.

As it follows from the **Table 5**, the sum amount of heavy metals in waters of rivers and lakes of Taimyr lowland makes 2.5-10.4 mkg/L. The average amount of Co is 0.07, Pb–0.59, Ni–1.02, Cu–3.33 mkg/L. It was stated that the average concentration of heavy metals in river and fresh waters of the Earth hydrosphere as a whole makes: Co–0.25 (margins of variation 0.04-8), Pb–1.0 (0.06-120), Ni–2.5 (0.02-27) and Cu–7.0 (0.2-30) mkg/L [14,15]. Comprised given numbers allow to ascertain that the river and lake waters of the discussed area are not polluted by heavy metals. According to the **Figure 2** the most contribution to enrichment of the discussed category of waters is made by the following heavy metals: copper on the average 64.2% (varying 45.9-82.2%), nickel 19,6% (6.8-41.1), lead—14% (3.7-26.7) and cobalt—2.2% (0.7-4.1).

In waters of bog ecosystems related in geochemical coupling to subordinate landscapes the total concentration of heavy metals is visibly higher—4.5-19.0 mkg/L. Bog waters which characterize the natural background accumulate nickel 4,9 times, cobalt 2.4 times, copper 1,9 times more. As it follows from the **Figure 2b**, the nickel contribution to enriching the water phase of bog ecosystems by heavy metals increases on the average up to 39,7% (varying makes 20.4-62.3). However, the leading role as before is played by copper—51.6% (33.8-78.0). Lead contribution decreases visibly. Reaching the bog ecosystems it is evidently adsorbed by peat substrate independently of a source of coming.

The total concentration of heavy metals in polluted bog waters increases up to 145-800 mkg/L. The exceeding order in relation to natural background of bogs makes: Co (64.4) > Ni (48.9) > Cu (35.3) > Pb (1.75). As before nickel and copper contribute mostly to pollution (**Figure 2c**). Therewith the nickel share in the total pollution by heavy metals becomes decisive and achieves on the average 57.5% (varying is 35.7-85.1), Copper share is 39.8% (13.6-60.7). The role of cobalt and especially of lead is very small.

Assessment of water pollution level was realized according to the exceeding order (factor) of levels of maximum permissible concentration [16]. The exceeding order of norms was calculated by the formula:

$$K_i = C_i / C_{MPC},$$

Table 4. Heavy metal amount in surface waters of the north- siberian (Taimyr) lowland, mkg/l (the mean water phase).

№ of samples*	Ni	Cu	Co	Pb	№ of samples	Ni	Cu	Co	Pb
Waters of rivers, lakes, waterfall					Bog waters (continuation)				
1 *r*	0,16	1,62	<0,01	0,57	17 *b*	3,43	8,53	<0,01	0,35
3 *r*	0,99	2,69	0,27	0,52	18 *b*	3,15	10,5	0,47	<0,10
4 *r*	0,92	1,84	<0,01	0,31	21 *b*	4,21	4,28	<0,01	0,59
5 *r*	1,10	6,46	<0,01	0,29	22 *b*	285,0	485,00	25,40	3,40
19 *r*	0,88	4,73	<0,01	0,65	23 *b*	6,79	10,90	<0,01	0,87
20 *r*	2,24	7,02	<0,01	1,19	24 *b*	102,0	16,30	0,85	0,71
28 *r*	2,15	2,40	<0,01	0,67	25 *b*	259,0	229,00	4,63	<0,1
6 *l*	0,28	1,24	0,29	0,66	26 *b*	345,0	314,00	6,01	<0,1
15 *w*	0,47	1,99	<0,01	0,45	27 *b*	293,0	158,00	19,00	0,48
Bog waters					29 *b*	9,12	6,47	<0,01	0,93
2 *b*	1,37	5,24	<0,01	<0,1	30 *b*	85,60	55,50	6,01	1,22
7 *b*	2,96	3,96	<0,01	0,82	31 *b*	9,45	8,67	<0,01	0,90
8 *b*	4,29	4,82	<0,01	0,78	32 *b*	6,14	5,17	<0,01	1,32
12 *b*	8,36	9,44	<0,01	0,86	33 *b*	1,76	2,12	<0,01	0,60
13 *b*	0,10	0,10	<0,01	<0,10	34 *b*	5,27	7,28	0,96	<0,10
14 *b*	1,40	2,42	<0,01	0,44	35 *b*	5,66	7,83	1,16	0,45
16 *b*	5,97	3,24	<0,01	1,36					

* Points of water sampling and indices of waters are given in the **Table 1**.

Table 5. Descriptive statistics* of heavy metal amount in surface waters of the North- Siberian(Taimyr) lowland (the mean water phase).

Elements	m	s_x	min	max	R	S^2_x	S_x	C_v
1	2	3	4	5	6	7	8	9
Waters of rivers, lakes, waterfall, $\sum_{HM}$ – 2,5-10,4 mkg/L								
Co	0,07	0,039	0,01	0,29	0,28	0,014	0,119	170
Pb	0,59	0,089	0,29	1,19	0,9	0,071	0,266	45
Ni	1,02	0,247	0,16	2,24	2,08	0,549	0,741	72
Cu	3,33	0,726	1,24	7,02	5,78	4,744	2,178	65
Waters of peat bogs of natural background, $\sum_{HM}$** –4,5-19,0 mkg/L								
Co	0,16	0,087	0,01	1,16	1,15	0,128	0,358	223
Pb	0,57	0,088	0,1	1,32	1,22	0,131	0,361	63
1	2	3	4	5	6	7	8	9
Ni	4,67	0,675	0,1	9,45	9,35	7,751	2,784	60
Cu	5,94	0,755	0,1	10,9	10,8	9,685	3,112	52
Waters of peat bogs of technogenic pollution, $\sum_{HM}$ –145-800 mkg/L								
Co	10,31	3,924	0,85	25.4	24,55	92,392	9,612	93
Pb	1,00	0,509	0,1	3.4	3,3	1,556	1,248	124
Ni	228,27	44,075	85,6	345	259,4	11655,5	107,96	47
Cu	209,63	70,92	16,3	485	468,7	30179	173,72	82

*Legend: m–mean, mkg/L, s_χ–error of the mean, min–minimum, max–maximum, R–amplitude (range), S^2_x–dispersion, S_x–standard deviation, C_v–variation coefficient,**)$\sum_{HM}$–sum of water soluble heavy metals.

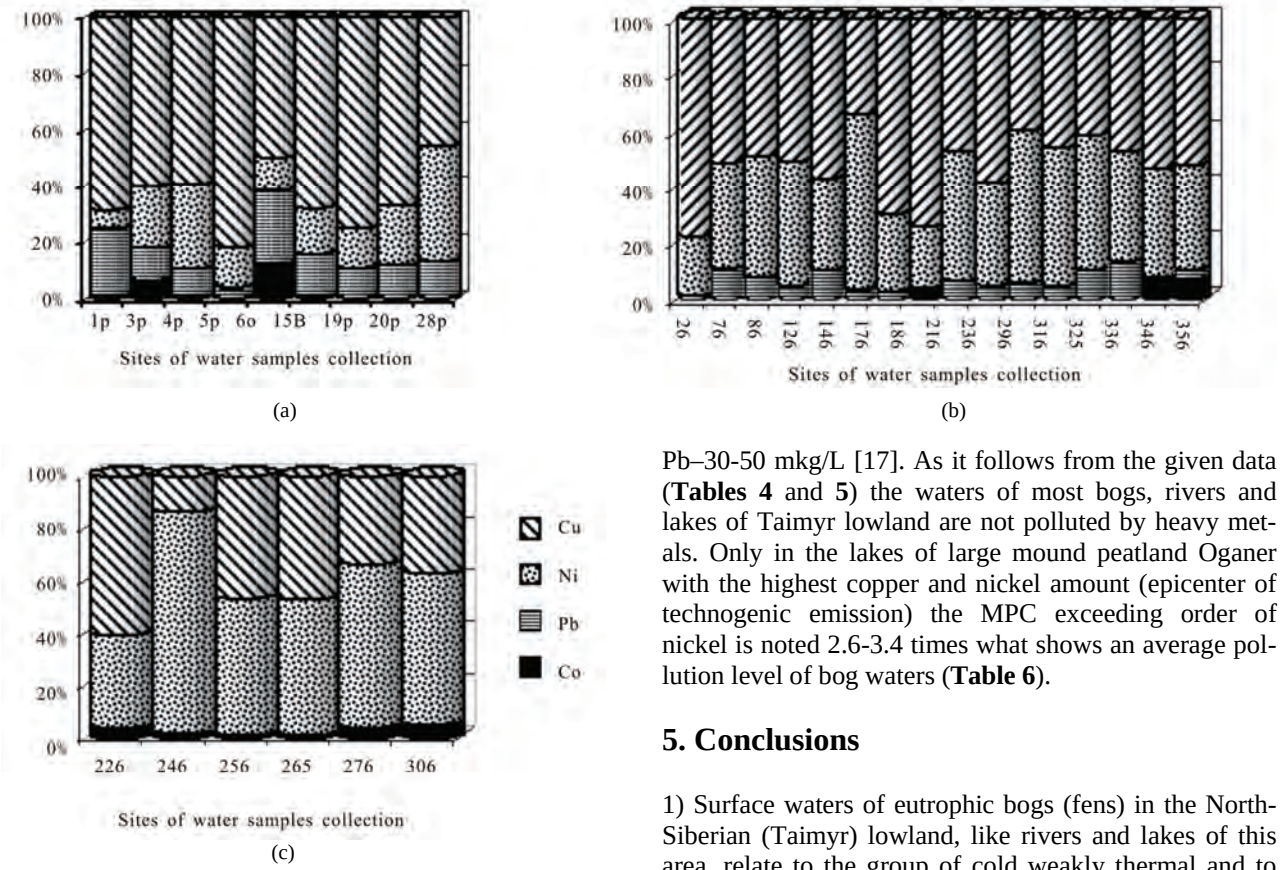

Figure 2. Cu, Ni, Co, Pb contribution to enriching waters of rivers, lakes and waterfall (a), bog waters of natural background (b) and bog waters with signs of technogenic pollution (c). Captions (legends) and points of water sampling are in the Table 1.

where K_i–the exceeding order of maximum permissible concentration by i–ingredient; C_i–concentration of i–ingredient in the water object, mkg/L; C_{MPC}–maximum permissible concentration of i–ingredient, mkg/L. If the exceeding makes not more than 2 units then the pollution level is considered to be low; 2-10 it is middle, 10-50 it is high, 50-100 units it is considered to be very high.

The MPC levels which are established for fresh drinkable water are the following: Co and Ni–100, Cu–1000, Pb–30-50 mkg/L [17]. As it follows from the given data (**Tables 4** and **5**) the waters of most bogs, rivers and lakes of Taimyr lowland are not polluted by heavy metals. Only in the lakes of large mound peatland Oganer with the highest copper and nickel amount (epicenter of technogenic emission) the MPC exceeding order of nickel is noted 2.6-3.4 times what shows an average pollution level of bog waters (**Table 6**).

5. Conclusions

1) Surface waters of eutrophic bogs (fens) in the North-Siberian (Taimyr) lowland, like rivers and lakes of this area, relate to the group of cold weakly thermal and to the type of oxygen waters, mainly, to the class of neutral weakly alkaline and to the family of ultrafresh and fresh waters and to the kind of waters poor with dissolved or ganic matter. The hydrochemical background is presented by hydrocarbonate, sulfate as well as hydro carbonate-sulfate calcium-magnesium waters which show regional; specificity connected with deposits in depths of sulfide copper and nickel ores.

2) Sulfate waters are inherent only in bog ecosystems. In their alkaline- acidic properties they relate to different water classes and characterize indirectly the mechanisms of medium reaction. In our opinion, neutral and weakly alkaline waters reveal the subalkaline trend of the intrachamber differentiation of sulfide fields in the Norilsk

Table 6. Assessment of pollution level[1] of bog waters in lakes of the large mound peatland (vicinity of Oganer suburb).

N of sample	Location of lakes	Nickel amount		Copper amount	
		K[2]	Level of pollution	K	Level of pollution
22 *b*	Peat mound with fire evidences	2,8	mean	0,5	not polluted
	Height from a peatland foot:				
25 *b*	5 m	2,6	mean	0,2	not polluted
26 *b*	10 m	3,4	mean	0,3	not polluted
27 *b*	15 m	2,9	mean	0,2	not polluted

[1]according to: [16], [2]Multiplicity of exceeding of a maximum concentration limit (MCL): Values of MCL are brought in the text.

ore region. Acid sulfate bog waters related, as a rule, to vicinity of industrial complexes are formed most likely under technogenic fluxes of sulfur oxides. An active acidification of neutral and weakly alkaline hydrocarbonate (hydrocarbonate-sulfate) waters points to instability of aquatic phase of bogs to industrial emissions because of lack of mechanisms which support it in stable state (low mineralization, high dissolving ability, deficit of bases). Strongly alkaline sulfate-hydrocarbonate-sodium waters are connected with cryogenic processes and are formed in the result of interaction of waters with salinized mineral grounds which are cropped out owing to earthflow of melted peat thickness (solifluction).

3) Natural hydrochemical background of bog ecosystems makes in heavy metals in the first approximation: Co–0.16, Pb–0.57, Ni–4.67 and Cu–5.94 mkg/L. In most cases the surface waters are not polluted by heavy metals: their migration in neutral and weakly alkaline waters is limited. As Ni, Cu, Co, Pb increase in bog water composition, it appears the trend of increase of nickel contribution to the sum amount of heavy metals. Bog waters are polluted by nickel at mid-level when being located in immediate closeness from sources of industrial emissions.

6. References

[1] N. Y. Kats, "Bogs of the Globe," Nauka, Moscow, 1971, p. 295.

[2] N. I. P'yavchenko, "On Studying Bogs of Krasnoyarsk krai," In: "Paludified Forests and Bogs of Siberia", Press of the USSR Academy of Sciences, Moscow, 1963, pp. 5-32.

[3] "Middle Siberia," Nauka, Moscow, 1964, p. 480.

[4] O. A. Dyuzhikov, V. V. Distler, B. M. Strunin *et al*., "Geology and Ore-Bearing Capacity of Norilsk Region," Nauka, Moscow, 1988, p. 279.

[5] T. T. Taisaev, "Geochemistry of Taiga-Frozen Landscapes and Searching the Ore Fields," Nauka, Novosibirsk, 1981, p. 136.

[6] "Standard Methods for Analyzing Water," Chemistry, Moscow, 1973, p. 376.

[7] Methodical Instructions, "Methodology for Performing Measurements of the Mass Sulfate Concentration in Waters Using The Titrimetric Method with Barium Salt," Rostov-na-Donu, 2006, p. 23.

[8] Methodical Instructions, "Methodology for Performing Measurements of the Mass Sodium and Potassium Concentration in Surface Waters of the Land Using the Flaming-Photometric Method," Rostov-na-Donu, 2008, p. 14.

[9] "Water Quality. Definition of Cobalt, Nickel, Copper, Zinc, Cadmium, Lead. Flaming Atomic and Absorption Spectro-Photometric Methods," p. 20.

[10] A. I. Perel'man and N. S. Kasimov, "Geochemistry of Landscape," Astreya-2000 Press, Moscow, 1999, p. 768.

[11] S. P. Suslov, "Physical Geography of the USSR," Asian Part. State Education Pedagogical Press, Vol. II, Moscow, 1954, p. 711.

[12] O. A. Alekin, "General Hydrochemistry," Hydrometeo Press, Leningrad, 1948, p. 206.

[13] O. A. Alekin, "Essential Principles of Hydrochemistry," Hydrometeo Press, Leningrad, 1970, p. 444.

[14] V. V. Dobrovols'ky, "Essential Principles of Biogeochemistry," Higher School Press, Moscow, 1998, p. 413.

[15] H. J. M. Bowen, "Environmental Chemistry of the Elements," Academic Press, London, 1979, p. 333.

[16] V. P. Yemeliyanova, G. N. Danilova and T. K. Kolesnikova, "Assessment of Surface Water Quality of the Land in Hydrochemical Figures," *Hydrochemical materials*, Hydrometeo Press, Leningrad, Vol. 88, 1983, pp. 119-129.

[17] "Drinkable Water. Hygienic Specifications for Water Quality of Central Systems of Water Supply for Drinking: Sanitary Rules and Norms," Press Centre of the Russian Goskomsanepidemnadzor, Moscow, 1996, p. 111.

J. Water Resource and Protection, **2010, 2, 675-682**
doi:10.4236/jwarp.2010.27078 Published Online July 2010 (http://www.SciRP.org/journal/jwarp)

Prioritizing Riparian Corridors for Water Quality Protection in Urbanizing Watersheds

Samuel F. Atkinson[1], Bruce A. Hunter[1], April R. English[2]
[1]*Institute of Applied Science, University of North Texas, Denton, USA*
[2]*Halff Associates, Inc, Richardson, USA*
E-mail: *atkinson@unt.edu*
Received February 11, 2010; *revised May* 18, 2010; *accepted May* 21, 2010

Abstract

The cumulative effects of urbanization on riparian corridors can decrease the quality of water entering local streams, and ultimately adversely impact drinking water reservoirs of local municipalities. As such, a GIS and remote sensing based analysis tool called the Water Quality Corridor Management (WQCM) model was designed to identify and prioritize highly functioning riparian ecosystems for the preservation of stream corridor conditions. Preservation priority among various riparian corridors is established in the model by analyzing five parameters associated with stream corridor conditions (vegetation type, erosion potential, surface slope, percent of the stream contained within the Federal Emergency Management Agency (FEMA) 100-year floodplain, and amount of the stream corridor contained within a subwatershed); and each parameter is weighted and scaled based on what conditions are most important to protect. Because data associated with each parameter are readily available and easily manipulated via spatial analysis techniques, the WQCM model functions as a flexible methodology for predicting stream corridor conditions and allows watershed managers to identify potential preservation opportunities to ensure long term ecological functioning that protects water quality. These corridors can then also provide urban planners with potential natural spaces for urban dwellers, meeting multiple benefits requirements imposed by many municipalities.

Keywords: Watershed Management Planning, GIS Modeling, Remote Sensing, Riparian Assessment, Riparian Preservation and Restoration, WQCM Model

1. Introduction

In scientific parlance the term *riparian* refers to biotic communities on the shores of streams and lakes. Ecologists have long studied riparian corridors as ecosystems of forested and/or vegetative buffers that link aquatic and terrestrial environments [1]. Those studies show that healthy riparian stream corridors perform a multitude of valuable tasks for their adjacent waterways, including their overall influence on water quality [2], biological diversity [3], ecosystem maintenance [4] and protection of intermittent streams and the residual pools that they provide as refuges for multiple species during dry periods [5]. Nutrient cycling, contaminant filtration, water purification, bank stabilization, stream temperature maintenance, flow stabilization, flood attenuation, and habitat preservation are some of the numerous functions carried out by riparian zones [6].

1.1. Effects of Urbanization

Urbanization and its subsequent activities, without proper planning, often leads to the degradation of streams and their corridors. Such degradation inhibits the natural cycles of biological and physical activities normally carried out within riparian ecosystems [7], and also cause social and economic problems at regional and local levels. For example, Withers and Jarvie [2] state that the problems can influence human health (algal toxins), species abundance and diversity, amenity value and costs of water treatment for drinking. Streams and rivers on the periphery of urbanizing areas are particularly vulnerable due to population centers, sensitivity to land use change and ubiquitous exploitation [8]. Furthermore, many of those aquatic systems at the urban periphery are already experiencing agricultural practices, such as grazing and the direct access of cattle to streams. This has resulted in increased erosion of stream banks due to trampling, as well as direct deposition and indirect flow of animal waste into waterways, a principal component of non-pointsource pollution [9]. An EPA National Water Quality Inventory [10] assessing 19% of the waterways in the United States found pathogens in over 93,000 miles of streams and rivers. Ultimately, the dynamic equilibrium

of stream ecosystems is altered by the cumulative effects of channelization, clear-cutting, illegal dumping, and increased chemical usage, all consequences of urbanization surrounding riparian corridors.

Many places throughout the world are experiencing the same pattern of land use change that can be seen in north central Texas, the site of this study. Former "rural" areas are becoming a part of an ever increasing urban landscape. As residential developments, commercial properties, and industrial facilities proliferate, they cover the natural landscape with roads, buildings, parking lots, and other impervious surfaces [6]. Stream health is directly linked to urbanization, the effects of which simultaneously decrease bank stability and increase pollutant presence and transfer. Healthy riparian buffer zones have been shown to filter out up to 97% of soil sediment prior to stream entrance [11]. However, removing trees in riparian zones is often one of the first activities associated with urban and suburban development, leading to increased soil erosion. Increased erosivity results in a decrease in the depth of fertile topsoil and an increase of sediment within streams. These sediments often contain contaminants such as metals, pesticides such as DDT, other organics such as polychlorinated biphenyls (PCBs) and polycyclic aromatic hydrocarbons (PAHs), and other synthetic chemicals that may be toxic to aquatic and terrestrial plant and animal species and are linked to human health via the food chain [12].

1.2. Riparian Corridor Preservation Versus Restoration

While a stream's ecosystem functions and water quality are directly related to the condition of riparian corridors, the quality of the services provided by the corridors are not completely obvious to the untrained eye. Therefore, a number of methods have been developed which allow ecologists to measure various physical/chemical/biological parameters in the field, and convert those measurements into a score that represents riparian quality. In fact the National Research Council [6] recommend that stream corridor assessment and management strategies need to be available not only to ecologists wanting to understand stream ecosystems, but to the landowners and developers who have riparian corridors on their properties. With ever increasing development pressures, the protection of riparian corridors should be seen as a critical management goal for the sustainability of stream ecosystems and the safeguarding of water quality entering drinking water reservoirs. As a result, and the principle topic of this communication, a geographic information system (GIS) model is proposed that classifies stream segments and their adjoining riparian corridors on a scale that allows for the identification of those stream segments that are highly functioning in terms of protecting water quality so that they can be placed at the front of the "preservation" line.

We point out that the proposed model ranks stream segments in terms of the importance of preserving them for water quality purposes as opposed to ranking them for restoration purposes. Ecological restoration in this context involves re-establishing the biological and physical system among streams that have been disrupted from human activities such as urbanizing development [13]. Restoring a complicated network of biotic interactions is tedious, requires a detailed knowledge base, is a potentially-expensive endeavor for any entity, whether private, government, or academic, and is often unsuccessfully implemented [14]. A viable alternative to the restoration of degraded stream systems is the protection and preservation of waterways and their surrounding corridors. The maintenance of healthy riparian ecosystems not only provides example environments by which restoration practices can be modeled, but is also a more economical alternative when funding is limited and efforts need to be focused on less intensive approaches [15].

1.3. Objectives of Study

It is the ultimate goal of preservation strategies to curtail the loss of valuable resources. Protection strategies provide the solid foundation by which more politically and environmentally complicated restoration efforts can evolve over time. The objective of our efforts was to produce a GIS model that can establish the underpinning for the portion of a watershed management plan that protects water quality in the headwater streams of drinking water reservoirs. The goal is to be able to identify and prioritize stream corridors based on existing watershed data that are easily accessible. Fortunately, this leads to a secondary goal because protecting stream corridors under the goal of drinking water protection, also results in protecting other services that riparian corridors provide such as habitat protection, nutrient cycling and recreational opportunities are also protected.

2. Materials and Methods

GIS and remote sensing have modernized the monitoring and implementation of best management practices for the protection of stream ecosystems. Such techniques allow for the manipulation of large and complex datasets, while providing easy access to data retrieval. In addition, complex interactions can be evaluated through the GIS layering of various data montages, such as land use classifications via remote sensing and satellite images, feature files, and raster datasets. GIS technology also allows for simplified data sharing, making it logistically easier and more cost-effective to employ interdisciplinary teams working towards the goal of environmental sustainability [16].

We propose a GIS and remote sensing based model, the Water Quality Corridor Management (WQCM) model, designed to (1) utilize easily accessible data for the purpose of identifying and assessing potential water quality issues and (2) to classify stream segments in order of priority for preservation as a component of an overall watershed management plan.

2.1. GIS Materials

To establish the relative priority of stream reaches, five variables were chosen based on their availability and capacity for manipulation within spatial analysis software, as well as their ability to predict current riparian conditions (**Table 1**). These variables include vegetation type, erosion potential, surface slope, percent of the stream contained within the Federal Emergency Management Agency (FEMA) 100-year floodplain, and amount of the stream corridor contained within the subwatershed. Each of the five variables consists of an importance weight and a scaling function. Importance weights and scaling functions assigned to each model variable range from 0 to 5, with 5 indicating a greater need for protection. For example, vegetation class is considered the most important variable in the model, receiving 5 importance points, and the scaling function for vegetation indicates that forested areas within the riparian buffer receive 5 points while residential areas within the riparian buffer receive 2 points. Each variable's scaling function is based on the same concept: what conditions are more important to protect via preservation. **Table 2** through 6 provides the functional scales for each variable [16].

2.2. The WQCM Model

WQCM scores are calculated for each subwatershed based on watershed characteristics for each of the five variables considered by the model. Values are calculated for each stream segment in a study area, generating an overall WQCM score for the stream segment that defines each subwatershed. Based on the WQCM scores, we suggest that each stream segment be grouped into one of four preservation priority quartiles: low, moderate, high, and highest priority. The WQCM model produces a score that can range from 0 to 50, with the highest scores assigned to the highest preservation priority category and indicating the greater need for protection of a stream corridor under future development. The underpinning model is presented in Equation (1) :

$$\text{WQCM Score} = V_iV_f + E_iE_f + S_iS_f + F_iF_f + C_iC_f \quad (1)$$

where the subscripts "i" and "f" represent "importance" (**Table 1**) and "functional scale" (**Tables 2-6**).

The Dallas-Fort Worth, Texas region currently contains a population of more than 6.6 million people, and has experienced an average growth of about 150,000 people per year over the past decade, resulting in more than 500,000 new housing units built over that time [18]. The North Central Texas Council of Goverments currently predicts that the regional population in 2030 will exceed 9 million people. This rapid rate of urbanization has raised concerns about water supply, and the need to protect the quality of water entering the region's drinking water reservoirs. WQCM was developed specifically for this type of planning need. WQCM was applied to two different study areas in north central Texas of different sizes: 60,300 hectares (149,000 acres) with 133 subwatersheds; and 240,000 hectares (593,000 acres) with 90 subwatersheds that drain to one of the region's large drinking water reservoirs [16]. The smaller area was examined first, and was considered a pilot project to test the applicability and verify the relationship between the newly developed GIS/remote sensing models to a more traditional field-based assessment tool.

3. Results

3.1. Validating WQCM

The field-based tool developed by the U.S. Department of Agriculture [17] to quantitatively score the physical conditions of aquatic ecosystems was chosen to validate the WQCM model. The technique, known as the Stream

Table 1. Variables included in the WQCM model.

WQCM Variable	Brief Description
Vegetation (V) *Importance* = 3	Eight classes were generated. The more the native the vegetative cover (forested riparian zones) within the stream corridor, the greater need for protection.
Erosivity (E) *Importance* = 2	Erosivity (Kw) in study area ranged from 0 to 0.43; higher Kw soils have a greater need for protection.
Slope (S) *Importance* = 2	Slope range from <1% to 5%; Greater slope percentage surfaces have a greater need for protection.
Floodplain (F) *Importance* = 1	Ratio of FEMA designated floodway area to stream buffer area; Because FEMA floodway designation provides inherent protection, the greater the area outside the designated floodplain, the greater need for protection.
Corridor (C) *Importance* = 1	Ratio of corridor area to subwatershed area; Larger ratios suggest less room for development and therefore more pressure to develop inside stream corridor area.

Table 2. Vegetation classes, class importance and functional scores.

Land cover	class importance
f = forest	5
w = water	5
s = shrub/brush	4
c = crop/pasture	5
b = barren	3
u = urban	2
r = residential	2
u = unclassified	5

$V_f = (c_f a_f + c_w a_w + c_s a_s + c_c a_c + c_c a_b + c_u a_u + c_r a_r + c_u a_u)/SWa$

where V_f is the vegetation function, c_i is class importance, "a_i" represents area in hectares of vegetation class c_i, and SWa is the subwatershed area.

Table 3. Erosivity classes, class importance and functional scores.

Erosivity class	class importance
Kw = 0.00	1
Kw = 0.17	3
Kw = 0.20	3
Kw = 0.24	3
Kw = 0.28	4
Kw = 0.32	4
Kw = 0.37	5
Kw = 0.43	5

$E_f=(c_f a_f + c_w a_w + c_s a_s + c_c a_c + c_c a_b + c_u a_u + c_r a_r + c_u a_u)/SWa$

where E_f is the erosivity function, c_i is class importance, "a_i" represents area in hectares of erosivity class c_i, and SWa is the subwatershed area.

Table 4. Slope classes, class importance and functional scores.

Slope class	class importance
slope < 1%	1
slope = 1% to 2%	2
slope = 2% to 2%	3
slope = 3% to 4%	4
slope = 4% to 5%	5

$S_f=(c_f a_f + c_w a_w + c_s a_s + c_c a_c + c_c a_b + c_u a_u + c_r a_r + c_u a_u)/SWa$

where S_f is the slope function, c_i is class importance, "a_i" represents area in hectares of slope class c_i, and SWa is the subwatershed area.

Table 5. Floodplain classes, class importance and functional scores.

Floodplain class	Floodplain function
100 year floodplain less than 5% of stream corridor	0
100 year floodplain 5% to 85% of stream corridor	1
100 year floodplain 85% to 150% of stream corridor	2
100 year floodplain 150% to 200% of stream corridor	3
100 year floodplain 200% to 350% of stream corridor	4
100 year floodplain greater than 350% of stream corridor	5

Table 6. Corridor classes, class importance and functional scores.

Corridor class	Corridor function
stream corridor area less than 5% of subwatershed area	1
stream corridor area 5% to 6% of subwatershed area	2
stream corridor area 6% to 7% of subwatershed area	3
stream corridor area 7% to 8% of subwatershed area	4
stream corridor area greater than 8% of subwatershed area	5

Visual Assessment Protocol (SVAP), is similar to the WQCM in that multiple variables are measured for each stream segment, and each measurement is scored by a functional scaling relationship. Like WQCM, higher SVAP scores indicate higher quality (and by extension a higher priority for preservation). This similarity allows the two very different approaches for evaluating aquatic ecosystems (field measurements versus GIS/remote sensing modeling) to be compared. Of the 133 subwatersheds developed for the WQCM pilot project, 10 subwatersheds from each of the 4 priority quartiles were randomly selected for SVAP assessment. For these 40 subwatersheds, a Spearman-rank correlation coefficient indicates a highly significant positive relationship between the two approaches ($p < 0.0001$), albeit a relatively low correlation coefficient ($r_s = 0.58$). We suggest that the relatively low correlation coefficient may in part be due to the different purposes for which SVAP and WQCM were prepared: SVAP was designed to rate a "stream's health" [19], while WQCM was designed to rate a stream corridor's potential for continuing to deliver high quality water to a drinking water reservoir. None-the less, both provide a measure of a stream's ecological quality, but the ease of applying WQCM over SVAP, and the relationship shown in **Figure 1**, offers an

adequate level of justification for proposing the use of WQCM.

3.2. Applying WQCM in North Central Texas

In an early paper that addressed how riparian corridors were linked to water quality [1] it was pointed out that that in undisturbed watersheds, biological communities and water quality are in dynamic equilibrium. Under normal rainfall events, there is relatively little surface runoff because the rain is adsorbed by the land and vegetation, and few nutrients are lost to drainage waters. When the vegetation is removed, instabilities in the terrestrial environment are inevitable, which in turn alter the water quality equilibrium of natural states. Urbanization often includes attempts to improve drainage of the land's surface by modifying stream channels (straightening and bank stabilization), the combined effects of which result in disequilibrium in both biological and water quality systems. We suggest that preservation of well functioning riparian corridors will result in the most economic way to protect water quality. Further, a prioritized list of riparian corridors will allow urban planners and developers alike to become part of a water quality protection strategy for their community.

The WQCM model was applied to each subwatershed in our two study areas, and a final WQCM score was calculated and a corresponding WQCM priority quartile (low, moderate, high, or highest) was designated for each stream corridor within each of the 133 subwatersheds of the pilot study area and 90 subwatersheds of the Lewisville Lake watershed. **Figure 2** represents the summary type of output that WQCM generates that can allow watershed managers to visualize where stream corridor preservation activities will be most beneficial across a moderately large watershed. **Figure 3** illustrates the detail that can be provided for stream corridors in specific subwatersheds. **Figure 3** highlights two subwatersheds, one with a low WQCM score and one with a high score, draped over a satellite image. The upper of the two subwatersheds contains a "high priority" corridor (WQCM rating = 35.1), and it can be clearly seen that this subwatershed has very little urbanization and the lower reaches of the stream corridor offers ample tree canopy resulting in high preservation priority. The adjacent lower subwatershed, however, is highly urbanized and much of the tree canopy cover along the stream corridor has been removed. This corridor is beyond preservation, and would need restoration, resulting in a "low priority" rating (WQCM rating = 26.4). A valuable aspect of the WQCM model is that landuse, soil erosivity, surface slope and floodplain data are also available for each corridor, allowing a watershed manager to glean insight as to why a particular corridor should be preserved.

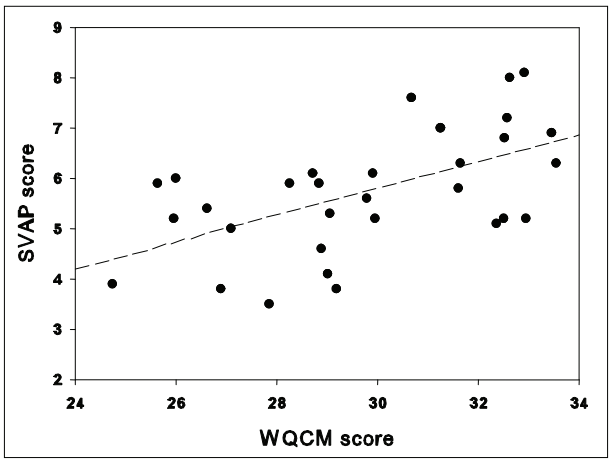

Figure 1. Relationship between proposed Water Quality Corridor Management (WQCM) model and the U.S. Department of Agriculture's Stream Visual Assessment Protocol (SVAP) for 40 subwatersheds (r = 0.58, p < 0.0001).

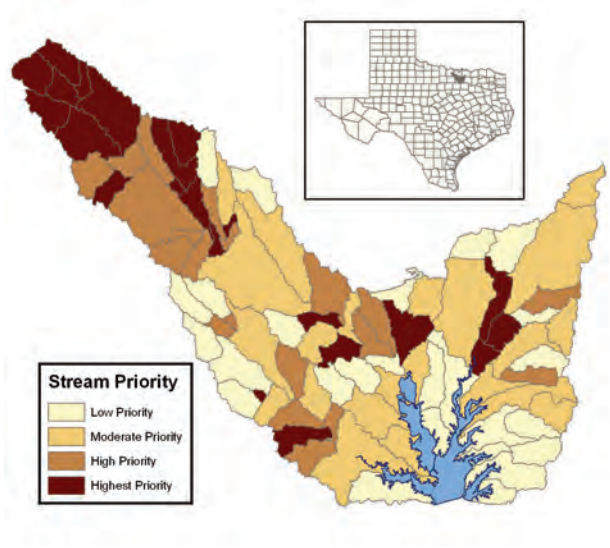

Figure 2. Stream corridor preservation priority based upon WQCM scores. Red is highest priority, light yellow is lowest priority (Study area is approximately 80 kilometers (50 miles) by 70 kilometers (43 miles) in dimensions). Lewisville Lake, at the bottom of the watershed, is one of several major sources of drinking water for the Dallas-Fort Worth region.

4. Concluding Remarks

The results of WQCM showed that subwatersheds that had little urbanizing development tended to have vegetated riparian corridors (the most important factor in the model), with varying degrees of slope, erosivity and FEMA floodplain protection. These combinations typically lead to preservation priority scores in the upper half of the subwatershed scores. The highest rated stream corridors were found to have high habitat quality along

the stream banks, and had a general appearance of providing many ecosystem services (see **Figure 4** for an example). On the other hand, the subwatershed with the highest levels of urbanizing development tended to have little vegetation in the riparian corridors, and no matter what levels of the other parameters were contained within those subwatersheds, they rarely scored in the upper half of the preservation priority (see **Figure 5** for an example). These findings quickly lead us to realize that the same data set, with different importance weights and scaling functions, can lead to a second model that prioritizes watersheds based on restoration goals. A restoration prioritization model is now under development.

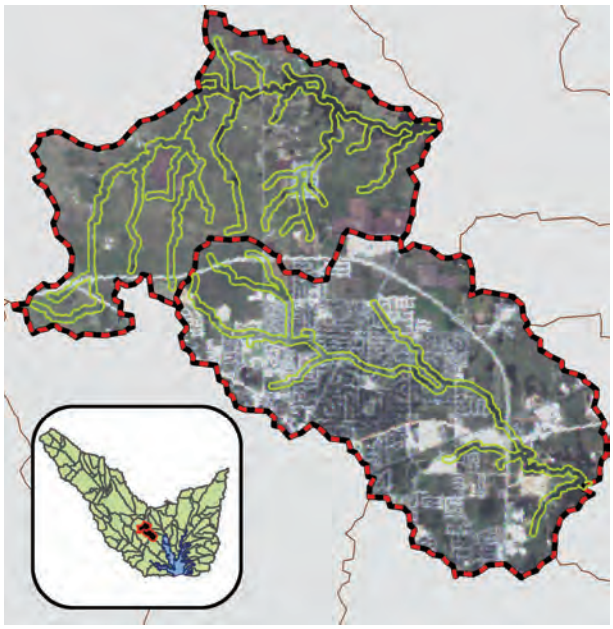

Figure 3. WQCM results for a "high priority" stream corridor (upper subwatershed: WQCM = 35.6), and an adjacent "low priority" stream corridor (lower subwatershed: WQCM = 26.4).

Figure 4. Field site #28, example of site designated as WQCM highest priority quartile.

Figure 5. Field site #34, example of site designated as WQCM lowest priority quartile.

A comparison analysis of the five WQCM model components, applied to both the pilot study region and the Lewisville Lake watershed, showed that the parameters most likely to influence the WQCM model's scores were vegetation, followed by the erosivity and floodplain components. The slope and corridor parameters were not driving factors for any of the WQCM model's scores within either of the studies. These findings were as expected, since the importance weight given to the vegetation component of the WQCM model (5) is higher than the weight assigned to any of the other four components. Furthermore, the vegetation, erosivity, and floodplain components were the predominant parameters influencing the WQCM scores even without including the corresponding importance weights. Due to these consistent comparison results, the pairing of protection strategies will be discussed for the three primary driving WQCM components of vegetation/land use type, the bank stability parameter of erosivity, and the floodplain component.

In relation to vegetation/land use type, the encroachment of suburban communities and commercial developments factors prominently into the degradation of stream ecosystems. In fact, the primary source of sediment runoff originates from the vast number of construction sites so commonly found among developing areas. Accordingly, simple protective measures need to be enforced at all construction zones. For example, the cessation of vegetation clear-cutting around construction sites leaves buffer zones intact and able to entrap harmful nonpoint source pollutants before they enter stream systems [14]. Furthermore, negligent lawn care and waste disposal habits throughout residential communities necessitates better management practices, such as using organic compost to treat lawns instead of the synthetic chemicals found in fertilizers and pesticides that are easily carried into streams during rainfall events (EPA Measure 9, 2005). Stream bank erosion, vegetation trampling, and the presence of manure are just a few of

Table 7. Impact sources and management practices for stream water quality and corridor protection based on land use.

WQCM Land Use Type	Sources	Impacts to Stream Water and Corridor Quality	Suggested Management Practices	References
Urban/ Residential	Construction sites	Presence of sediment, pesticides, fertilizers, trash, and other harmful chemicals in streams.	Protect natural vegetative buffers; Stabilize construction site entrance & exit locations; Install silt or fabric filter fences in areas of non-concentrated flow around site; Install sediment basins.	[16]
Urban/ Residential	Impervious Cover, Negligent waste disposal and landscape practices	Increased flooding risk; Increased transport of non-point source pollutants to water sources; Runoff pollutants such as lawn fertilizers, household chemicals, and pet waste; Increased algae presence in streams; Increased stream bank erosion.	Public education outreach programs; Protect natural vegetative buffers; Limit the use of pesticides and fertilizers; Increase the use of organic compost; Recycle yard clippings into organic compost; If use fertilizer, use organic or encapsulated nitrogen fertilizer; Plant vegetation native to the regional climatic conditions; Water lawns only when necessary; Properly dispose of pet waste; Do not wash cars at home; Label storm drains; Post "no pollution signs" warning of legal ramifications.	[16,22,23]
Pasture	Cattle grazing	Trampling and disturbance of stream banks and vegetation; Increased soil compaction; Increased erosion; Decrease in detritus for aquatic organisms; Decrease in stream biodiversity; Presence of livestock urine and manure in stream; Increase in disease causing bacteria and oxygen-depleting organics.	Fence off cattle access to streams and riparian corridors; Decrease or tightly regulate cattle access to streams and riparian corridors; Rotate areas subjected to cattle grazing.	[7,17,18,22]

the detrimental impacts caused by the grazing of livestock in and near streams on pastureland, the most effective remedy for which being the total exclusion of cattle from accessing streams and their surrounding corridors [20].

Just as the complex interactions of ecosystems are intertwined, so are the parameters outlined in the WQCM model. The stability of a stream bank, measured in the WQCM model by erosion potential, is both directly and indirectly affected by land use. For instance, stream channelization to improve aesthetics in residential developments disturbs the delicate balance among stream ecosystems, leading to amplified water flow and the subsequent increase in stream bank erosion, channel incision, and habitat degradation [21]. In other words, if erosivity is an implicating parameter for a particular WQCM score, the first step in establishing abatement practices is analyzing how stream bank erosion characteristics is related to the land use practices surrounding the stream and on the neighboring land parcels. Once the relationship between land usage and channel erosion has been established, the appropriate management practices, as outlined in **Table 7**, can be implemented. Based on the results of this study, the conclusion is that the WQCM model provides a potential system for predicting stream corridor quality within the north central Texas area, but the approach should be applicable for other rapidly urbanizing areas.

5. Acknowledgements

We are grateful to the U.S. Environmental Protection Agency and the Upper Trinity Regional Water District for providing support for this research, and Brian Boe and Matt Dameron for their assistance in this research.

6. References

[1] J. R. C. Karr and I. J. Schlosser, "Water Resources and the Land-Water Interface," *Science*, Vol. 201, No. 4352, 1978, pp. 229- 234.

[2] P. J. A. Withers and H. P. Jarvie, "Delivery and Cycling of Phosphorous in Rivers: A Review," *Science of the Total Environment*, Vol. 400, No. 1-3, 2008, pp. 379-395.

[3] D. D. Tullos and M. Neumann, "A Qualitative Model for Analyzing the Effects of Anthropogenic Activities in the Watershed on Benthic Macroinvertebrate Communities," *Ecological Modeling*, Vol. 196, No. 1-2, 2006, pp. 209-220.

[4] D. Montgomery, "Geomorphology, River Ecology and Ecosystem Management in Geomorphic Processes and Riverine Habitat," *Water Science Applications*, Vol. 4, pp. 2001, 247-253.

[5] P. J. Wigington Jr., J. L. Ebersole, M. E. Colvin, *et al*., "Coho Salmon Dependence on Intermittent Streams," *Frontiers in Ecology and the Environment*, Vol. 4, No. 10, 2006, pp. 513-518.

[6] NRC (National Research Council), "Riparian Areas: Functions and Strategies for Management," National Academies Press, Washington, D.C., 2002.

[7] D. L. Correll, "Principles of Planning and Establishment of Buffer Zones," *Ecological Engineering*, Vol. 24, No. 5, pp. 2005, 433-439.

[8] P. A. Hamilton and T. L. Miller, "Lessons from the National Water-Quality Assessment," *Journal of Soil and Water Conservation*, Vol. 57, No. 1, 2002, pp. 16A-21A.

[9] EPA, "National Water Quality Inventory, Chapter 2: Rivers and Streams", U.S. Environmental Protection Agency, EPA/305b, Washington, D.C., 2000, pp. 7-15.

[10] R. L. France, "Potential for Soil Erosion from Decreased Litterfall due to Riparian Clear-Cutting: Implications for Boreal Forestry and Warm-and-Cool-Water Fisheries," *Journal of Soil and Water Conservation*, Vol. 52, 1997, pp. 452-455.

[11] J. B. Kauffman, R. L. Beschta, N. Otting and D. Lytjen, "An Ecological Perspective of Riparian and Stream Restoration in the Western United States," *Fisheries*, Vol. 22, No. 5, 1997, pp. 12-24.

[12] R. J. Naiman and H. Décamps "The Ecology of Interfaces: Riparian Zones," *Annual Review of Ecology and Systematics*, Vol. 28, 1997, pp. 621-658.

[13] P. M. Groffman, D. J. Bain, E. Lawrence, *et al*., "Down by the Riverside: Urban Riparian Ecology," *Frontiers in Ecology and the Environment*, Vol. 1, No. 6, 2003, pp. 315-321.

[14] EPA, "National Management Measures to Control Nonpoint Source Pollution from Urban Areas. Introduction and Management Measures 8, 9, 12," U.S. Environmental Protection Agency, EPA/841/B-05/004, Washington, D.C., 2005, pp. 1-518.

[15] S. F. Atkinson, B. A. Hunter, A. English, B. Boe and M. Dameron, "Lewisville Lake Watershed Protection and Management Strategies," Technical Report Prepared for the Upper Trinity Regional Water District, 2007, p. 155.

[16] NCTCOG (North Central Council of Governments), Arlington, 10 February 2010. http://www.nctcog.org/ris/demographics/population.asp

[17] U.S. Department of Agriculture, "Stream Visual Assessment Protocol (SVAP)," National Resource Conservation Service, National Water and Climate Center Technical Note 99-1, Portland, 1998, p. 36.

[18] A. J. Belsky, A. Matzke and S. Uselman, "Survey of Livestock Influences on Stream and Riparian Ecosystems in the Western United States," *Journal of Soil and Water Conservation*, Vol. 54, No. 1, 1999, pp. 419-431.

[19] T. Pirim, S. Bennett and B. Barkdoll, "Effect of Riparian Vegetation Density on Stream Flow Velocity," Joint Conference on Water Resource Engineering and Water Resources Planning and Management, *Water Resources*, Vol. 104, 2000, p. 347.

[20] K. Kennedy, "Storm Water: Why Take it Personally?" Fourth Annual Region VI MS4 Operators' Conference, North Central Texas Council of Governments (NCTCOG), Arlington, 2005.

[21] NCTCOG, "12 Lessons Student's Can Learn from Smart Scape," North Central Texas Council of Governments, Texas Smartscape Program, Environment and Development Department, Arlington, 2006.

[22] C. T. Agouridis, "Cattle Production in a Small Grazed Watershed of Central Kentucky," Proquest Dissertations and Theses, 2004, p. 485.

[23] NRCS, "Animal Manure Management—Brief 7," National Resource Conservation Service, Resources Conservation Act, Washington, D.C., 1995.

J. Water Resource and Protection, **2010, 2, 683-689**
doi:10.4236/jwarp.2010.27079 Published Online July 2010 (http://www.SciRP.org/journal/jwarp)

Geo-Hydrodynamics of Bagjata Area and its Significance with Respect to Seasonal Fluctuation of Groundwater

Bijay Singh[1], A. S. Singh[2]
[1]*University Department of Geology, Ranchi University, Ranchi, India*
[2]*National Mineral Development Corporation Limited, Kirandul Complex, Chhattisgarh, India*
E-mail: *bsingh*6029*@gmail.com, ajayshekhar1@rediffmail.com*
Received February 2, 2010*; revised March* 25, 2010; *accepted May* 26, 2010

Abstract

Bagjata area is a part of Singhbhum Shear Zone (SSZ) falling within Survey of India Toposheets No. 73J/6, J/7, J/10 and J/11. The Subarnarekha River, Sankh Nala and Gohala faults are major discontinuities in the area. An attempt has been made to simulate the regional groundwater hydrodynamics. Few dug-wells were monitored for more than a year to find out the seasonal fluctuation changes in the drainage pattern and groundwater level. Groundwater samples were analyzed for physical and chemical analysis. Results show that one of the major discontinuities in the area—the Gohala Fault controls largely the geohydrodynamics of the area. Discharge of groundwater is of effluence type during all the three seasons. The water is safe for drinking as most of the contaminations are much below the permissible limits. No such previous work has been attempted in this area to investigate the groundwater dynamics and hence the selection of few parameters were assumed and taken from similar surrounding aquifer systems for modeling. The groundwater flow was also assumed to be in steady state. The present paper deals with some important aspects related to the hydrological significance of the Bagjata Uranium mining area and its relationship with the local climate, physiography and meteorology. An attempt is also made to simulate the status of groundwater conditions of hard rock aquifers in the region. Further it envisages the necessity of such study being undertaken in the entire SSZ belt to secure precise information about the surface manifestations which govern the groundwater recharge potentiality as well as its quality.

Keywords: Geo-hydrodynamics, Bagjata Groundwater, Singhbhum Shear Zone (SSZ), Gohala Fault, Effluence, Uranium-Copper Mineralization

1. Introduction

Bagjata is located in Dalbhumgarh subdivision of East Singhbhum district of Jharkhand state at a distance of about 6.5 km SE of the copper mining town of Musabani. The nearest Railway station is Dalbhumgarh. It can also be accessed by road from Jamshedpur and Jaduguda townships. The geohydrological significance in this area is important due to various misconceptions about the contamination of radiogenic contents in the water bodies of the entire Uranium belt. No such previous information / data are available for this area to allay the fears of local populace. This work assumes importance as being the first attempt of its kind in the SSZ. During the research important aspects of groundwater and its movement within aquifers have been studied vis-à-vis the geological setting of the area. It was noticed carefully and found to be very much linked with the subsurface water transport mechanism and the quality and its ground water. The investigation includes planning, sample collection, analytical chemistry, quality and data management. The sub surface water was routinely analyzed, geohydrodynamics discussed and modeling studies done on the basis of the well inventory data.

2. Materials and Methods

The Bagjata area is confined to the sheared rock types of Singhbhum Thrust Zone. Geologically, the thrust belt is constituted by Archaean metasediments such as mica-schist, quartzite, phyllites and altered tuffs. During the field mapping authors find the rock formation trending along NW-SE with variable dip of 35º to 45º due North-East. The shear zone has been a major

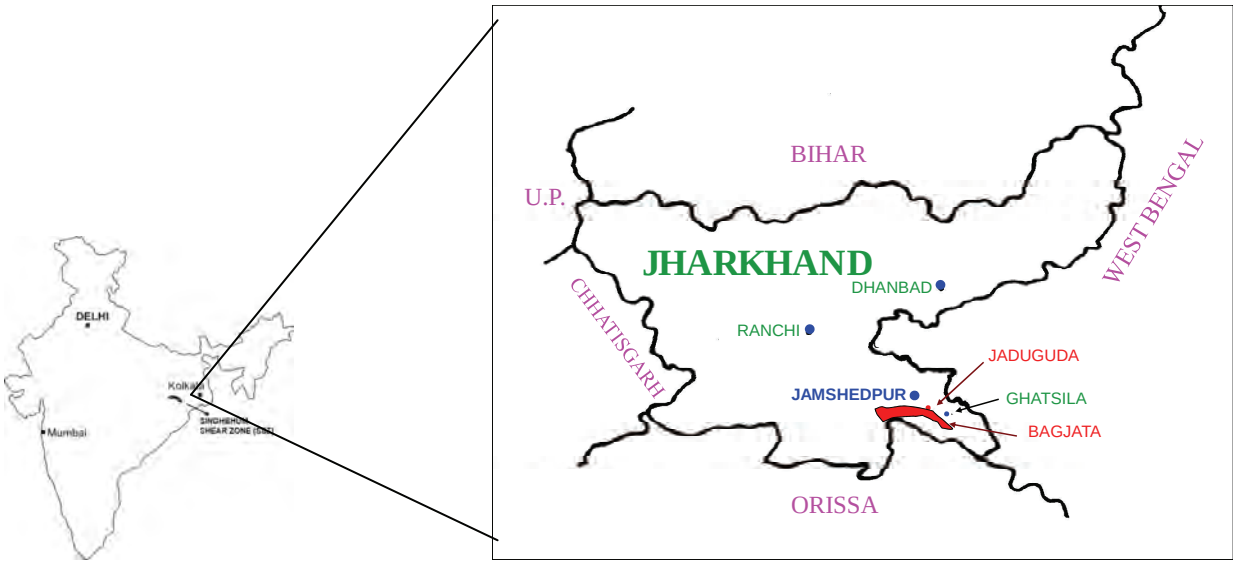

Figure 1. Location of bagjata area, east Singhbhum, Jharkhand, India.

site for intense mineralization in the region.

The geological mapping in the area was carried out with the help of GPS and other traditional field equipments in order to investigate an area falling under four SOI toposheets integrated with the help of Surfer 8.0 and AutoCAD software followed by intensive groundtruthings.

The principle planar structures at Bagjata are foliation planes, joint planes and shear planes. The foliation planes are the dominant planar feature in the rocks. There are three sets of joint planes present in the rocks.

J-1:—The most prominent one is nearly parallel to foliation strike but having dips of 30º to 50º towards SW (opposite to the Uranium lode). A few of them are nearly vertical.

J-2:—The second set of joints is the dip joints which are vertical or having dips of 30º to 50º towards NW or SE.

J-3:—In general this is not prominent, but present at places with variable directions.

On the basis of field investigations, authors find the area with a gentle to moderately steep or steep slopes. The selected area is to the north and west of a small hill range. The ground level of the area is at 120-144 m RL whereas hilltops to the east are at about 300 m RL and those to the south are mostly at 350-400 m RL. There is another hill range which is within the study zone. These hills are however, less steep and made up of quartzite. General ground level gradually slopes towards the North. The NE quadrant of the area is blocked by Gohala Fault. The natural drainage system is dendritic in nature due to hilly topography and well defined gradients in parts of the study area. The area is very important in terms of lithology and hydrogeological characteristics.

The River Subarnarekha flows from the NW to the SE to the northeast part. The area lies in a valley of about 5 km wide extending in the NW to SE direction. This valley is drained by the Sankh Nalla, which flows northeastern part of the study area and joined the Subarnarekha River 5 km northeast of the Bagjata. Major part of the area has a dendritic drainage pattern.

The hill ranges are drained by seasonal streams which form the part of the Subarnarekha River System. The Sankh Nalla receives water through streams flowing down from the hills on both its banks. High flood level of the Sankh Nalla and Subarnarekha River is well below the study area.

The area lies in tropical region where climate is characterized by very hot summer and cold winter. Summer is typically from mid March to mid June when temperature ranges from 44ºC in day to 19ºC in night. Eighty percent of the rainfall occurs during period from mid June to mid September. The average rainfall in the region is 1391 mm as recorded by IMD observatory at Jamshedpur. This paper describes the fluctuations of Ground water with seasons and responses with respect to recharge/discharge.

The Geological map was prepared on the basis of field investigations with the help of a modern GPS system. Existing wells were selected for sampling and plotted on this map with the help of AutoCAD software (**Figure 2**). The selected wells were observed for a period more than a year and data for depth of water level are collected during all the three seasons. The depth to water level data with respect to mean sea level (**Table 2**) and ground water level contours has been prepared to ascertain the general groundwater hydraulic gradient. An application

Table 1. Litho-Stratigraphic sequence.

Group	Formation	Lithological Units
Iron Ore Group	Chaibasa Formation	Garnetiferous mica schist with basic and ultra basic intrusives.
		Sericite schist.
		Quartzite and Quartz schist.
	Shear Zone Assemblages	Sericite schist with impersistent Quartz-kyanite-granulite.
		Banded Quartz-sericite-biotite schist with bands of metabasic and Quartz-tourmaline-magnetite rock.
		Quartz-biotite-chlorite schist with bands of Quartzite.
	Dhanjori Formation	Quartz and sheared Conglomerate.
		Biotite schist and Quartzite
		Talc schist.
		Traps and Quartzite.

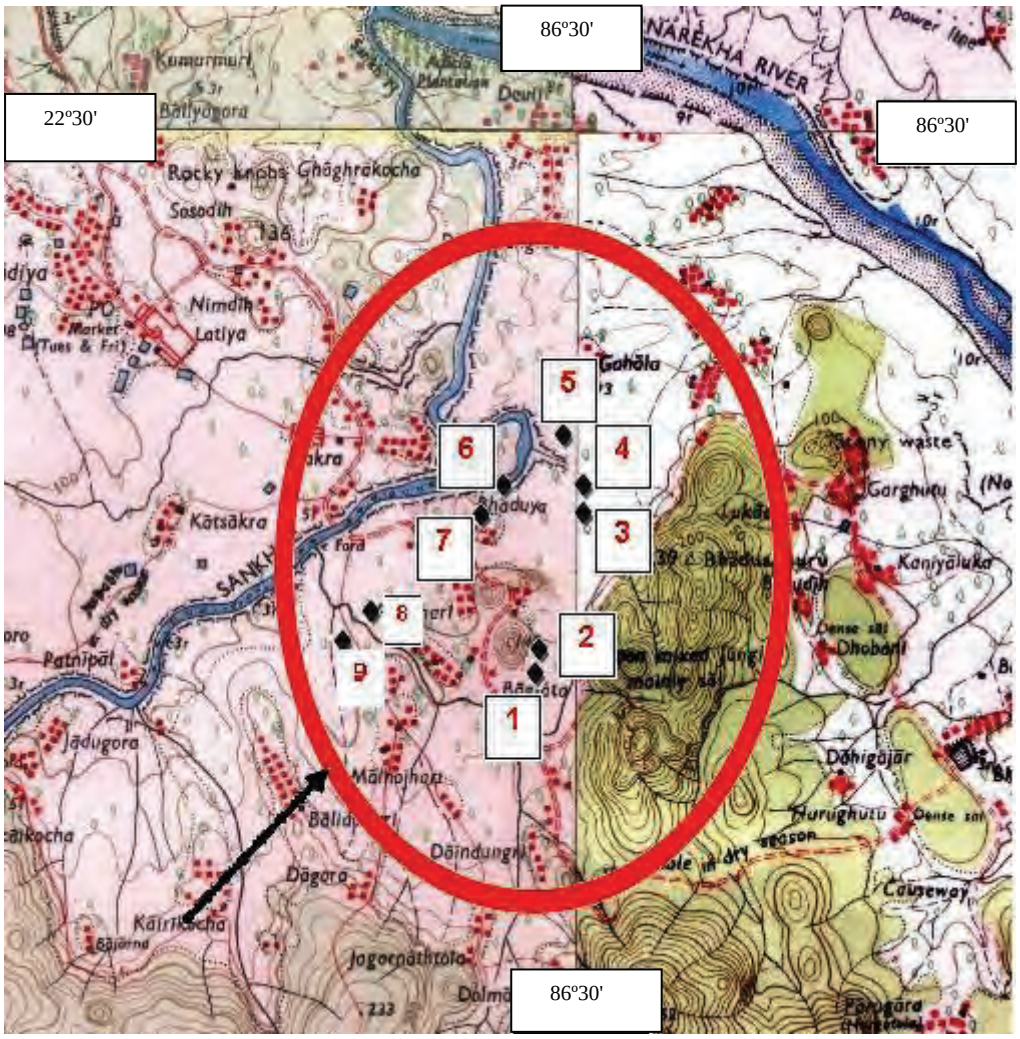

Figure 2. GPS measured sampling locations of Bagjata area, east Singhbhun, Jharkhand.

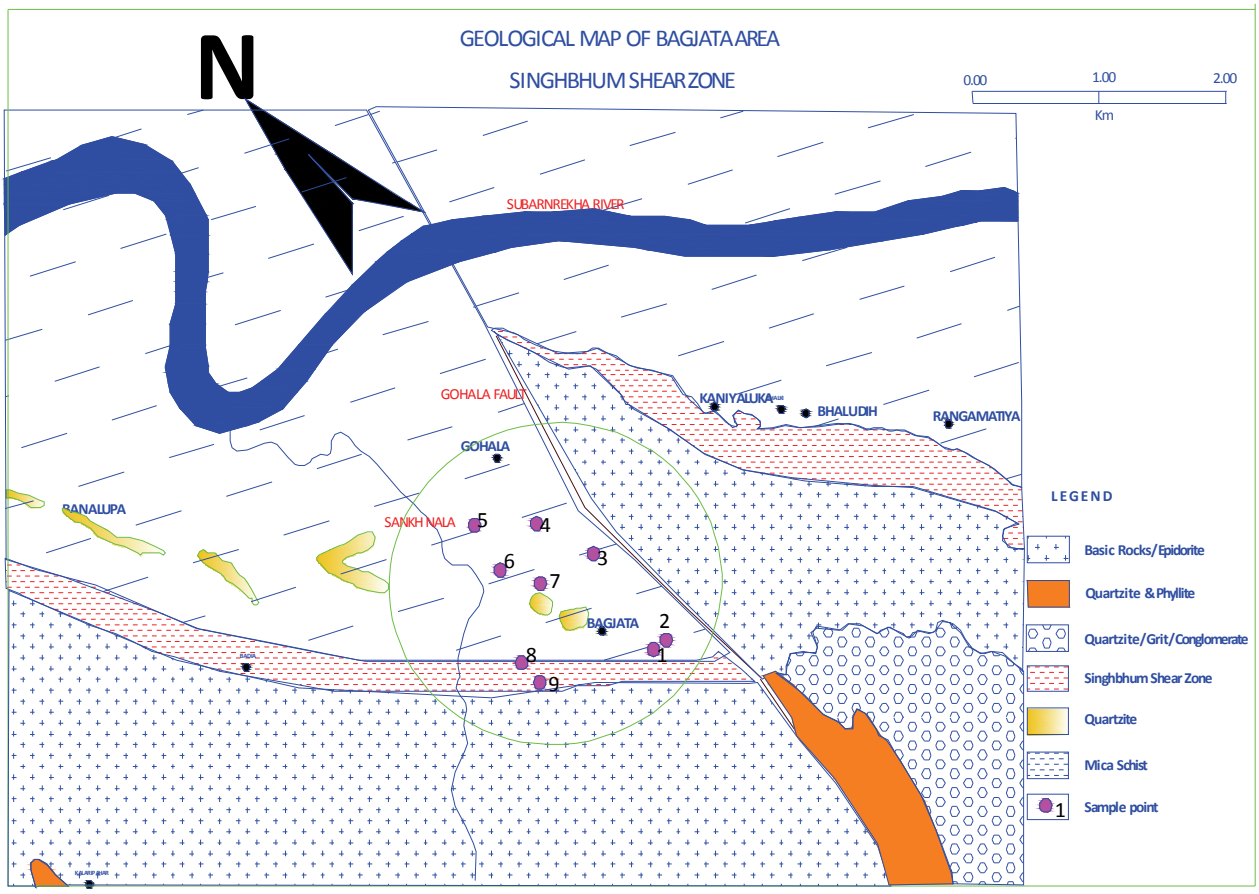

Figure 3. Location of collected samples plotted on the geological map, east Singhbhum, Jharkhand, India.

Table 2. Water table (AMSL) at bagjata area.

Sample No	Winter Season (Nov.) (mm)	Summer Season (May) (mm)	Rainy Season (July) (mm)
1	4600	5870	1500
2	680	3180	650
3	1560	8830	1120
4	5100	9370	1410
5	1520	4450	1050
6	1300	4000	1200
7	2100	6580	1320
8	7200	8600	2370
9	4390	7050	1630

of software Surfer 8.0 is done for contour generation. The collected samples were also analyzed for physical and chemical methods (**Table 3**). The pH of groundwater samples were measured at site using direct reading probe. Before taking reading pH meter was calibrated using a pH = 7, buffer for natural water, single point calibration method. The other radicals for samples were analyzed in laboratories by chemical analysis methods. Radium analysis is carried out by batch adsorption from water sample. 133 Ba is added to allow the measurement of

the overall chemical yield by γ counting. Radium is recovered with a few milliliters of 1.5 M HCl, and lead is removed by a chromatographic column filled with Dowex 2 × 8. Finally 50 μg of barium carrier is added, and the radium is co-precipitated as sulfate on a pre-formed bed of barium sulfate, to prepare a sample suitable for α and γ counting.

Groundwater Sampling:

Sampling points are located based on the available open well position in the area and its durability to continue for a long period. The chosen well were monitored for a year in all the three seasons. **Table 1** Shows the depth data measured in the three sea sons with respect to the re-spective reduced level in millimeter (mm). The samples

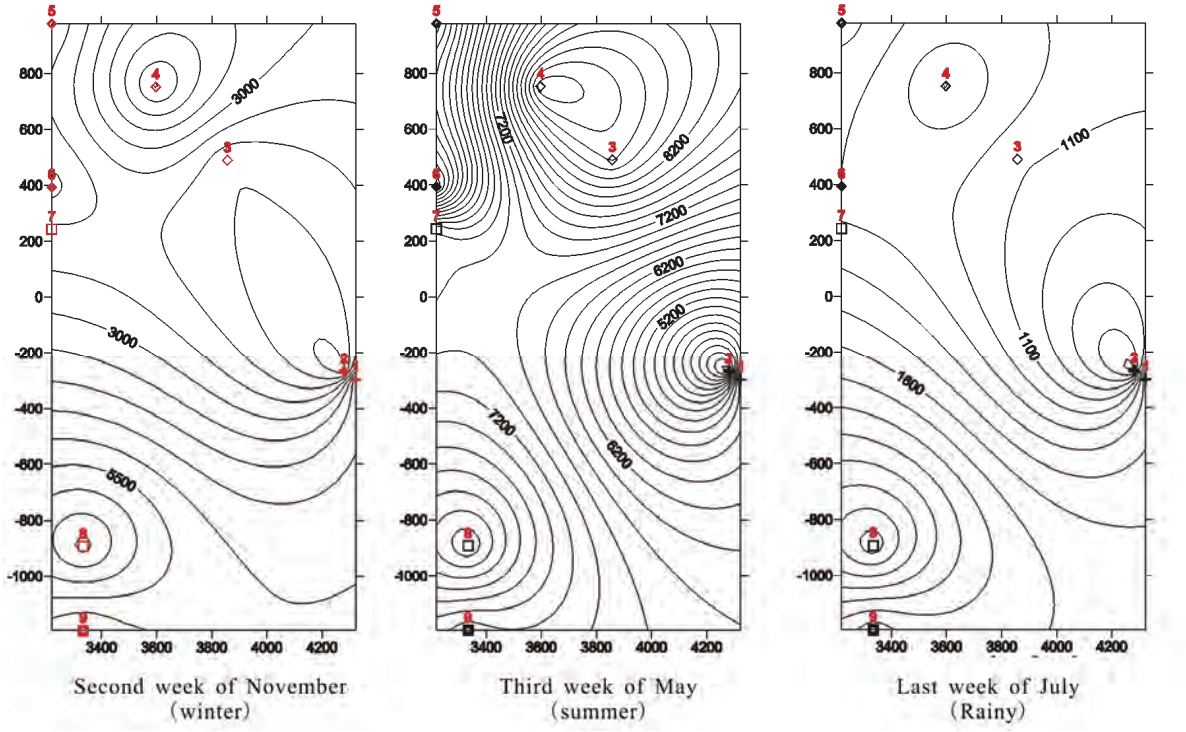

Figure 4. Groundwater level contours at bagjata area, east singhbhum, Jharkhand.

Table 3. (a & b) The chemical composition of groundwater around bagjata area collected during month november.

(a)

Sample No	pH	Total Hardness ($CaCO_3$), mg/L	Iron (Fe), mg/L	Chloride (Cl), mg/L	Fluoride (F), mg/L	Dissolved solids, mg/L	Calcium (Ca), mg/L	Magnesium (Mg), mg/L	Copper (Cu), mg/L	Manganese (Mn), mg/L
1	7.0	330	0.3	78	0.5	500	52	56	< 0.01	0.056
2	7.2	326	0.5	68	0.4	356	26	26	< 0.01	0.024
3	7.5	356	0.8	79	0.9	782	35	31	< 0.01	0.036
4	7.2	358	0.4	64	0.2	300	45	21	< 0.01	0.058
5	7.4	381	0.9	78	1.2	568	65	26	< 0.01	0.025
6	7.0	415	1.2	124	0.7	986	35	33	< 0.01	0.014
7	7.5	398	0.9	26	0.5	642	52	34	< 0.01	0.065
8	7.0	425	0.7	63	0.9	564	25	11	< 0.01	0.082
9	7.4	386	0.9	89	1.9	268	56	6	< 0.01	0.015

(b)

Sample No	Sulphate (SO_4), mg/L	Nitrate (NO_3), mg/L	Arsenic (As), mg/L	Lead (Pb), mg/L	Zinc (Zn), mg/L	Chro-mium (Cr^{6+}), mg/L	Alumin-ium (Al), mg/L	Boron (B), mg/L	U (nat) mg/m^3	Ra-dium(Ra^{226}), Bq/m^3
1	56	5	< 0.02	< 0.05	0.035	< 0.01	< 0.01	< 0.1	2.5	25
2	6	12	< 0.02	< 0.05	0.08	< 0.01	< 0.01	< 0.1	3.5	36
3	58	35	< 0.02	< 0.05	0.06	< 0.01	< 0.01	< 0.1	4.0	41
4	59	5	< 0.02	< 0.05	0.058	< 0.01	< 0.01	< 0.1	2.6	32
5	87	68	< 0.02	< 0.05	0.069	< 0.01	< 0.01	< 0.1	< 0.5	12
6	125	34	< 0.02	< 0.05	0.042	< 0.01	< 0.01	< 0.1	< 0.5	25
7	56	26	< 0.02	< 0.05	0.026	< 0.01	< 0.01	< 0.1	< 0.5	14
8	36	6	< 0.02	< 0.05	0.085	< 0.01	< 0.01	< 0.1	0.8	18
9	89	11	< 0.02	< 0.05	0.062	< 0.01	< 0.01	< 0.1	1.6	23

were also collected from these chosen open well during the winter (November) season. The Poly-ethylene bottles are used for sample collection. Each sample bottle is identified by date, site name and an adhesive bar-code label. The bar-code allows each sample to be tracked through sample analysis and data entry. All bottles for sampling were given the unique bar-code identification number. Collected samples were protected by reducing temperature method to avoid any further contamination, loss or other unintended changes. The sample bottles were completely filled to avoid any evaporation loss. Raw data for all analyses are entered into a Visual dBase database.

3. Hydro-Geochemical Characteristics

The chemical composition of Ground water is shown **Table 2**. The pH of water samples collected from Bagjata area is mildly alkaline to natural. The most of radicals falls within the permissible limit of drinking water except the Iron content at few locations. The presence of radioactivity is purely due to the Uranium mineral rich area. This value is far beyond the radium activity admissible for drinking waters.

4. Discussion and Conclusions

The collected samples were analyzed for groundwater position, its fluctuation in respect of seasonal variation. Data were first analyzed through manual formation of reduced level and then schematic drawing is formulated with the help of the software for contour generation. **Figure 4(a)** shows the ground water contour during the winter season where maturity in the domain can be seen easily. **Figure 4(b)** is the contour diagram of summer season, the dense contour reflects to the scarcity of water in the ground water domain and thus velocity is fast. **Figure 4(c)** is the contour diagram for rainy season. Again a maturity in the horizon is returned back. Since at any point the water table equals the energy head as a consequence, flow lines lie perpendicular to water table contours. Therefore in all the three season the direction of ground water movement is parallel and sub parallel to North direction which is the direction of Gohala Fault. Gohala Fault is the major discontinuity in the area. Authors find the groundwater movement is very much controlled by the Gohala Fault which is lying along in the N-S direction. Also the wide contour intervals show the higher permeabilities than those of the narrower spacing. Therefore prospects for a good yielding well are better in rainy and winter seasons respectively than in the summer session.

Also the major discontinuity in the area that is Gohala fault is very much controlling the flow direction. Authors observe an effluence type of discharge of groundwater where it is in a position to recharge/feed the rivers during all the three seasons. Groundwater quality is mildly alkaline to natural. Radioactive contamination in water is very low and much below the limit. Other radicals are also within the permissible limits and designated safe for drinking. Further it envisages the necessity of such study being undertaken in the entire SSZ belt to secure precise information about the surface manifestations which govern the groundwater recharge potentiality as well as its quality.

5. Acknowledgements

The authors are thankful to the C.M.D. Mr. R. Gupta and Mr. A.K.Sarangi T.S. to the C.M.D. of the Uranium

Corporation of India Limited (a Govt. of India Undertaking) at Jaduguda near Jamshedpur for their support and encouragement rendered during the course of the fieldwork. The kind co-operation and necessary infrastructural facilities provided by the Head of the University Department of Geology, Ranchi University, Ranchi (Jharkhand, India) is thankfully acknowledged.

6. References

[1] A. K. Bannerji, "Cross Folding Migmatisation and Ore Location along Part of the Singhbhum Shear Zone, South of Tatanagar, Bihar," *Economic Geology*, Vol. 57, No. 1, 1962 pp. 50-71.

[2] S. B. Bhattacharjee, A. K. Ghosh, L. Bhattacharjee and S. R. Svananda, "Uranium Mineralisation and Trace Element Distribution in the Jaduguda Uranium Deposit, Singhbhum Thrust Belt, Bihar, Contributions to the Geology of Singhbhum," Jadavpur University, Calcutta, 1966, pp. 59-75.

[3] S. B. Bhattacharjee, A. K. Ghosh, L. Bhattacharjee and S. Bhattacharjee, "Minor Elements in Some Rocks and Minerals of the Rakha Mines Area, Singhbhum, India," *Mineralogical Magazine*, Vol. 36, No. 281, 1968, pp. 671-675.

[4] K. L. Bhola, G. R. Udas, N. R. Mehta and G. H. Sahasrabudhe, "Uranium Ore Deposits at Jaduguda in Bihar State India," In: *Peaceful Uses of Atomic Energy*, *Proceedings of Second Internet Conference*, Vol. 2, 1958, pp. 704-708.

[5] J. A. Dunn and A. K. Dey, "Geology and Petrology of Eastern Singhbhum and Surrounding Areas," Memoirs of Geological Survey, India, Vol. 69, No. 2, 1942.

[6] J. M. McDonald and A. W. Harbaugh, "A Modular Three-Dimensional Finite-Difference Groundwater Flow Model. Techniques of Water Resources Investigations of U.S.," Geological Survey Book, 1988, p. 586.

[7] H. M. Ragunah and D. K. Todd, "Ground Water," In: H. M. Raghunath and D. K. Todd, Eds.

[8] S. C. Sarkar, "Geology and Ore Mineralisation of the Singhbhum Copper-Uranium Belt, Eastern India," INA Press, Kolkata, 1985.

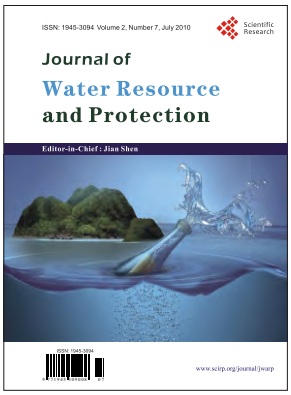

Call for Papers

Journal of Water Resource and Protection (JWARP)

http://www.scirp.org/journal/jwarp
ISSN:1945-3094 (Print), 1945-3108 (Online)

JWARP is an international refereed journal dedicated to the latest advancement of water resource and protection. The goal of this journal is to keep a record of the state-of-the-art research and promote the research work in these fast moving areas.

Editor-in-Chief

Editorial Board

Subject Coverage

This journal invites original research and review papers that address the following issues in water resource and protection. Topics of interest include, but are not limited to:

- Water resources and quality assessment
- Rivers, lakes and estuary systems
- Wastewater treatment and sludge biotreatment
- Water purification and water supply
- Water source protection and sustainable use
- Modeling, measuring and prediction of water pollution
- Ground water pollution control
- Reactions and degradation of wastewater contaminants
- Other topics about water pollution

We are also interested in short papers (letters) that clearly address a specific problem, and short survey or position papers that sketch the results or problems on a specific topic. Authors of selected short papers would be invited to write a regular paper on the same topic for future issues of the *JWARP.*

Notes for Intending Authors

Submitted papers should not have been previously published nor be currently under consideration for publication elsewhere. Paper submission will be handled electronically through the website. All papers are refereed through a peer review process. For more details about the submissions, please access the website.

Website and E-Mail

http://www.scirp.org/journal/jwarp Email: jwarp@scirp.org

J. Water Resource and Protection, 2010, 2, 609-689.
Published Online July 2010 in SciRes (http://www.SciRP.org/journal/jwarp).

TABLE OF CONTENTS

Volume 2 Number 7 **July 2010**

